Development of Membrane Bioreactor Employing Commercial and Modified Membranes for Wastewater Treatment in Bangladesh

A Thesis Submitted in Partial Fulfillment of the Requirements for the Degree

of

DOCTOR OF PHILOSOPHY

in

Applied Chemistry and Chemical Engineering,

University of Dhaka

BY

MD. NUR-E-ALAM

(Registration No.: 57/2021-2022)

Department of Applied Chemistry and Chemical Engineering

Faculty of Engineering and Technology

University of Dhaka

Dhaka 1000, Bangladesh

June, 2024

DECLARATION

I certify that the work contained in the thesis is original and has been done by myself under the supervision of my supervisors. I also declare that this work has not been submitted to any other institute for any degree.

Signature of the Candidate

Md. Nur-E-Alam
Registration No.: 57/2021-2022
Session: 2021-2022

CERTIFICATE

This is to certify that the work contained in the thesis entitled **"Development of Membrane Bioreactor Employing Commercial and Modified Membranes for Wastewater Treatment in Bangladesh"** submitted by **Md. Nur-E-Alam, Registration No.: 57/2021-2022, Session: 2021-2022** for the award of the degree of **Doctor of Philosophy (Ph.D.)** to the **Department of Applied Chemistry and Chemical Engineering, Faculty of Engineering and Technology, University of Dhaka, Bangladesh,** is a record of authentic research works carried out by him under our joint supervisions and steerage.

We considered that the thesis has reached the standards and fulfilling the requirements of the rules and regulations relating to the nature of the degree. The contents embodied in the thesis have not been submitted for the award of any other degree or diploma in this or any other university.

Supervisors:

1. …….

   Dr. Md. Nurnabi
   Professor
   Department of Applied Chemistry and Chemical Engineering
   University of Dhaka
   Dhaka 1000, Bangladesh

2. …….

   Dr. Shamim Ahmed Deowan
   Associate Professor
   Department of Robotics and Mechatronics Engineering
   University of Dhaka
   Dhaka 1000, Bangladesh

Dedicated

To

My parents and All Teachers

ACKNOWLEDGEMENTS

The author extends heartfelt gratitude to the most merciful and Almighty Allah for His blessings and guidance throughout the journey of this research.

The author would also like to express sincere appreciation to Professor Dr. Md. Nurnabi, Chairman, Department of Applied Chemistry and Chemical Engineering, University of Dhaka, and Associate Professor Dr. Shamim Ahmed Deowan, Department of Robotics and Mechatronics Engineering, University of Dhaka, Bangladesh. The unwavering support, encouragement, valuable advice, constructive criticism, motivation, and profound scientific insight provided by Prof. Dr. Md. Nurnabi and Assoc. Prof. Dr. Shamim Ahmed Deowan have been instrumental in shaping the author's growth as a researcher. Their wisdom has not only inspired but also significantly enriched the entire research process.

The author like to thank Professor Dr. Md. Zahangir Alam, Vice Chancellor of Atish Dipankar University of Science and Technology (ADUST), his invaluable support and guidance.

The author expresses his kindhearted gratefulness to Professor Dr. Mohammad Ismail, Dr. Md. Nuruzzaman Khan, Associate Professor, and Sadit Bihongo Malitha, Lecturer, Department of Applied Chemistry and Chemical Engineering, University of Dhaka for their valued advice and kind cooperation.

The author desires to reveal his profound gratitude to Dr. Md. Abu Sayid Mia, Postdoctoral Fellow, Centre for Advanced Research in Sciences (CARS), University of Dhaka, for his invaluable support.

The author is grateful to Mr. Shimul Chakma and Mrs. Kanish Fatema, Senior Scientific officer, Leather Research institute, Bangladesh Council of Scientific and Industrial Research (BCSIR), for their support.

The author expresses his special appreciation and thanks to Bappa Kar, Esrafil Hossain, Shakil Shahriar Efty, and Md. Ahsanul Haque Milon, MSc students for their invaluable help, suggestions, and encouragement throughout the research work.

The author is grateful to acknowledge the support extended by the Bangladesh Council of Scientific and Industrial Research (BCSIR) for facilitating the pursuit of this degree.

The financial support from the Prime Minister's Education Assistance Trust (PMEAT), Bangladesh to carry out the research is highly acknowledged.

The author wishes to thank all the teachers of the Department of Applied Chemistry and Chemical Engineering, the University of Dhaka for their cordial support. The author is also grateful to all the staff at the Department of Applied Chemistry and Chemical Engineering, the University of Dhaka for their amiable technical support and other facilities.

Last but not least, the author is grateful to his family members for their cooperation and supports him throughout his life.

(Md. Nur-E-Alam)
nalam1980@yahoo.com

ABSTRACT

Industries across various sectors are exacerbating water pollution through the direct discharge of untreated wastewater into natural ecosystems. Traditional wastewater treatment approaches often prove inadequate in mitigating pollutants. However, membrane bioreactors (MBRs) emerge as a promising remedy with membranes constituting the fundamental element of the system. MBRs are the favored choice for treating high-strength wastewater as all the bacteria are retained within the reactor which can degrade the toxic and bio-degradable matters present in the wastewater. Globally, MBR systems with different setups have been seen widespread utilization for treating various wastewater across lab and pilot scales. However, implementation of MBR technology for wastewater treatment in Bangladesh is relatively new, and research conducted at both laboratory and industrial scales remains limited.

This research investigates the fabrication and effectiveness of blended membranes using polyethersulfone (PES) and commercially available polysulfone (PSF) as matrix for wastewater treatment in a submerged MBR. In the first phase, commercially available PSF polymer was mixed with polyethylene glycol (PEG) and sodium alginate (SA) to fabricate PSF-PEG and PSF-SA blended membranes applying the non-solvent induced phase separation (NIPS) method, where PSF-PEG membranes exhibited higher performance in terms of porosity (9.25%) and flux (308 L/m^2h) compared to PSF-control and PSF-SA membranes. For synthetic textile wastewater treatment using MBR, both PSF-PEG and PSF-SA membranes achieved 87-89% removal of COD and about 90% removal of BOD_5 while PES-commercial membrane demonstrated 90% COD and 92% BOD_5 removal. However, color removal efficiency of fabricated membranes was lower compared to a PES-based commercial membrane. In the second phase, PES polymer was blended with PEG and polyvinylpyrrolidone (PVP) to fabricate PES-PEG and PES-PVP membranes. The PES-PEG blended membrane, incorporating 3 wt.% PEG, exhibited the highest porosity of 28.64% and a flux of 1328 L/m^2h, outperforming the PES-control membrane with a porosity of 2.73% and a flux of 226 L/m^2h. Conversely, the PES-PVP blended membrane, optimized with 5 wt.% PVP, showed porosity of 15.04% and a flux of 660 L/m^2h. During MBR operation of synthetic textile treatment, PES-PEG and PES-PVP membranes showed high efficiency in removing BOD_5 (93-94%), COD (95-96%), and color (93-94%) compared to the PES-based commercial membrane. Despite differences in permeate flux, all fabricated membranes demonstrated significant efficacy in microorganism removal akin to the PES-based

commercial membrane. In the third phase, a real industrial wastewater collected from a CETP was subjected to treatment using both fabricated (PES-3PEG) and commercial membranes using MBR. The results demonstrated exceptional efficiency in eliminating organic matter removal across both membranes, achieving about 93% removal for COD and 88-89% for BOD_5 after 28 days of continuous operation.

TABLE OF CONTENTS

LIST OF FIGURES

LIST OF TABLES

LIST OF ABBREVIATIONS

CM	Commercial membrane
MBR	Membrane bioreactor
MF	Microfiltration
NF	Nanofiltration
PEG	Polyethylene glycol
PES	Polyethersulfone
PSF	Polysulfone
PVP	Polyvinylpyrrolidone
RO	Reverse osmosis
SA	Sodium alginate
TFC	Thin film composite
UF	Ultrafiltration

CHAPTER 1: INTRODUCTION

1.1 Background of study

Membrane bioreactor (MBR) is considered as an energy efficient and low footprint wastewater treatment process in many industries in recent years. It is the combination of conventional biological process and membrane filtration. Due to its complete solid removal capacity, substantial disinfection capability, high efficiency of organic substance elimination and small footprint, it is a fascinating alternative over the conventional wastewater treatments particularly biological treatment plants (Lubello, CCaffaz et al., 2007). Reverse osmosis (RO), microfiltration (MF), ultrafiltration (UF), nanofiltration (NF), and electrodialysis (ED) are the membrane separation processes which are most frequently utilized (Tamime, 2013). Generally, MF and UF membranes are used in MBR plants, and this technology is new for Bangladesh. Since there is no operation of MBR technology, there is a room for development and implementation of this technology in Bangladesh and everything for this research work needs to be started from scratch. Different design aspects such as reactor size, amount of volume to be treated, suitable membrane polymer, support materials, necessary accessories like micrometer, pumps, sensors etc., have been considered and a design methodology has been adapted for this work.

The industrial sector of Bangladesh has the significant contribution to the country's economic growth. Among them, leather, textile, tea, jute, and pharmaceutical industries are major contributors in terms of foreign exchange and engendering employment, where textile and textile-related goods contribute to over 78% of the total export earnings (Roy et al., 2018). But this industry is a water intensive industry and producing wastewater encompassing varying concentrations of both organic and inorganic pollutants. It has been estimated that about 2 million m^3 effluents are discharged every day from textile sector in Bangladesh (Dey et al., 2015). The average water consumption is of about 160 L/kg of finished product and the textile production is responsible for an estimated 17 to 20% of industrial water contamination, according to the World Bank (Kant, 2012). Textile wastewater comprises different effluent coming from different manufacturing operations (Roy et al., 2018). The common characteristics of textile effluent are high dissolved organic and inorganic content, high chemical oxygen demand (COD) and biological oxygen demand (BOD), excessive suspended solids, high pH and temperature, strong color, too high fats, oils, fibers, nitrogen, phosphorus, and often heavy metals concentrations (Hassan et al., 2014)(De Jager et al., 2012)(Carliell et al., 1994). On the other hand, the

leather sector, another offender for polluting the environment, is well established, and ranked fourth in terms of earning foreign exchange. The processing of finished leather requires approximately 40 to 45 liters of water per kg of raw hide or skin (Sundar et al., 2001). Such a huge volume of water used in tanning poses various problems, notably contributing to issues such as increased pollution in water and soil. Tannery effluents are also characterized by high COD, high BOD_5, high concentrations of suspended solids, chromium, and sulfide contents.

The release of such hazardous effluents without proper and sufficient treatment to the environment causes degradation of water bodies, soil, and ecosystems. For this, many nations have now implemented stricter discharge standards for industrial wastewater. In the present era, the treatment of industrial effluent faces major problems because of the existence of recalcitrant organic and inorganic chemical substances. So, the removal of these molecules is still challenging issue, however, this toxic effluent can be treated effectively and efficiently by membrane biological (MBR) process rather than the conventional treatment processes (Pandy, 2015).

In this research work, we fabricated flat sheet membranes employing polysulfone (PSF) and polyethersulfone (PES) as base polymers with sodium alginate (SA), polyethylene glycol (PEG), and polyvinylpyrrolidone (PVP) as additives. These fabricated membranes along with a PES based commercial one were used in submerged bioreactor which removed almost all colloidal particles, color, and macromolecules larger than the membrane pore size from water. This MBR technology development for industrial effluent treatment is quite new in Bangladesh, representing a unique research endeavor in the country.

1.2 Problem statement

The escalating industrial activities in Bangladesh, particularly in textile, tanning, and other manufacturing, have led to a significant surge in wastewater generation. Unfortunately, the inadequate treatment of this wastewater, in violation of environmental regulations, has resulted in adverse environmental effects. Membrane Bioreactors (MBRs) have emerged as a promising technology for wastewater treatment, combining activated sludge and filtration processes to enhance solids and organic removal. MBR excel in suspended growth systems, offering advantages such as a smaller footprint, minimal sludge production, ease of operation, no chemical addition, etc. Despite the global increase in studies on MBRs over the past two decades to meet strict discharge standards and address the growing demand for wastewater reuse, the

application of MBRs in the industrial sector of Bangladesh remains rare. Limited research has been conducted on MBR technology specially in the context of Bangladesh (Uddin et al., 2022). Consequently, there is a pressing need for a thorough investigation on the fabrication of membrane and assessment of their effectiveness in MBRs. This would aim to address the wastewater management challenges emanating from the rapid growth of industries in the country.

1.3 Objectives of the study

The study aims to achieve the following primary goals:

1. To fabricate low cost PSF and PES membrane using PEG, SA, and PVP as additives
2. To design and fabricate flat sheet membrane module using locally available materials
3. To design and fabricate lab scale MBR system for wastewater treatment
4. To characterize the wastewater (synthetic textile wastewater and effluent from a CETP)
5. To study the removal efficiency of COD, BOD_5, and color from the wastewater and compare the results with a PES based commercial membrane using MBR
6. To compare water quality parameters from MBR with the water standard (DoE, 1997) of Bangladesh.

1.4 Membrane separation processes

Membrane separation processes have been established as a very effective and efficient attractive option for separation and purification methods in various industrial treatments. These are now precise alternative over the conventional techniques due to its no chemical addition, low energy consumption, low sludge production, and relatively low footprint.

1.5 Definition of membrane

The name membrane coins after the Latin word '*membrana*' that refers to a skin. Membrane passes materials selectively which is acts as a blockade that separates two phases and impedes transport of different species in a selective way (Nath, 2008).

Membrane is a semi-permeable barrier that lets some molecules cross them while rejecting others. It selectively separates the feed stream into two distinct phases: one is stated as permeate (filtrate) which passes across the membrane and other is retentate (concentrate) which is retained by the membrane (Tamime, 2013). A conventional filter can be regarded as membrane, though

the name “filter” that is typically restricted to structures which remove particulate substances larger than 1–10 μm in size (Wang et al., 2011).

An alternative description for a membrane is that it serves as an interphase between two neighboring phases, functioning as a selective barrier that controls the movement of substances between the two compartments (Ulbricht, 2006).

1.5.1 Historical development of membrane

The capability of membranes to separate water from solutes dated back to 1748, when the French physicist Abb´e Nolet (Jean-Antoine Nollet) was the first to observe the connection involving a semipermeable membrane with osmotic pressure. He experienced that the bladder of pigs transports ethanol favorably when taken in contact with a water- ethanol mixture on one side and pure water on the other side. The attribution of the term ‘Osmosis’ to describe the process credited either Abb´e Nolet or Dutorchet. In the 18th and 19th centuries, membranes were completely employed for laboratory purposes and typically crafted from materials such as animal intestines’ sausage casings or the bladder of pigs, cattle, or fish (Tamime, 2013).

Membranes gained significant importance in Germany and other parts of Europe during the aftermath of World War II when supply of potable water has been compromised due to air raids. Hence, there was an extreme need of an efficient alternative to test the water safely with convenient and short time (Baker, 2012).

The significant development in membrane technologies began in 1960 which was regarded as the golden age of membrane technology. A breakthrough came in 1960s when two UCLA (University of California, Los Angeles) engineering graduate students, Srinivasa Sourirajan and Sidney Loeb, made the high flux, defect free first asymmetric skinned cellulose acetate reverse osmosis (RO) membrane which had ten times greater fluxes than any membrane available then. The modern development was begun in the mid-1990s for making reliable and cost-effective (MF and UF) processes for the purification of municipal wastewater as well as treatment of sewage wastewater by membrane bioreactors (MBRs). Membrane pore and pore size distribution, operating parameters, selectivity, membrane lifespan, capital, and operational costs, etc., dictate the membrane-based applications which in turn are manipulated by many factors such as membrane materials, element configuration, and system design (Baker, 2012) (Baker et al., 1990) (Tamime, 2013). Table 1.1 shows the historical development of different membrane processes.

Table 1.1: Historical evolution of membrane technology (pre-1980s) (Fane et al., 2011)

Year	Development	Scientists
1748	Osmosis, the passage of water through pig bladders	Abbe´ Nollet
1833	The principle of gases diffusion	Thomas Graham
1855	The empirical principles of diffusion	Adolf Fick
1860–1880s	Semi-permeable membranes and the concept of osmotic pressure	M. Traube (1867), W. Pfeffer (1877), J.W. Gibbs (1878), J.H. van't Hoff (1887)
1907–1920	Membranes with micropores	R. Zsigmondy
1920s	A reverse osmosis prototype	L. Michaelis (1926), E. Manegod (1929), J.W. McBain (1931)
1930s	Modern membrane electrodes used in electrodialysis (ED)	T. Teorell (1935), K.H. Meyer and J.F. Sievers (1936)
1950s	ED, MF, hemodialysis, and ion-exchange membranes	Many
1963	Anisotropic reverse osmosis membranes with defect-free and high-flux,	S. Loeb and S. Sourirajan
1968	Fundamental principles of pervaporation Spiral-wound RO module	P. Aptel, and J. Neel J. Westmorland
1977	Thin film composite (TFC) membrane	J. Cadotte
1970–1980	Reverse osmosis, UF, MF, ED	Many
1980s	Gas separation processes utilizing industrial membrane	J.M.S. Henis and M.K. Tripodi (1980)
1989	Submerged MBR	K. Yamamoto

1.5.2 Types of membranes

Membranes come in diverse forms, including homogenous (symmetric) or heterogeneous (asymmetric) in structures, both solid and liquid compositions, such as positive charges, negative charges, neutrality, or bipolar attributes. Transport through these membranes can take place through convection, the diffusion of individual species, or can be persuaded by factors like an electric field, pressure, concentration, or temperature gradients. Membranes can be classified according to the following viewpoints (Nath, 2008) (Baker, 2012) (Jiang, 2016):

a) Based on sources

i. Natural membrane: These are obtained from natural sources, example, cellulose.
ii. Synthetic membrane: These membranes are man-made which do not directly obtain from the nature, example, polysulfone (PSF), polyethersulfone (PES), polyamide, etc.

b) Based on morphology or structure

Based on morphology or structure, membranes are categorized as solid membrane and liquid membrane.

1. Solid membranes

Solid membranes are subdivided as follows:

i) Isotropic (symmetric) membrane, ii) Asymmetric (skinned), and iii) Inorganic membrane

i) Isotropic membrane

These membranes have an identical composition in their structure, which can be either porous or dense. The total thickness of these membranes determines the mass transfer through them while a decline in thickness causes an improved filtration rate.

a) Microporous membrane: This membrane closely resembles a traditional filter both in structure and function. A microporous membrane (Fig 1.1) possesses a highly rigid and voided structure with pores that are casually distributed and interconnected. But microporous membrane differs from the conventional filter by its exceptional pore size on the range of diameter from 0.01-10 μm. Species or molecules bigger than the largest pores of the membrane are fully excluded while that are smaller but bigger than the smallest pores are moderately eliminated, based on the sieving effect.

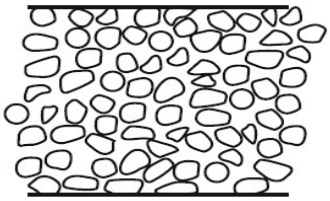

Fig 1.1: Isotropic (symmetric) microporous membrane (Baker, 2012)

b) Non-porous, dense membranes: These types of membranes (Fig 1.2) are composed of a compact film through which permeants are conveyed via diffusion, driven by factors like pressure, temperature, feed solution concentration, or electrical potential gradients. The non-porous membranes do not have visible pores and transportation occurs due to diffusion through these membranes. These types of membranes are generally employed for RO, gas separation, and pervaporation that have anisotropic properties to enhance flux.

Fig 1.2: Isotropic (symmetric) dense membrane (Baker, 2012)

c) Electrically charged/ion exchange membranes: These membranes (Fig 1.3) contain extremely swollen gels with permanently attached positive or negative charges and may exhibit either a dense or microporous structure. A membrane which is fixed with positively charged ions is regarded as anion-exchange membrane (AEM) since it attracts and transports the negatively charged anions from the solution while repelling the positively charged cations. The reverse situation is applicable for the cation exchange membrane (CEM). Charge exclusion is the main separation mechanism of these membranes and are used preferentially for electrodialysis.

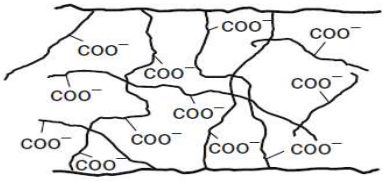

Fig 1.3: Isotropic (symmetric) charged membrane (Baker, 2012)

ii) Asymmetric (skinned)

Asymmetric membranes are characterized by their anisotropic nature, featuring two primary layers with varying properties, including differences in morphology and permeability.

a) Integrally skinned asymmetric membrane: This membrane (Fig 1.4.a) was invented by Loeb and Sourirajan in 1963 for RO which constituted of two or more structural planes of non-identical morphologies. These are characterized by a thin (0.1 to 1.0 um) skin upon the membrane surface. The layers beneath the skin may consist of voids which serve to support the skin layer.

b) Thin film composite (TFC) membrane: TFC membranes (Fig 1.4.b) typically consist of multiple materials layered together to create a unified membrane. The porous backing material serves as a structural support, while the skin layer primarily serves selective functions. These are primarily developed for RO and NF applications.

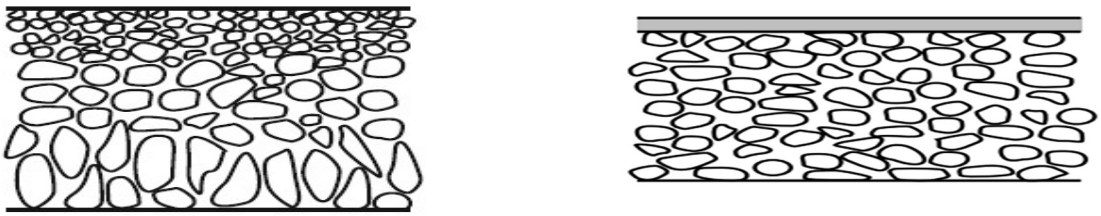

(a) Integrally skinned membrane (b) Thin film composite (TFC) membrane

Fig 1.4: Thin film composite membrane (Baker, 2012)

iii) Inorganic membrane

Inorganic membranes (or ceramic membrane) denote membranes made of materials include zeolite, carbon, ceramic, silica, and metals like silver, palladium, and their alloys. Metal membranes are durable at temperatures ranging from 500 - 800°C, however, lots of ceramic membranes are operational above 1000°C and very much resistant to various chemical attacks. Fig 1.5 shows examples of the inorganic membranes.

Fig 1.5: Inorganic membranes (Kalayni, 2020)

Inorganic membranes are categorized fundamentally into two main groups depend on their structure. One is microporous and the other is dense (non-porous) membranes.

Table 1.2 provides the comparison between inorganic and polymeric membranes.

Table 1.2: Comparison between inorganic and polymeric membranes (Daramola et al., 2012)

Criteria	Inorganic membrane	Polymeric membrane
Swelling	Unswell	Swell
Uniformity	Likelihood of uniform, molecular sized pores	Lack of uniform, molecular sized pores
Chemical stability	Resistant to chemical exposure from solvents and low pH levels	Unstable and denatured at low pH
Thermal stability	Stable	Unstable and denatured at elevated temperature
Production cost	High	Low
Brittleness	More brittle	Less brittle

2. Liquid membranes (LMs)

Liquid membranes are composed of liquid typically in the shape of a thin oil layer. It can be found both in a supported and unsupported state and functions as an obstacle between two phases, such as liquid solutions or combination of gases ('Introduction to Membrane').

i. Supported liquid membrane (SLM): SLM membranes possess a microporous framework saturated with the liquid membrane phase. This microporous framework offers structural integrity, while the liquid-filled microporous serve as a selective filtration barrier (Purkait, Sinha, et al., 2018).

ii. Unsupported liquid membrane: These membranes consist of thin liquid films stabilized within an emulsion-type mixture by a surfactant. Fig 1.6 shows the various LMs.

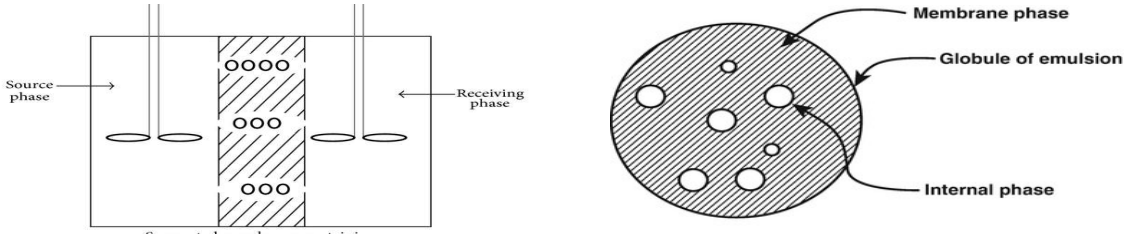

a. Supported liquid membrane b. Emulsion liquid membrane

Fig 1.6: Diagrams of liquid membranes a) supported liquid membrane (SLM) (Parhi, 2013) **b) emulsion liquid membrane (ELM)** (Mondal et al., 2018)

c) Based on structure of the membrane

i) Porous membranes: These are generally applied for MF and UF. The pore size of microfiltration membrane ranging from 0.1-10 μm, while for ultrafiltration membrane it is ranging from 0.001-0.1μm.

ii) Nonporous membrane: These are primarily employed for reverse osmosis, nanofiltration, or molecular separation in various gas phases. A nonporous membrane consists of a dense film across which permeates diffuse due to concentration, pressure, or electrical potential gradient.

d) Based on membrane geometry

According to this classification, membrane can be:

i. Flat sheet (FS) membrane: These membranes (Fig 1.7 a) have planar configuration and are generally rectangular, while other geometries exist for membrane modules.

ii. Hollow fiber/ capillary membrane: These are a class of synthetic membranes comprising a semi-permeable obstacle in the shape of a hollow fiber (Fig 2.7b). Because of its small strand diameter, these membranes feature a very high packing density.

iii. Tubular membrane: These are not self-supported and located within a specially designated tube made of a unique material. The tubular membrane (Fig 1.7c) has a diameter of about 5 to 15 mm. The distinction between hollow fiber and tubular membrane is based on their diameters. Hollow fibers have much smaller diameters (0.1–1 mm diameter) than that of tubular membranes.

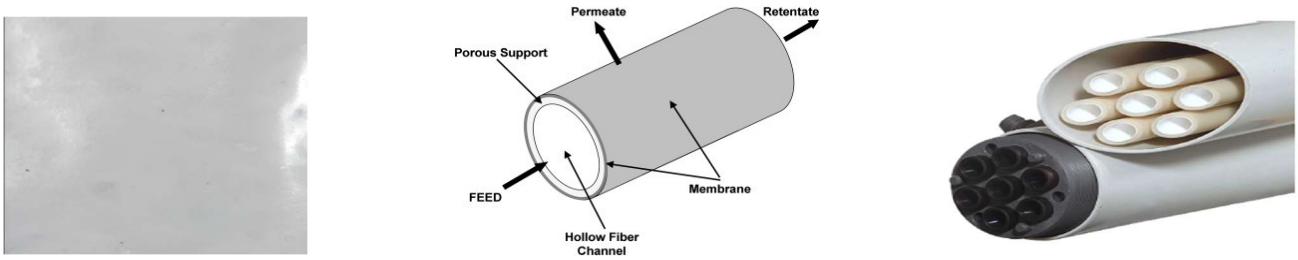

(a) Flat sheet membrane (Authors) (b) Hollow fiber membrane (McKeen, 2012) (c) Tubular membrane (PCI membranes)

Fig 1.7: Membranes based on geometry

e) Based on mechanism of action

Based on these criteria, membranes are grouped as adsorptive or diffusive, ion-exchange, osmotic or non-selective (inert) membranes.

The overall general membrane classification is illustrated in the following Fig 1.8.

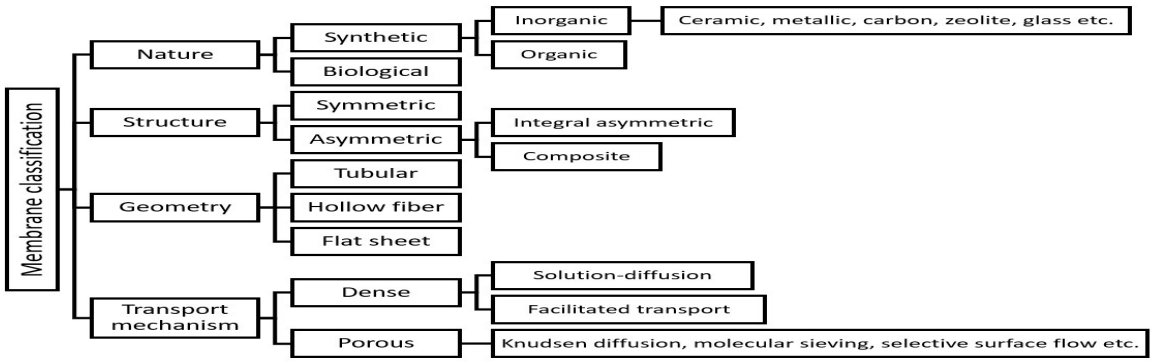

Fig 1.8: General membrane classification (Dai et al., 2016)

1.6 Mechanisms of membrane separation process

Transport within membranes can be broadly categorized into two types of diffusion. The first type involves diffusion through a dense membrane, such as NF and RO membranes, following Fick's law. The second type of diffusion occurs in porous membranes like MF and UF membranes, where the porous structure and channel characteristics play a crucial role.

1.6.1 Solution diffusion (S-D) theory through dense membranes

The prevalent mechanism for mass transport through non-porous membranes is the solution-diffusion process (Fig 1.9), initially postulated by Graham (Fane et al., 2011).

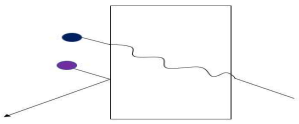

Fig 1.9: Molecular transport through membranes by S-D model (adapted from (Baker, 2012)**)**

Fick's first law is related to diffusive flux and concentration, operating under the assumption of steady state. It points out that the flux moves from areas of high concentration towards low concentration, and its magnitude is proportional to the concentration gradient. The mathematical expression for Fick's first law of diffusion is as follows (Eq. 1.1):

$$J = -D\frac{dC}{dZ} \qquad \text{(Eq. 1.1)}$$

Where J is the rate of transfer (g/cm^2.s) per unit area of the membrane, D is the diffusion coefficient (cm^2.s), C is the concentration of diffusing substances, and $\frac{dC}{dZ}$ is the concentration gradient. S-D model applies to nanofiltration, reverse osmosis, pervaporation, and gas permeation in polymer films.

1.6.2 Convective transport through a porous membrane layer

Pressure-driven convective flow serves as the foundational principle for the pore flow model (Fig 1.10), commonly employed to elucidate flow in capillary tubes. The essential mechanism underlying both MF and UF is the sieving process, selectively preventing the passage of molecules larger than the membrane's pore size.

Fig 1.10: Molecular transport through membranes by pore-flow model (adapted from (Baker, 2012))

There are two prevalent approaches to articulate permeability through porous membranes. In the first approach, when the membrane exhibits a configuration akin to near-spherical particles, the Carman–Kozeny equation is applicable, as depicted in the following equation (Eq. 1.2):

$$J = \frac{\varepsilon^3}{k.\mu.S^2\ (1-\varepsilon)^2\ l_{pore}} \qquad \text{(Eq. 1.2)}$$

Where J is the permeate flux, ε is surface porosity, μ is the dynamic viscosity of the permeate, K is a constant, l_{pore} is the thickness of the porous layer, ΔP is the pressure drop, and S is the specific area per unit volume.

Both K and S are influenced by the inherent characteristics of the membrane's porous structure. The permeability constant, K, is determined by factors like the membrane's pore size distribution, porosity, and the viscosity of the permeate.

In the second approach, where the laminar fluid flow occurs through the capillaries, the well-known Hagen-Poiseuille equation is employed for calculating the permeate flux, as described by equation (Eq. 1.3):

$$J = \left(\frac{\varepsilon r^2}{8\eta\ \tau\ \Delta X}\right)\Delta P \qquad \text{(Eq.1.3)}$$

Where ε is the number of pores or porosity; r is the average pore radius; η is the viscosity of the solvent or solution; τ is the tortuosity of the pores; ΔX is the thickness of the membrane, and ΔP is the pressure drop (transmembrane pressure). The term $\frac{\varepsilon r^2}{8\eta\ \tau\ \Delta X}$ is correlated with the permeability of the membrane (L_p) to solvent or solution, thus Eq.1.3 may be represented in Eq. 1.4:

$$J = L_p\ \Delta P \qquad \text{(Eq. 1.4)}$$

Furthermore, when dealing with a porous medium, the fundamental equation for describing the rate of fluid flow is Darcy's law and it states that volumetric flux or filtration rate is directly proportional to the pressure (ΔP) drop, as showed in equation (Eq.1.5):

$$J = A\ \Delta P \qquad \text{(Eq. 1.5)}$$

Where A is the permeability constant which depends upon pore size, pore shapes, pore distribution, viscosity, etc., ΔP is the pressure drop.

1.7 Membrane flow configurations

Basically, there are four different flow patterns for membrane separation processes.

a) Complete mixing

Both the feed side and the filtrate side of the membrane are well mixed shown in Fig 1.11 a. Like continuous-stirred tank reactor, the retentate or residue and the product or permeate compositions are equal to their respective uniform composition in the chamber.

b) Cocurrent flow

Here the fluid on the feed or concentrated side moves along and parallel to the upstream membrane surface. The filtrate fluid has passed through the membrane shown in Fig 1.11b.

c) Cross flow

Here the incoming stream of feed flows in parallel with the surface of the membrane and only a segment of the incoming stream of feed crosses the membranes due to the applied pressure gradient shown in Fig 1.11c. When the feed flow is directed tangentially across the surface of the membrane, it can lead to significantly increased flux rates because this flow continuously sweeps away retained materials.

d) Countercurrent flow

Both the feed stream and the filtrate stream are in plug flow countercurrent to each other shown in Fig 1.11 d. The composition of each stream varies along its flow path.

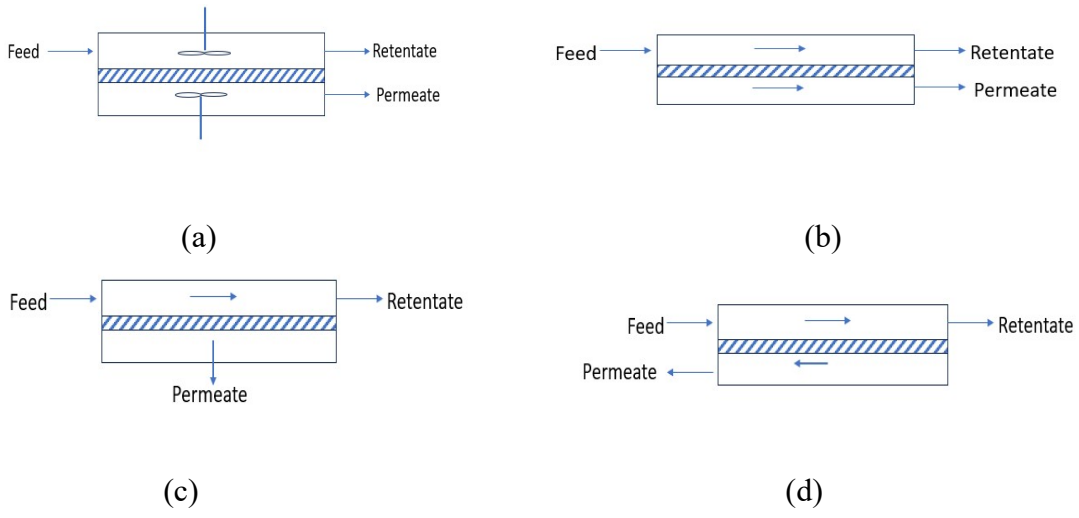

Fig 1.11: Basic flow patterns in membrane separation (Nath, 2008) **: a) complete mixing; b) cocurrent flow; c) cross flow; and d) countercurrent flow**

1.8 Modes of operation

Membrane separations are operated fundamentally in two forms: one is dead-end, and another is cross flow (illustrated in Fig 1.12).

a. Dead-end form

Dead-end mode of filtration is the most basic separation where the feed is pushed through the filter medium. The whole feed flow is pushed perpendicularly across the membrane and then the filtered substance is gathered on the membrane surface. It is a batch process, and the accumulated substance decreases the filtration capacity of membrane because of clogging. This method is very efficient for concentrating compounds and is primarily used for water with solid matter lower than 0.1 % (Sarbatly, 2020). This process is also an energy efficient technique.

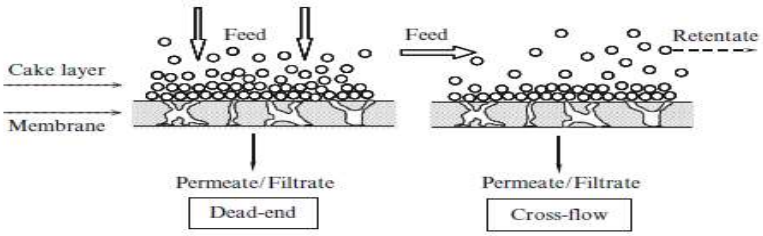

Fig 1.12: Diagram illustrating the dead-end and crossflow filtrations processes (Fane et al., 2011)

b. Cross flow form

In this process, the feed stream passages in a parallel direction with the surface of the membrane while a segment of the incoming feed can permit across the membranes due to the applied pressure. Consequently, the membrane's surface experiencing a constant turbulent flow, prevents the deposition of particles on its surface. The process is stated to as "crossflow" as the direction of feed flow and filtration flow direction are perpendicular. Generally, this mode is used for water with solid matter 0.5 % or higher (Sarbatly, 2020).

1.9 Membrane modules

Membranes are installed or mounted in a suitable device known as 'membrane module'. In other words, membrane module is the arrangement of the membrane within devices designed to separate the feed stream into filtrate stream and concentrate stream (Cui et al., 2010). There are fundamentally four main classes of membrane modules that are most commonly used:

a. **Plate-and-frame:** This module represents the most basic configuration in which two set membranes are arranged in a configuration resembling a sandwich, with their feed sides oriented toward each other (Fig 1.13).

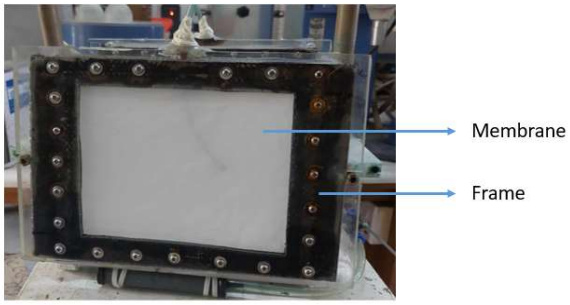

Fig 1.13: Plate and frame membrane module (Authors)

A suitable spacer is inserted into both the feed and permeate compartment.

a. **Tubular module:** Membranes are inserted usually in the inside of a tube, with the feed stream being pushed across the tube. Unlike hollow fibers, these membranes do not have inherent self-support. Generally, these are put inner side of a tube which is generally made of porous materials such as stainless steel (SS), plastic, or ceramic having diameter of more than about 10 mm and the feed stream is forced across the tube shown in Fig 1.14.

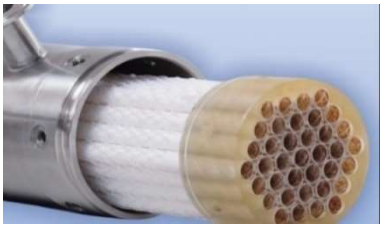

Fig 1.14: Tubular membrane module (PCI membranes)

b. **Hollow fiber module:** These membrane modules are fabricated of collections of hollow fibers contained within a pressure vessel. They can have a shell-side feed design where the feed permits along the outside of the fibers and exits from their ends and the opposite also available. The structure of the fiber walls resembles that of an asymmetric membrane, with the active skin layer positioned on to the side facing the feed stream and is illustrated in Fig 1.15.

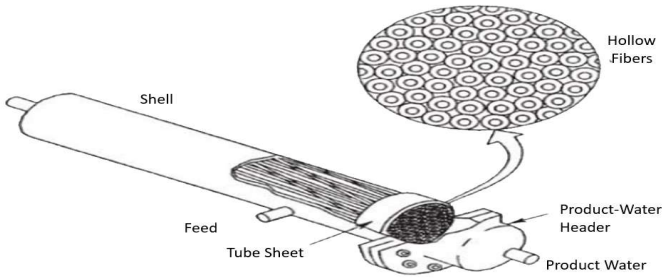

Fig 1.15: Diagram of hollow fiber membrane module (Sharaai et al., 2009)

c. **Spiral wound module:** For dense membranes like nanofiltration and reverse osmosis, spiral wound modules (shown in Fig. 1.16) are the most preferred choice which composed of flat sheet membranes that are tightly wound around a punched or perforated permeate collection tube. A permeate spacer is inserted between the two membranes. These membranes are mostly assembled with flat sheet membranes made from either a cellulose diacetate (CA) or triacetate (CA) blend or a thin film composite (TFC).

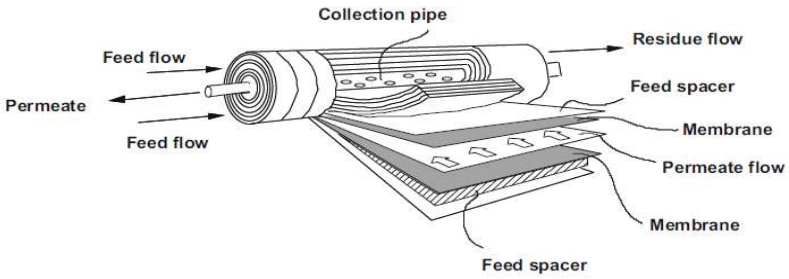

Fig 1.16: Spiral wound membrane module (Balster, 2013)

These modules are employed in situation where the pressure drop must be taken into consideration, while the counter current flow is not required for increasing the separation performance.

1.10 Classification of membrane processes

The membrane filtration systems can be grouped according to equilibrium-based membrane processes and non-equilibrium (rate governed) based membrane processes. Both of these are further divided into pressure and non-pressure driven separation methods shown in Fig 1.17 (Ezugbe et al., 2020). Pressure driven procedures comprise of microfiltration (MF), ultrafiltration (UF), nanofiltration (NF), reverse osmosis (RO), pervaporation, and gas separation. These processes depend on hydraulic pressure to achieve separation.

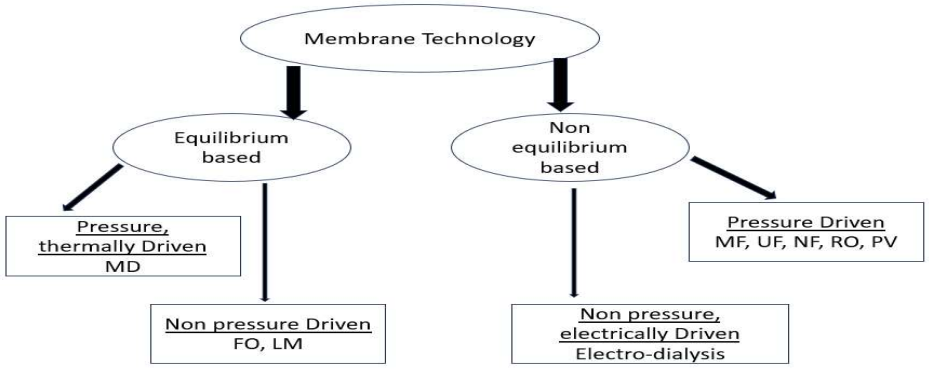

Fig 1.17: Classification of membrane separation methods (Ezugbe et al., 2020)

1.10.1 Microfiltration membrane (MF)

These types of membranes are employed for filtration of micron sized particles or biological entities with a pore size ranging from 0.1-10 micron (μm) (Sarbatly, 2020). Materials eliminated by MF involve clays, sand, silt, Giardia lamblia and Crypotosporidium cysts, algae, and some bacterial species. MF membranes do not offer a complete obstruction to viruses. The separation procedure of MF is established on a sieving effect mechanism and impurities are sorted based on their sizes while some charge or adsorptive filtration is also possible. MF has required a very low pressure (0.1-3 bars) (Sarbatly, 2020) compared with other membrane processes.

1.10.2 Ultrafiltration (UF)

It has evolved since 1960 with a primary purpose of making high-flux RO membranes (Fane et al., 2011). UF is driven by applied pressure where water as well as low molecular weight particles can pass across the membrane, but particulate, colloids and macromolecules are excluded. It possesses a pore size ranging approximately from 0.001-0.1 μm (Sarbatly, 2020) with a molecular weight cut off ranging approximately from 10 to 500 kilodaltons (Federation, 2012), and an operating pressure ranges from 3-5 bar. UF can separate all microbiological substances eliminated by microfiltration (partial elimination of bacteria), with few viruses (not a complete barrier to viruses) and humic materials. The mechanism of ultrafiltration is size exclusion though electrical charge as well as surface chemistry of the elements on membrane could affect the separation. The mode of transport through a UF membrane is mostly by convection (Gupta et al.,

2023). Fouling is a major drawback of the UF process, which is related to the hydrophobicity of membrane.

1.10.3 Nanofiltration (NF)

NF term was established by FilmTec company in the late 1980s to define a process similar to "RO" which intentionally permits some specific ionic substances in a feed stream to selectively pass through. Typically, the NF process requires hydraulic pressure within a range of 5–15 bars with the pore size ranging from 1 to 10 nm. This is also called "loose" RO and this "loose" phenomena of nanofiltration membranes can be run significantly at lower pressure compared to RO membranes. Nanofiltration membranes have a MWCO of 150 to 2,000 Daltons and it is in between RO and UF. This process can effectively remove a wide range of substances, including pigments, certain ions, sugars, salts, and small organic molecules, due to their extremely tiny pores. In addition to the size-exclusion mechanism, adsorption on the membrane surface is also significant in filtering out specific solutes. NF membranes can possess some level of charge because of adsorbing charged molecules or the dissociation of functional groups on the membrane surface (Fane et al., 2011) (Gupta et al., 2023).

1.10.4 Reverse osmosis (RO)

RO is a highly pressure driven (15-80 bar) filtration method that uses a semi-permeable thin membrane with MWCO near 100 Daltons and pores <1nm to pass pure water while refusing larger molecules such as dissolved salts (ions) and other impurities such as bacteria. Pressure gradient and chemical potential gradient are the driving forces of RO. The mode of mass transport in this type of process is solution diffusion and a preferential sorption mechanism. RO can effectively separate almost all inorganic pollutants from water and wastewater. Ionic diffusion is the main mechanism of reverse osmosis filtration instead of size exclusion. The main drawback is concentration polarization (CP) and fouling which can be decreased by appropriate maintenance, backwash and chemical cleaning.

The applicability ranges of various processes based on sizes are shown in Fig 1.18.

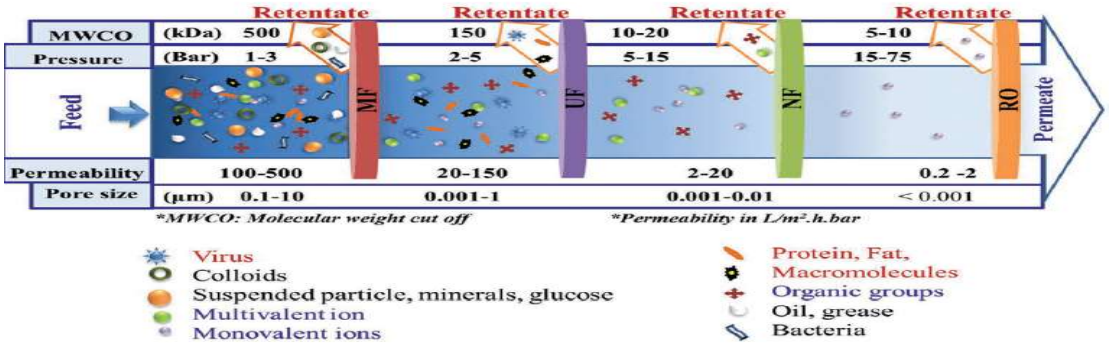

Fig 1.18: Illustration of basic characteristics of pressure-driven membranes (Gupta et al., 2023)

1.11 Membranes materials

Usually, membrane materials are categorized into three groups: i) Organic or polymeric materials, ii) inorganic (ceramic) materials, and iii) biological materials.

A brief description of some commonly used polymeric materials are given below:

i. **Polysulfone (PSF):** PSF (Fig 1.19) was first prepared by A. G. Farnham and R. N. Johnson of Union Carbide in 1965. It consists of repeating diphenylene sulphone units $[(C_6H_5)_2SO_2]_n$, creating a sturdy polymer characterized by excellent strength and resistance to compression. Additionally, diphenylene sulfone exhibits remarkable stability when exposed to elevated temperature and oxidative conditions. It is a thermoplastic amorphous polymer.

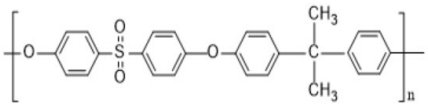

Fig 1.19: Polysulfone polymer

ii. **Polyethersulfone (PES):** It is a thermoplastic amorphous material and consists of a harder benzene structure with a softer ether bond. In 1972 Union Carbide and Imperial Chemical Industries (ICI) developed PES (Fig 1.20). It shows higher thermal and chemical stability, solvent resistance, and improved toughness compared to PSF. This is primarily used in UF, MF, and dialysis membranes (Ren et al., 2011)(Ladewig et al., 2017)

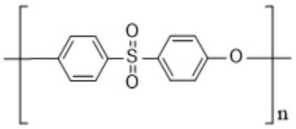

Fig 1.20: Polyethersulfone

iii. **Cellulose acetate (CA):** It is an organic material that is commonly used for membrane preparation. It is composed of cellulose units with different degrees of acetylation, and are composed of β-1,4 linked glucose units. All glucose molecule has three free OH groups that can be substituted by acetyl groups as shown in Fig 1.21. It is a hydrophilic polymer and has high salt rejection, high water permeability, good film-forming capability, and high mechanical properties (Tamime, 2013).

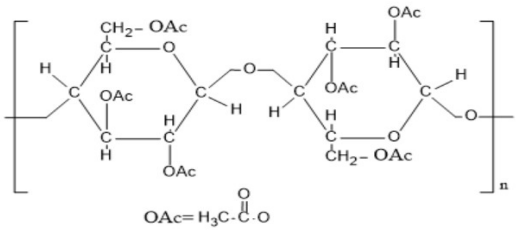

Fig 1.21: Cellulose triacetate

iv. **Polyamide (PA):** Polyamide relates to a group of polymer-forming substances that have an amide bond (CONH) in their backbone as shown in Fig 1.22. Polybenzimidazole, polyurethane, polybenzamide, polybenzhydrazide, and nylon belong to PA compounds. These membranes usually are less tolerance to chlorine than CA (Tamime, 2013).

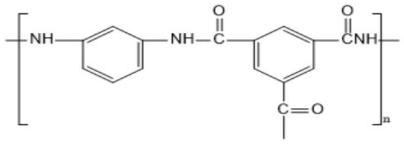

Fig 1.22: Structure of polyamide

v. **Polycarbonate (PC):** In 1953, both D. W. Fox at General Electric Company (USA) and H. Schnell at Bayer AG (Germany) separately discovered the PC with the same distinctive higher tough, heat-resistant, excellent electrical properties, transparent, and amorphous properties. The structure of the PC is shown in Fig 1.23.

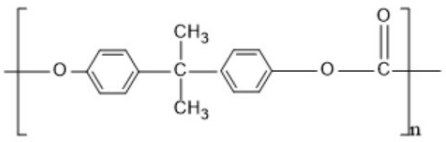

Fig 1.23: Structure of polycarbonate

vi. **Polyvinylidene fluoride (PVDF):** It (Fig 1.24) is an excellent polymeric material for MF membrane because of its chemical, thermal, and hydrophobic, semi-crystalline nature.

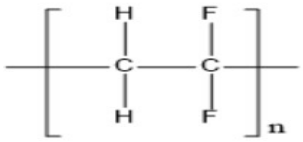

Fig 1.24: Structure of PVDF

Polymeric materials that are most usually employed in membrane fabrication are given in Table 1.3.

Table 1.3: Commonly used polymeric membrane materials (Nath, 2008) (Omnexus, 2021)(Scott, 1995) (Pinnau et al., 2000)

Materials	T_g/°C	T_m/°C	Membrane process	Commonly used solvents
Cellulose acetate (CA)	100-130	230-300	RO, MF, UF, ED, GS	NMP, Acetic acid, DMF, dichloromethane (DCM), acetone.
Polyvinyl chloride (PVC)	87	85	MF	NMP, DMAc, DMF.
Polyvinyl alcohol (PVA)	65-85	228-256	PV, MF, UF	Water, DMAc, NMP.
Polyacrylonitrile (PAN)	80-104	300	UF, MF	DMF, DMSO, DMAc, NMP, dioxanone, dimethyl phosphite, conc. Sulfuric acid, nitric acid.
Polysulfone (PSF)	190	187	GS, UF, MF	NMP, DMF, DMSO, DMAc.
Polyethersulfone (PES)	230	227-238	UF, MF	NMP, DMF, DMSO, DMAc.
Polyvinylidene fluoride (PVDF)	-40	160-185	UF, MF	DMF, DMAc, DMSO, NMP.
Polycarbonate (PC)	150-155	240	GS, UF, MF	NMP, DCM, chloroform.
Polyimide (PI)	250-340	190-205	GS, UF, RO	Chloroform, dioxane tetrahydrofuran, DMAc, DMSO, DMF, NMP.
Polyamide (PA)	60	226-266	RO, NF, UF, MF	NMP, DMF, DMSO, tetrachloroethane (TCE).

MF= microfiltration, UF= ultrafiltration, NF= nanofiltration, RO= reverse osmosis,
ED= electrodialysis, GS= gas separation, PV= pervaporation

1.12 Membrane fouling

Membrane fouling represents a stubborn and inevitable challenge in all membrane-based processes, particularly with membrane bioreactor (MBR). It results in increased operational pressure, more frequent membrane cleaning, reduced membrane lifespan, and a decline in the produced water quality (Ladewig et al., 2017).

1.12.1 Types of membrane pore blocking / models of membrane fouling

Four fouling models (Fig 1.25) are used to explain the mechanisms of membrane fouling during filtration.

1. **Cake filtration—**When the particle sizes are bigger than the pore sizes of the membrane, cake filtration occurs. For cleaning the membrane, water flushing or backwashing are usually employed.
2. **Complete pore blocking or plugging—**It is predicted that each element that reaches the membrane surface blocks the membrane pores without overlapping with other particles and thus the pore area is reduced for water flow.
3. **Standard blocking—**In this case, the pores of the membrane are narrowing because of the deposition of elements around the pore entry.
4. **Intermediate pore blocking—**In this situation, addition of foulants on membrane surface and pore happens simultaneously during membrane filtration. This is the combination of standard and complete pore blocking as the buildup of deposited particles begins to bridge the pore opening.

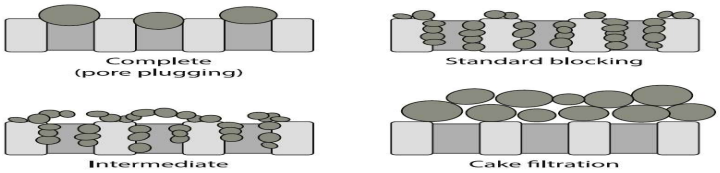

Fig 1.25: Different fouling models (Ladewig et al., 2017)

1.12.2 Mechanism of membrane fouling

A conventional flux-time curve observed in UF membrane is shown in Fig 1.26, begins with (I) an abrupt initial decline in permeates flux, (II) followed by a long period of gradual decline of flux that (III) completed with a steady-state flux.

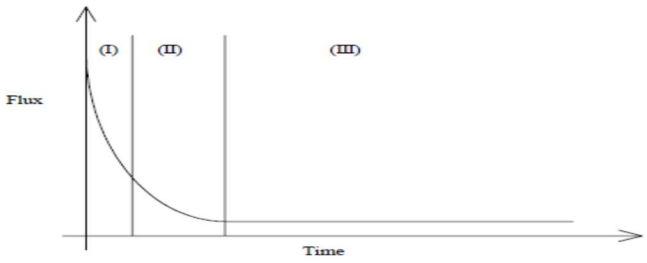

Fig 1.26: A diagram illustrating the three phases of flux reduction (Abdelrasoul et al., 2013)

Flux decrease can be attributed because of the addition in the membrane resistance due to the blockage of the membrane's pore as well as the generation of a cake layer on the membrane's surface. Pore blocking contributes to an rises in membrane resistance, while the generation of a cake layer adds an external level of resistance to the flow of permeate. Both of these phenomena can be regarded as fundamental mechanisms responsible for fouling.

The rapid initial decrease in permeate flux is primarily a result of the rapid pore blockage within the membrane. The maximum permeate flux consistently happens at the beginning of separation since, during this phase, membrane pores are in a clean and open state. Pore blockage is more likely to be partial, with the extent of blockage being contingent on the shape and relative size of both particles and pores.

After pore blockage, further flux decline occurs because of the formation and expansion of a cake layer on the membrane's surface. This layer adds extra resistance to permeate flow, and its resistance increases as the cake layer thickness grows. Therefore, the permeate flux declines over time.

1.12.3 Types of membrane fouling

Membrane fouling is typically categorized based on the chemical characteristics of foulants, the membrane fabrication method, the types of foulants and their interactions with the surface of the membrane. They are i) inorganic fouling/scaling ii) particle/colloids fouling iii) microbial fouling iv) organic fouling, and v) Reversible and irreversible fouling (Ladewig et al., 2017).

1.12.3.1 Inorganic fouling/scaling

Scaling, also recognized as inorganic or precipitation fouling, arises when crystallized salts, oxides, and hydroxides are present in the feed stream. Scaling problem is a vital issue for RO and NF membranes as these membranes reject inorganic substances that accumulate near the membrane-liquid interface- an incident known as 'concentration polarization' (CP). While microfiltration and ultrafiltration membranes are less susceptible to inorganic fouling due to CP, it can still occur, possibly because of chemical bonding between ions and other fouling agents like organic polymers (SAMCO, 2018).

1.12.3.2 Particle/colloids fouling

This type of fouling appears when suspended particles block the pores of a membrane or cling to its surface. Algae, bacteria, and certain natural organic substances fall within the range of

particles and colloids. Though, they differ from inert particles and colloids like silts and clays (SAMCO, 2018).

1.12.3.3 Microbial fouling/ biofouling

This fouling is a result of the development of biofilms on the membrane's surface and contributes more than 45 % of all membrane fouling. This is a vital obstacle in NF and RO filtration processes (Nguyen et al., 2012). When the bacteria are adhered to the membrane's surface, they initiate to multiple and produce extracellular polymeric substances (EPS) to create a viscous, slimy, and hydrated gel. This gel structure serves to shield bacterial cells from hydraulic shear forces, rendering them resistant to standard cleaning procedures such as backwashing or uses of biocides, like chlorine (SAMCO, 2018).

1.12.3.4 Organic fouling

It is identified as the collection of carbon-based substance during a membrane filtration procedure. It is an irreversible process. Natural organic matter (NOM) includes carbon-based materials found in soil and water from decomposition of plant and animal materials which are usually highly reactive. Fouling risk depends on factors like membrane material compatibility. Organic fouling can be minimized by choosing a membrane polymer with more hydrophilic which resists adsorption of organic material on its surface (Ladewig et al., 2017)(SAMCO, 2018).

1.12.3.5 Reversible and irreversible fouling

It is affected by strong attachment of materials to the membrane like pore blocking, creation of gel layer or formation of biofilm. Irreversible fouling cannot be eliminated by any methods including chemical methods.

1.12.4 Impacts of membrane fouling

There are various impacts associated with membrane fouling. First, it declines the permeate flux of the membrane, either in a permanent or temporary manner. If the fouling of membrane is temporary, it is typically possible to restore the initial flux through the cleaning procedures or by employing backpressures. On the other hand, membranes that are permanently fouled cannot be returned to their initial condition. Second, fouling can substantially diminish membrane performance, lower separation efficacy, rise maintenance and operational expenses, result in sudden rise in transmembrane pressure (TMP), shorten lifespan of membrane, and finally lead to

frequent membrane cleaning or replacement of the existing membrane. It's worth emphasizing that while a decline in flux is also linked with the concentration polarization (CP), this incident is not classified as fouling since it disappears when the separation procedure is finished (Ladewig et al., 2017).

1.12.5 Causes of membrane fouling in MBRs

Fouling occurs when foulants, such as particles, biomolecules, or colloids, interact with the membrane surface, leading to the adhesion of microorganisms and other biomolecules, which can block or reduce membrane pores and decrease separation efficiency. The interaction can cause chemical degradation of the membrane material, leading to a significant decline in permeation flux. Several factors influence membrane fouling including the type of wastewater, sludge age and loading rate, permeate flux, aeration intensity, MLSS concentration, mechanical stress, SRT, F/M ratio, and hydraulic retention time. The properties of mixed liquor, such as soluble compounds, SMP, EPS, particle size distribution, and viscosity, also affect membrane fouling (Ladewig et al., 2017).

1.12.6 Influential factors of fouling

The fundamental causes of fouling can be attributed to three key factors: membrane properties, characteristics of sludge, and operating factors which are illustrated in Fig 1.27

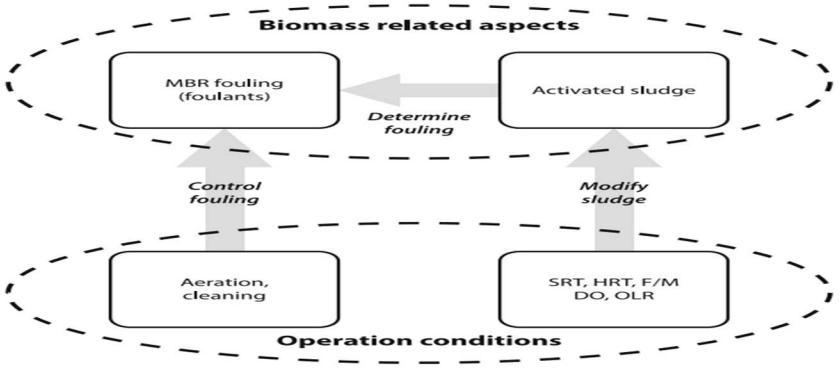

Fig 1.27: Influencing factors of membrane fouling 137 (Ladewig et al., 2017)

- Characteristics of Membrane, including pore size, pore size distribution, hydrophilicity, and membrane material, are significant factors.
- Properties of solution, such as concentration of solid particles, the size of the particle, and nature of its components play an important role.
- Operational conditions include pH, temperature, flow, rate, and pressure.

1.12.7 Fouling control

Membrane fouling can be reversible in some cases, but not in all instances. Therefore, it is advisable to protectively implement preventative measures to avoid or minimize membrane fouling initially. Several typical preventative measures to mitigate membrane fouling are given below:

1.12.7.1 Scheduled cleaning

A systematic cleaning regimen can help minimizing the deposition of foulants on the membrane. It's advisable to set up cleaning cycles on a monthly basis or according to a predetermined regular schedule. The choice of maintenance procedures can differ based on the specific design of the membrane separation system and the types of contaminants present, and may include one or more cleaning techniques, such as:

- **Mechanical cleaning** encompasses the use of physical force to dislodge foulants from the membrane and eject them from the system. Typical methods involve vibration, as well as backward or forward flushing.
- **Chemical cleaning** entails using a variety of substances like detergents, caustics, acids, antiscalants, or dispersants to effectively break down and eliminate foulants from the surface of the membrane.

1.12.7.2 Pretreatment

RO and NF membranes possess smaller pore sizes compared to microfiltration and ultrafiltration membranes, making them more liable to potential membrane fouling. When dealing with streams containing high concentration of foulants, it is often necessary to implement pretreatment steps before employing membrane filtration process to mitigate the jeopardy of membrane fouling. These pretreatment options encompasses a range of techniques, including coagulation for colloidal particles removal, gravity settling (sedimentation), flocculation, and media filtration to eliminate larger or coagulated particles.

1.12.7.3 System design

The most effective way to prevent membrane fouling is through good planning and design. A membrane separation process is influenced by numerous variables, and each of these factors

should be taken into account replacing an existing membrane or installing a new system. These involve:

i. **Membrane material:** The characteristics of the membrane material dictate the membrane resistant to specific types of fouling, as well as its ability to endure process conditions and required maintenance procedures.

ii. **Membrane pore size:** Choosing the appropriate pore size can help to prevent fouling during filtration process.

iii. **Operational conditions:** Membrane fouling can be intensified by specific ranges of temperature, pH, TMP, and flow rate. A well-designed system will harmonize these factors to guarantee that fouling does not accumulate on the membrane's surface.

1.13 Membrane fabrication

The membrane serves as the heart of membrane filtration method. The primary role of a membrane is to act as a selective barrier either to permit or retain the passage of permeating species. Different kinds of natural and synthetic materials are used for preparing membranes. Various methods are available to fabricate synthetic membranes, some of which are applicable to both organic (polymeric) and inorganic membranes. Among these methods, the widely used methods are sintering, coating, stretching, track-etching, and phase inversion.

1.13.1 Sintering

Sintering (Fig 1.28), a relatively simple method, fabricates porous membranes from various organic and inorganic materials. This process involves compressing a powder with specific-sized particles and subjecting it to high- temperature sintering. The necessary temperature varying with the material employed. At the time of sintering, the interface between the particles vanishes.

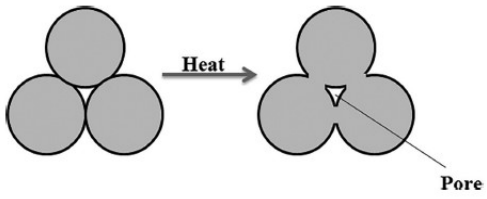

Fig 1.28: Diagram showing the sintering process (Das et al., 2019)

1.13.2 Stretching

In this technique (Fig 1.29), an extruded film or foil composed of partially crystalline polymer (such as PTFE, polypropylene, or polyethylene) is subjected to stretch in a direction

perpendicular to the extrusion, aligning the crystalline areas parallel to of the direction extrusion. This stretching imparts a mechanical stress on the thin film that results in the formation of pores with sizes in the range of 0.1 to 3.0 μm.

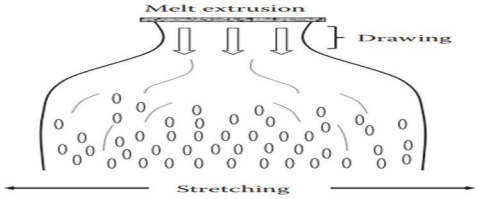

Fig 1.29: Diagram of stretching method (Purkait and Singh, 2018)

Polymeric materials of crystalline or semicrystalline nature are only suitable for the preparation of membranes by this method. Generally, microporous membranes are prepared by this method.

1.13.3 Track-etching

In this technique (Fig 1.30), a film or foil, typically made of materials like polycarbonate (PC), undergoes exposure to high-energy radiation directed perpendicular onto the film. These particles induce damage to the polymer matrix, resulting in the formation of tracks. Therefore, the film is immersed in an acid or alkaline solution, selectively etching away the polymeric material along these tracks, resulting in uniform cylindrical pores with a narrow pore size distribution. The level of porosity primarily depends on the radiation exposure duration, while the pore size depends on the duration of the etching process.

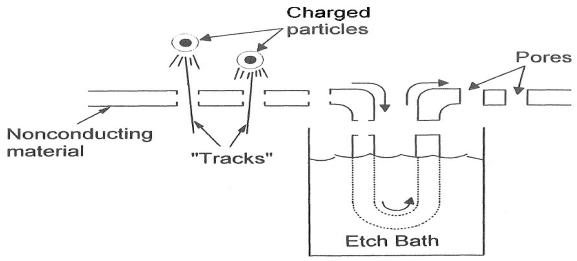

Fig 1.30: Diagram of track-etching process (Cheryan, 1998)

1.13.4 Phase inversion (PI)

Phase inversion method (Fig 1.31) is characterized as demixing process where homogeneous liquid polymer solution transformed into solid state in a controlled manner by immersing it in a coagulation or precipitation bath. This demixing process occurs as a consequence of the solvent exchange from polymer solution with non-solvent in the precipitation bath. This method is

applied for fabrication of asymmetric membrane with porous and dense skin layer. The morphology of polymeric membrane is affected by the mutual exchange of two solvents.

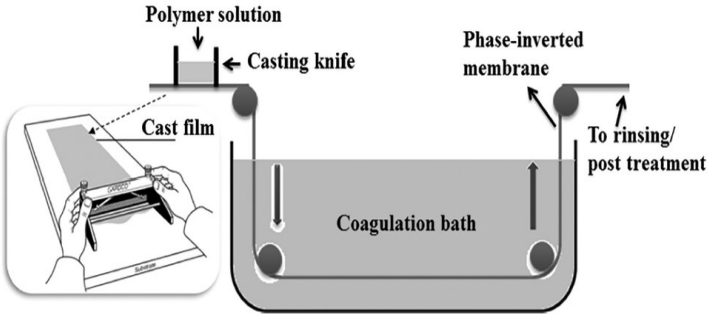

Fig 1.31: Schematic drawing of phase inversion process (Das et al., 2019)

The phase inversion process is the most adaptable membrane fabrication process.

1.13.5 Coating

This method (Fig 1.32) is generally employed to fabricate thin but dense structures that exhibit a high (intrinsic) selectivity with relatively high flux. These composite membranes are composed of two different materials, with a highly selective membrane material applied as a thin layer porous substrate. The main selectivity is governed by the thin top layer, while the porous substrate primarily function as a supporting material. A number of coating methods are employed such as dipcoating, plasma polymerisation, interfacial polymerisation, and in-situ polymerisation.

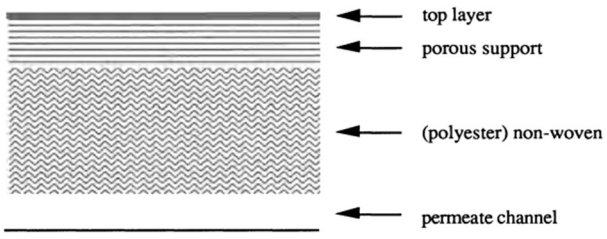

Fig 1.32: Schematic drawing of coating process (Mulder, 1996)

1.14 Brief of phase inversion (PI) process

This method is the most versatile method employed to fabricate membranes for RO, UF and NF. Loeb and Sourirajan in the 1960's first introduced this method in membrane technology which serves as the foundational basis for the preparation of most commercially available membranes. During phase inversion process, a dope solution that is initially thermodynamically stable undergoes a controlled transition from a liquid solution into a solid phase. This transformation of

solidification is preceded by a liquid–liquid demixing process. After a certain time following the initiation of this phase separation, the phase containing the highest polymer content will begin to solidify through mechanisms such as gelation, vitrification, or crystallisation. The liquid phase with a lower polymer content will subsequently form pores within the resulting solid matrix.

Phase inversion process is classified into four main techniques (a) Non solvent Induced Phase Inversion (NIPS) (b) Thermally Induced Phase Inversion (TIPS) (c) Vapor Induced Phase Inversion (VIPS) and (iv) Evaporation Induced Phase Inversion (EIPS).

1.14.1 Non solvent induced phase inversion (NIPS)

NIPS process is widely employed for fabrication of commercially available membranes due to its simplicity and low cost. In this method, a solution comprising of polymer dissolved in a solvent is applied onto a suitable support material and then submerged in a precipitation bath composed of nonsolvent. Precipitation takes place due to the interchange of solvent with the non-solvent. This method is frequently used for microfiltration (Alvi et al., 2019), ultrafiltration (Yuan et al., 2018) nanofiltration membrane, and reverse osmosis membranes (Mulder, 2000).

Dope solution preparation: The determined amount (wt.%) (e.g.,10% (Anadão et al., 2010), 12% (Urducea et al., 2020), 15%-17% (Kim et al., 2002), (Mokkapati et al., 2017), 18% (Mansourizadeh et al., 2010), 20% (Zinadini et al., 2014), 25% (Ganesh et al., 2013)) of base polymer (e.g., PSF (Ravishankar et al., 2018), polycarbonate (Idris et al., 2017), polyamide (Deng, 2013), PES (Fang et al., 2017), hydroxypropylcellulose (Guenoun et al., 2017), PAN (Kim et al., 2002), PVDF (Xu et al., 2019), PVC (Mei et al., 2011), sodium alginate (Chen et al., 2010)) is dissolved in a suitable solvent (e.g., DMF (Velu et al., 2015), NMP (Mahmoudian et al., 2018), DCM (Idris et al., 2017), DMAc (M. J. Park et al., 2015), triethyl phosphate (Yeow et al., 2004)) under stirring at fixed temperature (e.g., 60°C (Ionita et al., 2014), 45°C (Deng, 2013), 65°C (M. J. Park et al., 2015), 70°C (Aditya Kiran et al., 2016)) or room temperature (Zinadini et al., 2014) for a certain time (e.g., 4 h (Urducea et al., 2020), 8 h (Yuan et al., 2018), 12 h (Lee et al., 2013), 24 h (Ionita et al., 2014), 6 h (Deng, 2013)). For air bubbles removing from the dope solution, degassing with sonication (Zinadini et al., 2014), oven (Kahrs et al., 2020) or just left in room temperature for several hours (e.g., 1 h (Najjar et al., 2019), 3 h (Aditya Kiran et al., 2016), 12 h (Sinha et al., 2013), 48 h (Urducea et al., 2020)). Air bubbles in the solution can lead to the formation of discontinuities and implicit defects in the membrane structure. As polymer is the base material in the membrane matrix, its concentration in dope

solution will influence the membrane morphology. High polymer concentration will result in low gravimetric porosity and permeability. Furthermore, different polymer concentration shows different precipitation paths where increasing polymer concentration increases the probability of instantaneous demixing that leads to differences in membrane morphology (Tan et al., 2019).

Additives: Polymers used for membrane fabrication generally are hydrophobic in nature which enhances the membrane fouling. To avoid fouling, membrane surface is modified with some hydrophilic material (e.g., methylcellulose (Nadour et al., 2017), PVP (Deng, 2013), PEG (Kassim Shaari et al., 2017), GO (Aditya Kiran et al., 2016), Arabic gum (Najjar et al., 2019), poly acrylic acid, lithium chloride (Yeow et al., 2004), polyethylene glycol methyl ether (mPEG) (Sinha et al., 2013), ethanol (Yeow et al., 2004), glycerol (Yeow et al., 2004), TiO_2 (Hwang et al., 2016), polyethyleneoxide (Hwang et al., 2016), alumina (Hwang et al., 2016)) on the basis of base polymer (e.g., 0.1 to 1% (M. J. Park et al., 2015), 2% (Xue et al., 2014), 3% (Nasseri et al., 2018), 4% (Kahrs et al., 2020), 5% (Kahrs et al., 2020), 6% (Mokkapati et al., 2017)) into the membrane dope solution before membrane formation. A hydrophilic material in the dope solution will tend to migrate to the membrane and pore wall surfaces during phase inversion (Miller et al., 2017). These modifiers have been found to be most successful to improve membrane performances where GO has been gotten more attention because of its high surface area, strong hydrophilicity, anti- bacterial ability, and the characteristic of negative charge on the surface under whole pH range (Yuan et al., 2018).

Casting dope solution: The polymer solution is casted generally on a smooth glass plate to a pre-determined thickness (e.g., 100 µm (Deng, 2013), 150 µm (Hwang et al., 2016), 180 µm (Mokkapati et al., 2017), 200 µm (Mahmoudian et al., 2018), 250 µm (Anadão et al., 2010), 300 µm (Nadour et al., 2017), 350 µm (Fang et al., 2017), 400 µm (Aditya Kiran et al., 2016), 500 µm (Srivastava et al., 2011)) normally at room temperature with various humidity conditions (e.g., 55-65% (Yeow et al., 2004), 60-62% (Urducea et al., 2020), 84% (Yunos et al., 2012)).

Immersion/ demixing: The casted polymer solution is immerged in a coagulation bath (also called non-solvent bath) at definite temperature (e.g., 10°C (Aditya Kiran et al., 2016), 15°C (Zinadini et al., 2014), 25°C (Mahmoudian et al., 2018), 30°C (M. J. Park et al., 2015)) for a certain period of time (e.g., 10 min (Ravishankar et al., 2018), 1 h (Mahmoudian et al., 2018), 12 h (Srivastava et al., 2011), 24 h (Fang et al., 2017)). Before immersion polymer solution is

sometime allowed to evaporate for few seconds (e.g., 10 sec (Yeow et al., 2004), 15 sec (Zheng et al., 2018), 20 sec (Yuan et al., 2018), 30 sec (Kassim Shaari et al., 2017), 120 sec (Maximous et al., 2009)). In some cases, coagulation baths are composed of solvent and non-solvent composition (Najjar et al., 2019) or composition of water with other materials (Madaeni et al., 2009). Even additive such as GO can be used in coagulation bath (Mokkapati et al., 2017). Membrane sheets finally dried at room temperature (Sinha et al., 2013) or oven dried. Non-solvents that are used must be miscible to solvents. More porous membranes are prepared in case of high mutual affinity while dense membranes with asymmetric structure are obtained with low mutual affinity between the solvent and non-solvent. Generally, water is used as a non-solvent because it is environmentally friendly and low cost (Tan et al., 2019).

1.14.2 Thermally induced phase inversion (TIPS)

In this method, the polymer is kept at elevated temperature so that a single phase is formed followed by rapid cooling to split the solution into a polymer-rich phase and solvent-rich phase. This results in gelation of the polymer as well as its structure can then be set by cooling lower the freezing point of the solvent. Finally, a second solvent, known as non-solvent, can be used to leach out the solvent.

This method is also called thermal gelation. In TIPS process, desired amount (wt.%) (e.g.,15 (Cui et al., 2013), 20 (Jeon et al., 2017), 25 (Zuo et al., 2019), 30 (Cui et al., 2013), 35 (Su et al., 2007)) of polymer (e.g., PVDF (Liang et al., 2013), PAN (Wu et al., 2012), CA (Liang et al., 2013)) is dissolved in a diluent or solvent (e.g., Dimethylphthalate (Gu et al., 2006), Dimethyl sulfone (Wu et al., 2012), glycerol (Wu et al., 2012), Diethyl phthalate (DEP) (Rajabzadeh et al., 2012), Dibutyl phthalate (DBP) (Li et al., 2016)) at high temperature (e.g., 180°C (Cui et al., 2013), 160°C (Wu et al., 2012), 190°C (Rajabzadeh et al., 2012), 200°C (Matsuyama et al., 2003)), after that the dope solution is cooled to induce the phase separation. Finally, diluent is extracted or dried (Su et al., 2007). Solvents that use can act as a nonsolvent pore-former when the casting solution is cooled, and this enables membrane with high porosity. That's why, solvents or diluents used in TIPS process are called latent solvent (Juhn et al., 2010). Polymers which are not easily dissolved in solvents such as polyethylene and polypropylene are suitable for making membranes by TIPS method. This is also a preferred method of preparing crystalline polymer membranes, especially for semi-crystalline polymers. The uncontrolled pore size, pore diameter or pore width are the main disadvantages of TIPS method (Dommati et al., 2019).

TIPS differs from NIPS method in respect to phase system, NIPS is a ternary system (polymer, solvent, and non-solvent) whereas TIPS is typically binary system (polymer and solvent). Therefore, TIPS process offers higher reproducibility with few defect formation on the membrane fabrication (Kim et al., 2016). TIPS method gives several advantages over the conventional casting processes such as (Juhn et al., 2010):

- Greater flexibility
- Ease of control
- Defect free membrane formation
- Controlled pore size
- Can produce both isotropic and anisotropic membrane structures.

1.14.3 Vapor induced phase inversion (VIPS)

Zsigmondy was the first to employ this technique as early as 1918. Vapor Induced Phase Separation (VIPS) is used to prepare highly porous membranes, e.g., MF membranes. This process involves exposing cast film to an environment rich in non-solvent vapour, usually water, within a vapor chamber. Phase inversion occurs because of the inflowing of non-solvent vapors into polymeric casted film while the solvent is expelled from the film. For preparing dope solution, a specific amount (wt.%) of (e.g., 10% (Zhao et al., 2018), 12% (Nawi et al., 2020), 15% (Bikel et al., 2009), 16% (Ripoche et al., 2002), 20% (Li et al., 2010), 21% (Wang et al., 2019), 25% (Zhao et al., 2018), 26% (Wang et al., 2019), 30% (Chae Park et al., 1999)) base polymer (e.g., polyetherimide (Menut et al., 2008), PVDF (Li et al., 2010), PSF (Su et al., 2009), poly(methyl methacrylate) (Tsai et al., 2010)) is dissolved in a suitable solvent (e.g., NMP (Menut et al., 2008), DMAc (Nawi et al., 2020), DMF (Li et al., 2010)) at room temperature (Menut et al., 2008) or various dissolution temperature (T_d) (e.g., 25°C (Zhao et al., 2018), 40°C (Venault et al., 2013), 45°C (Zhao et al., 2018), 50°C (Wang et al., 2019), 60°C (Tsai et al., 2010), 65°C (Zhao et al., 2018), 80°C, 110°C, 130°C, 150°C (Li et al., 2010)) for a given time (e.g., 12h (Wang et al., 2019), 24 h (Venault et al., 2013)). The polymer concentration can affect the viscosity of the casting solution which controls the rate of non-solvent diffusion. Again, high polymer concentration increases the polymer volume friction at the interface that results the formation of a lower gravimetric porosity (Tan et al., 2019).

Then the polymer dope solution is cast on a glass plate with required thickness (e.g., 200 µm (Wang et al., 2019), 150 µm (Zhao et al., 2018), 200 µm(Nawi et al., 2021), 220 µm (Nawi et al., 2020), 250 µm (Ripoche et al., 2002), 300 µm (Su et al., 2009), 500 µm (Ye et al., 2011)) under

controlled temperature (e.g., 25°C (Tsai et al., 2010)). The solvent is dried with evaporating chamber of gas stream with certain vapor temperature (T_v) (e.g., 25°C (Su et al., 2009), 40°C (Ripoche et al., 2002)), at specific duration (e.g., 0.5 min (Zhao et al., 2018), 1 min (Zhao et al., 2018), 3 min (Tsai et al., 2010), 5 min (Zhao et al., 2018), 8 min (Lee et al., 2004), 10 min (Zhao et al., 2018), 15 min (Nawi et al., 2020), 20 min (Zhao et al., 2018), 30 min (Tsai et al., 2010), 180 min (Chae Park et al., 1999)) and relative humidity (e.g., 30% (Ripoche et al., 2002), 50% (Ripoche et al., 2002), 65% (Chae Park et al., 1999), 70% (Su et al., 2009), 80% (Ye et al., 2011), 90% (Wang et al., 2019), 95% (Venault et al., 2013)). Finally, solvent is extracted from the nascent membrane by immersing in water bath for specific a time (e.g., 24 h (Su et al., 2009)) and drying in air at room temperature (Tsai et al., 2006) or at given temperature (e.g., 22°C (Zhao et al., 2018), 70°C (Ripoche et al., 2002)). Additives such as PVP (Bikel et al., 2009), LiCl (Nawi et al., 2020), ethanol (Ye et al., 2011), PEG (Venault et al., 2013) etc., are used to modify the membrane surface.

VIPS method is used to fabricate commercial MF membranes as well as highly porous membranes. This technique differs from NIPS method, in which casted solution is directly immerged in the non-solvent or coagulation bath (Tsai et al., 2010).

1.14.4 Evaporation induced phase inversion (EIPS)

In this method, the polymer is dissolved in a suitable volatile solvent such as acetone, dioxane, pyridine, etc. and a swelling agent (e.g., magnesium per chlorate or formamide) is added. Phase inversion occurs as a result of the evaporation of solvent, due to its volatility, leads to demixing and subsequently forms a porous structure. The fast evaporation of solvent determines a dense homogenous membrane. This method also called dry casting process was pioneered by Kesting in 1973 (Pervin et al., 2019a). In EIPS process, known percentage (wt.%) (e.g., 2% (Solak et al., 2010), 3% (Kalyani et al., 2008), 8 % (Solak et al., 2011), 17% (Ahmad et al., 2018), 25% (Zhao et al., 2013)) (wt.%) of base polymer (e.g., PES (Ahmad et al., 2018), sodium alginate (Chen et al., 2010), PVP (Solak et al., 2011), silicon rubber (Zhao et al., 2013), poly(methyl methacrylate) (Pervin et al., 2019b), PSF (Plisko et al., 2019)) is dissolved in suitable solvents (e.g., NMP (Ahmad et al., 2018), DMF (Ahmad et al., 2018), DMAc (Plisko et al., 2019), demineralized water (Kalyani et al., 2008), tetrahydrofuran (Pervin et al., 2019b)) at certain temperature or room temperature (Plisko et al., 2019) for certain period of time (e.g., 24 h (Ahmad et al., 2018)).

The dope solution/casting solution is casted on a clean glass plate with a desired thickness (e.g., 180 µm (Ahmad et al., 2018), 200 µm (Zhao et al., 2013)). For removing solvent, the casted membrane solution is heated at certain temperature (e.g., 50°C (Pervin et al., 2019b), 60°C (Plisko et al., 2019), 90°C (Ahmad et al., 2018)) in oven (Kalyani et al., 2008)) for definite period of time (e.g., 5 h (Kalyani et al., 2008), 24 h (Ahmad et al., 2018)).

1.15 Impacts of various factors on membrane morphology

1.15.1 Selection of polymer

The selection of the polymer is very crucial as it plays a vital role in determining both the inherent characteristics and structural properties of the resultant film. Additionally, it also dictates the selection of suitable solvent as well as nonsolvent. PSF, PES, PVDF, PAN, CA, PI, poly etherimide (PEI), and polyamide (PA), among others, have been described as appropriate candidate for employing in the PI process (Mulder, 1996). Table 1.4 shows a partial listing of typical materials used in the fabrication of membranes.

Table 1.4: Materials used for the manufacture of membranes (Cheryan, 1998)

Material	MF	UF	RO
Alumina, Carbon-carbon composites, Polyamide, aliphatic (e.g., nylon), Cellulose esters (mixed), Cellulose nitrate, Polytetrafluoroethylene (PTFE), Polycarbonate (track-etch), Polyester (track-etch), Polypropylene (PP), PVC, PVDF, Sintered stainless steel.	✓		
Cellulose (regenerated), Ceramic composites (zirconia on alumina), PAN, PVA, PSF, PES.	✓	✓	
CA, Cellulose triacetate (CTA), Polyamide, aromatic (PA).	✓	✓	✓
Polyimide (PI)		✓	✓
CA/CTA blends, Composites (e.g., polyacrylic acid on zirconia or stainless steel), Composites-polymeric thin film (e.g., PA or polyetherurea on polysulfone), Polybenzimidazole (PBI), Polyetherimide (PEI).			✓

1.15.2 Selection of the solvent and non-solvent

While there are numerous solvents where the polymer can dissolve, it is wise to opt for a solvent that exhibits complete miscibility with the nonsolvent. The choice of solvent may also depend upon the specific PI technique employed, sometimes requiring a solvent having a higher boiling point. For cellulose acetate, solvents such as dimethylformamide (DMF), dimethylacetamide

(DMAc), acetone, dioxan, tetrahydrofuran (THF), acetic acid (HAc) and dimethylsulfoxide (DMSO) have been reported as solvents. Similarly, polysulfone has been reported to be compatible with solvents like DMAc, DMF, DMSO, N-methylpyrrolidone (NMP), formylpiperidine (FP), morpholine (MP), etc. The nonsolvent usually employed is water, although alcohols like propan-2-ol butan-1-ol methanol have been used. The selection of solvents and nonsolvents significantly influences the morphology of the membranes. Table 1.5 shows a general group of various solvent and nonsolvent pairs.

Table 1.5: Categorization of solvent and nonsolvent pairs (Mulder, 1996)

Solvent	Nonsolvent
Porous membrane	
Dimethylsulfoxide	Water
Dimethylformamide	Water
Dimethylacetamide	Water
N-methylpyrrolidone	Water
Nonporous membrane	
Dimethylacetamide	n-propanol
Dimethylacetamide	i-propanol
Dimethylacetamide	n-butanol
Trichloroethylene	Methanol/ethanol/propanol
Chloroform	Methanol/ethanol/propanol
Dichloromethane	Methanol/ethanol/propanol

1.15.3 Polymer concentration

Raising the initial polymer concentration within the dope solution leads to a raise in polymer concentration at the casting film interface. As a direct consequence, the final film experiences a reduction in porosity, accompanied by a simultaneous increase in the thickness of the dense top layer (Mulder, 1996). The gelation time (transformation time from liquid solution to solid form) also increases with increasing polymer concentration (Porter, 1990).

Porous ultrafiltration membranes usually have a concentration of 15-20 wt.%. In the context of RO and gas separation membranes, it's common to observe higher polymer casting solution concentrations, typically around 25 wt.%. In the case of making hollow fiber membranes through spinning, casting solutions with polymer concentrations as high as 35 wt.% can be employed, with the solution being heated to 60–80°C (Baker, 2012).

1.15.4 Constituents of the precipitation bath

When the precipitation bath contains solely water, demixing occurs instantly, resulting in the creation of a porous membrane structure. However, when a solvent is introduced into the precipitation bath, it leads to a decrease in the chemical potentials of both the solvent within the cast film and the non-solvent in the precipitation bath. This reduction in chemical potentials subsequently reduces the overall mass transfer rate, causing a delay in the demixing process of the dope solution. Hence, it becomes plausible to transition from porous to nonporous structures by incorporating solvent to the coagulation bath. Furthermore, the closer the bimodal curve approaches to the polymer-solvent axis on the ternary diagram, the more solvent are introduced into the coagulation bath (Mulder, 1996).

1.15.5 Composition of the casting solution

Modifiers are often added in small amounts to the dope solution to achieve the desired membrane properties. The casting solutions typically consists of two to four components, although contemporary commercial solutions exhibit greater complexity. Even with only 5 to 10 wt. % of modifiers, they can significantly alter the membrane's performance. The type of nonwoven support material used is also significant. Polyester fabric is common, but nonwoven polypropylene and polyphenylene sulfide papers are also applied. If the fabric surface is very rough, it may cause membrane pinholes, while the very smooth surface may result in insufficient adhesion with membrane's microporous layer (Baker, 2012). Again, the addition of nonsolvent to the dope solution leads to porous, skinned morphology due to the occurrence of instantaneous demixing occurs (Mulder, 1996).

1.15.6 Effect of precipitation rate on membrane structure

The rate of precipitation during the demixing process determines the various structures of the membrane. Finger-like and sponge-like structured membranes are obtained when the precipitation occurs rapidly and slowly, respectively. However, for sponge-like structure, the pore sizes are inversely proportional to rate of precipitation. Higher precipitation rate results in finer pore structures, while slower precipitation rate results in coarser structures (Porter, 1990). Table 1.6 shows the effect of precipitation rate on the membrane structure.

Table 1.6: Effect of precipitation rate on membrane structure (based on (Porter, 1990))

Precipitation rate	Membrane structure	Gelation time
High	Finger-like	Short
Slow	Asymmetric, sponge-like	Long
Very slow	Symmetric, no defined skin layer, uniform pore size distribution.	In between

1.16 Membrane modification

A membrane is an obstacle that selectively allows certain molecules to pass through but blocking others. Membranes are manufactured from a variety of materials, including organic and inorganic substances. For practical purposes, membranes should possess following qualities (Pinnau et al., 2000):

i. High flux and selectivity
ii. Chemical and mechanical strength
iii. Tolerance to feed solution and temperature variations
iv. Easy of fabrication
v. Low cost
vi. Ability to package into high surface area modules.

The development of highly efficient membranes involves choosing an appropriate membrane material and shaping it into the desired membrane structure. Consequently, it becomes essential to make modification either to the material itself or to the structure to improve the membrane's overall performance. Some membrane modification processes are briefly stated below:

1.16.1 Surface modification

Membrane separation is considered one of the surface phenomena, so performances of membranes rely on the properties of their surfaces. At present most of membranes are surface modified (Khulbe et al., 2010). Numerous surface modifications are done to enhance the selectivity as well as the permeability of the membrane (Pinnau et al., 2000). Several surface modification methods such as preadsorption (coating), plasma treatment, grafting, etc., have now been developed for enhancing the membrane properties.

1.16.2 Chemical modification

Membrane surface modification by chemical treatment is a promising method of attaining desirable surface properties without affecting the bulk polymer properties like mechanical, chemical resistance, and membrane structure. Mainly membranes are modified to enhance its

anti-fouling properties and permeability (Upadhyaya et al., 2018). Sulfonation, carboxylation, interfacial polymerization, etc., are commonly used chemical modification methods.

1.16.3 Polymer blending

Blending is a method where two (or more) polymers are physically blended to get the desired properties which can overcome their respective defects (Bhattacharya et al., 2004). It is a straightforward and effective technique for improving polymer properties.

1.17 Membrane bioreactor (MBR)

Membrane biological reactors (MBRs) refer to the technologies based on the combination of membranes and biological reactors for the treatment or resource recovery from wastewater. Combination of membrane separation with biochemical treatment has led to a variety of innovative environmental biotechnology purposes, namely, separation of biosolids, diffusion of gas, extractive, biocatalytic, and electrochemical membrane biological reactors (Haia et al., 2014) .

Recently the demand of membrane bioreactors (MBRs) in treating domestic and industrial wastewater has expanded dramatically due to their advantages such as lower footprint, higher efficiency and product quality, and small sludge production over the conventional treatment process (Federation, 2012)(Hamedi et al., 2019). MBR integrates a biological wastewater treatment process, usually activated sludge, with membrane filtration technology, commonly employing pressure-driven microfiltration (MF) or ultrafiltration (UF) membranes (American Membrane Technology Association, 2016). MBR was first introduced by Smith and coworkers who were assisted by the Dorr-Oliver research program in 1969, though it was not gaining popularity during its introduction. It was a flat sheet plate and frame UF membrane. MBR got considerable popularity in Japan in between 1970s to 1980s than that of North America. Yamamoto et al. gave a major breakthrough in MBR process by introducing submerge membrane bioreactor (SMBR) in 1989s. This represented a significant innovation compared to previous practice of external membrane in bioreactor (Radjenovi et al., 2008) (Ladewig et al., 2017). The market share of MBR has been increasing significantly. In 2005, the market value of MBR was $217 million and doubled in 2010. It has boosted about $1.81 billion in 2016 and $ 1.9 billion in 2019. In 2022 the market size was USD 3.35 billion and is expected to grow at a compound annual growth rate (CAGR) of 7.0% from 2023 to 2030 (Report, 2017)(McWilliam, 2019) (‘Membrane Bioreactor Market Size, Share & Trends Analysis Report By Product

(Hollow Fiber), By Configuration (Submerged), By Application (Municipal), By Region, And Segment Forecasts, 2023 - 2030', 2024). Another reason for the rapid growth of MBR in domestic and industrial wastewater treatment is its competitive advantages over the conventional treatment process. Producing very high-quality treated water, flexible design for upgradation of old treatment plants, complete solid retention, low sludge production, operation at higher mixed liquor suspended solids (MLSS), higher solid retention time (SRT) and shorter hydraulic retention time (HRT) make the MBR process superior to conventional activated sludge (CAS) process. MBR eliminates the gravity sedimentation tanks (clarifier) which results in a smaller footprint of the plant than CAS process (Treatment et al., 2008) (Faisal Ibney Hai et al., 2014).

1.17.1 Principle of MBR

MBR technology employs a bioreactor in conjunction with membrane separation to treat wastewater. The bioreactor in the MBR serves as the same purposes as the aerated tank in activated sludge processes, where microorganisms treat the wastewater. However, in MBR, porous membranes with pore diameters typically ranging from 0.05 to 0.1 µm (MF or UF) are employed to separate treated water and microorganisms, replacing the gravity separation of conventional activated sludge processes.

As shown in Fig 1.39, the pore diameter of the membranes employed in MBR are small enough to eliminate activated sludge flocs, free-living bacteria, even large-size viruses, or particles. Therefore, MBR yields exceptionally high-quality treated water with virtually no detectable suspended solids (SSs), comparable to tertiary treatment using activated sludge and depth filtration. This technique eliminates the need for gravity sedimentation tanks, making it a smaller

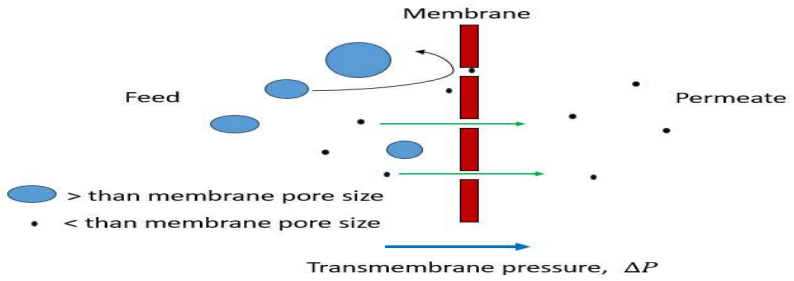

footprint than conventional activated sludge (CAS) processes.

Fig 1.33: Membrane separation process

Despite its advantages, MBR processes can experience membrane fouling due to various factors, including activated sludge, SSs, organics, and inorganics. To ensure stable MBR operation, it's essential to control membrane fouling addressing various approaches. For example, membrane manufacturers are trying to modify surface chemistry and module geometry to create fouling-resistant membranes, while process engineers are adjusting filtration cycles, ensuring backwashing, and providing scouring aeration (H.-D. Park et al., 2015).

1.17.2 Advantages and disadvantages of MBR

Conventional activated sludge (CAS) processes use activated sludge (i.e., active microorganisms) in a bioreactor to treat wastewater, and a sedimentation tank to separate treated water from the mixture of activated sludge and treated water. Sedimentation tanks don't completely settle all activated sludge, and some of it is washed away with the treated water. Even with properly functioning clarifiers, the concentration of SSs in the supernatant is usually around 5 mg/L (H.-D. Park et al., 2015). In MBR process, the membranes used have pore size smaller than activated sludge particles, so all activated sludge is separated from the treated water. This means there is almost no SSs concentration in the treated water, but dissolved matter can still pass through. As a result, tertiary treatments like sand filters and microfilters to remove SSs are not needed in MBR processes. Table 1.7 illustrates the pros and cons of MBR compared to CAS.

Table 1.7: Pros and cons of MBR compared to CAS (H.-D. Park et al., 2015)

Advantages	1. Production of reusable, high-quality treated water. Furthermore, it is possible to eliminate a significant portion of pathogenic bacteria and certain viruses. 2. Low footprint because of elimination of secondary clarifier and smaller bioreactor size. 3. Reduced excess or surplus sludge. 4. Precise control over solid retention time (SRT). 5. Possible to convert from existing activated sludge process (ASP)
Disadvantages	1. Increased operational and process intricacy. 2. Higher capital and operational expenditures; energy intensive 3. Greater foaming propensity 4. Membrane fouling 5. May need equalization for variable flow

1.17.3 MBR configuration

MBR filtration comes in two primary arrangements (Fig 1.40): A) vacuum-driven membranes submerged directly into the bioreactor (iMBR) and B) pressure-driven filtration in side-stream

MBRs (sMBR). The submersed MBR is generally preferred for wastewater treatment due to its better energy consumption, better hydraulic efficacy, and simpler design.

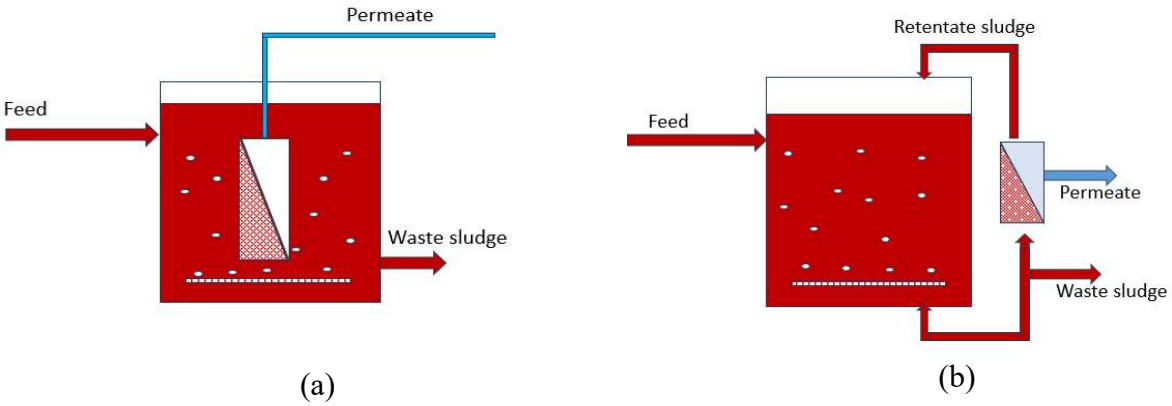

Fig 1.34: MBR configuration (a) immersed/submersed MBR (b) side-stream MBR

Though, the side-stream arrangement can also be used, where wastewater is forced across the membrane and then some of the permeate is collected whilst the rest is replaced to the bioreactor tank. This configuration can effectively control membrane fouling and maintain a constant flux, but it is limited by its higher energy consumption and more complex design (Ladewing et al., 2017).

1.17.4 Operating conditions for MBR

The MBR process operates over a significantly different range of parameters compared to the traditional activated sludge process. Different operating parameters used in designing the MBR plants are briefly discussed below:

1.17.4.1 Flux rate

Flux selection is a balance between cost and risk of membrane life. A lower design flux demands a larger membrane surface area and, therefore, higher capital costs; however, a lower design flux results in lower risk, longer membrane life, and, typically, less maintenance. Conversely, a higher design flux requires less membrane area (Federation, 2012) and lower capital costs, but higher risks, shorter membrane life, and potentially higher maintenance costs. Standard flux rate ranging from 20 to 50 L/m^{2}h have been commonly used. The MBR system should be designed to manage peak flows of the system to avoid flooding of the system. Alternately an equalization basin may be required if the membrane flux rate is inadequate.

1.17.4.2 Operating mode

MBRs commonly employ two operating modes: one with a constant TMP with variable permeate flux and the other with a constant permeate flux (L/m^2h) with variable TMP. The latter mode, maintaining a constant permeate flux rate, is typically preferred in membrane bioreactors as it can effectively control fluctuations in influent hydraulic loading. In this mode, membrane fouling is generally determined by observing a sudden TMP jump. Critical flux is required in constant flux operation as it is an essential factor in membrane bioreactor process (Iorhemen et al., 2016).

1.17.4.3 Mixed Liquor Suspended Solids (MLSS) concentration

Operating at higher MLSS concentrations (mg/L) allows the use of smaller biological reactor volumes and, hence, smaller plant footprints compared to conventional activated sludge (CAS) systems. Most manufacturers recommend MLSS concentrations between 4000 and 15000 mg/L in membrane tanks, while for CAS it is usually ranged in between 1500 to 3000 mg/L (Faisal Ibney Hai et al., 2014).

1.17.4.4 Aeration

Aeration serves dual purposes in aerobic membrane bioreactors. Firstly, it provides essential oxygen for biological activities, and secondly, it functions as a means of removing the cake layer that develops on the surface of the membrane, a process known as air scouring. The oxygen provided through aeration enables biodegradability and biomass cell synthesis. The operating costs tend to rise when the aeration rate exceeds the optimal level. Therefore, aeration needs to be optimized in MBR operation and typically it ranges from 180 to 600 L air/m^2 membrane area (Zaerpour, 2014). A minimum oxygen level of 1 mg/L must be maintained in the aeration basin, typically aiming for a range of 2-3 mg/L (H.-D. Park et al., 2015). Aeration serves a threefold purpose: aeration, mixing of the biomass, and cleaning the membrane (A. H. Konsowa et al., 2013).

1.17.4.5 Solids retention time (SRT)

SRT stands as another critical operating parameter in MBRs, serving the dual purpose of maintaining a constant MLSS concentration and regulating sludge production. Typically, MBRs are run with longer SRT values (>30 days) in contrast to the CAS processes, which usually

around 10 days (H.-D. Park et al., 2015). This extended SRT in MBRs results in reduced excess sludge production, primarily due to a decrease in the production of EPS. However, it's important to mention that SRT also influences the secretion of SMP by microorganism, which in turn, affects the membrane fouling propensity. At higher MLSS concentrations associated with higher SRT, MBRs can face elevated activated sludge viscosity that can lead to excessive membrane fouling.

1.17.4.6 Hydraulic retention time (HRT)

HRT represents the average time wastewater is retained in a tank or system. It indirectly influences membrane fouling in MBRs as it, in conjunction with other operating parameters, determines the sludge properties. It is found that as hydraulic retention time declines, the propensity of membrane fouling tends to increase. This can be attributed to rise in sludge viscosity and extracellular polymeric substances concentrations (Iorhemen et al., 2016). A decline in HRT generates several effects, including the generation of extracellular polymeric substances from bacterial cells, the proliferation of filamentous bacteria, and the production of irregularly big flocs. Furthermore, a reduction in HRT results in increased MLSS concentration as well as sludge viscosity that are primary influencing parameters which affect hydrodynamic environment with membrane bioreactor process. Typically, the HRT value in the membrane bioreactor does not noticeably differ from the CAS system and it falls in the range of 4 to 10 h (H.-D. Park et al., 2015).

1.17.4.7 Food to microorganisms (F/M) ratio

The Food to Microorganism (F/M) ratio is a crucial operational factors in biological wastewater treatment processes. It is observed that as the F/M ratio increases, the propensity of membrane fouling tends to rise as well. An elevated F/M ratio can also result in increased extra-cellular polymeric substances (EPS) concentrations because the biomass consumes a higher amount of available food. Therefore, operating at lower F/M values is preferred, typically in the range of 0.05 to 0.4 (H.-D. Park et al., 2015).

1.17.4.8 Organic loading rate (OLR)

This is a very influential factors impacted by the operation of biological wastewater treatment procedures, with membranes fouling becoming more pronounced as OLR rises (Iorhemen et al., 2016).

1.17.4.9 Temperature

Temperature plays a significant role in influencing the biodegradation rate. In MBRs, temperature effects the membrane fouling by changing the properties of MLSS (Iorhemen et al., 2016). It has been observed that declining operational temperature results in the bacteria tend to release more extracellular polymeric substances. Additionally, very low temperatures are associated with a prevalence of filamentous bacteria, that make more extracellular polymeric substances in the MLSS, thus increasing the likelihood of membrane fouling.

1.18 MBR for textile wastewater treatment

MBR technology has been increasingly employed in industrial wastewater treatment due to its inherent advantages over the traditional activated sludge processes. It is particularly effective for treating textile wastewater. Textile processing is one of the main polluters of water pollution which involves many different steps that produce wastewaters which depend on many different factors, such as the type of fabric, the type of process, and used chemicals. Textile industries constitute about 8% of manufacturing goods around the world and consume a huge amount of freshwater and emitting hazardous substance to the environment. This wastewater contains organic and inorganic substances that can cause pollution of the environment if discharged indiscriminately. Most of the wastewater generated is during the wet processing stage that includes slashing/sizing, bleaching, mercerizing, dyeing, and finishing. Little or no wastewater is generated at fiber preparation, weaving, knitting, and textile fabrication processes (Lubello, CCaffaz et al., 2007)(De Jager et al., 2012)(Pandy, 2015). An MBR can be a suitable alternative to the conventional textile wastewater treatment due to its high removal efficiency of COD, BOD, TSS, color, TSS, total nitrogen, turbidity, etc. Conventional MBR is operated at aerobic conditions which is not suitable for dye degradation. Rather, anoxic or anaerobic MBR (AnMBR) shows more potential of dye removal (Sun et al., 2010) (Boonyungyuen et al., 2014). A concise brief of textile wastewater treatment using MBR is shown in Table 2.1. Based on the table, 89.78 ± 7.78 % COD and 76.32±19.96 % BOD were removed from the textile wastewater. About 76 % color was removed though some studies showed almost all color removal (Deowan et al., 2016) (Luong et al., 2016)(Ali et al., 2016)(Badani et al., 2005). MBR processes are suitable for turbidity removal and some researchers achieved above 95 % turbidity removal (Berkessa et al., 2020) (Deowan et al., 2013). MBRS can also remove considerable amount of NH_3-N (Ben et al., 2015), TSS (Hai et al., 2005) and surfactants (Grilli et al., 2011) from the

textile wastewater. Operating parameters such as SRT (avg. 53 days), MLSS (avg. 8500 mg/L) were maintained. For HRT, lowest 6h and highest 216h were found. Grilli et al. investigated on MBR-NF hybrid process and found that addition of NF membrane allowed the further improvement in 50-80 % COD and 60-70 % color removal (Ibney et al., 2006). Another study showed 96% salt (NaCl) rejection using RO combined with MBR (Huang et al., 2009). Tubular (A. H. Konsowa et al., 2013), hollow fiber (Saha et al., 2014), and flat sheet (Lubello et al., 2004) membranes were used in various MBRs configurations with MF and UF types. Therefore, MBR technology proved itself as a potential and promising treatment method for textile wastewater. Table 1.8 gives a brief summary of MBRs used in textile wastewater treatment.

Table 1.8: Summery of MBR performance treatment of textile industry wastewater

SL	Characteristics of textile wastewater	Membrane and MBR Type	Operational Parameters	Treatment Efficiency	Ref.
1	High concentration of organics, dyes, COD, heavy metals, reducing agents, oxidizing agents, biocides, surfactants, etc.	MF (0.2 µm) Aerobic MBR	SRT: 50 day TMP: <0.35 bar Backwash: 30 sec/10 min MLSS: 9000-14000 mg/L	COD: 91 TSS: 99 Surfactants : 66-82	(Lubello, CCaffaz et al., 2007)
2		MF (0.2 µm) Side stream aerobic MBR	MLSS: 1300 mg/L	COD: 75 TSS: 19.6 Turbidity: 94 Phosphate: 14.5 Color: 28	(De Jager et al., 2012)
3		MF (0.1-0.2 µm) Aerobic MBR	pH: 8.5-8.7	COD: 90	(Pandy, 2015)
4		Tubular membrane Cut off: 100 KDa Coagulation-MBR	HRT: 8h MLSS: 8000 mg/L	COD: 82 Choma: 80	(Sun et al., 2010)
5		MF (0.4 µm) hollow fiber Aerobic MBR	HRT: 6-24 h	COD: 48-67 Color: 84-95 TKN: 51-65 TP: 52-61	(Boonyun gyuen et al., 2014)
6		UF (0.03-0.05 µm) Aerobic MBR	HRT: 25-150 h TMP: 30-50	COD: 94-96	(Deowan et al.,

		mbar MLSS: 8000-12000 mg/L F/M: 0.05-0.1	Red dye: 40-50 Blue dye: 55	2016)
7	UF (0.04 µm) Aerobic MBR	MLSS:4000-14000 mg/L TMP: 40-60 mbar F/M: 0.1-0.25	COD: 95 Red dye: 15-70 Blue dye: 30-80	(Luong et al., 2016)
8	UF (0.025 µm) RO (0.001 nm) Combined MBR-RO	MBR HRT: 20 h SRT: 30 day MLSS: 10,000 mg/L Pressure: 0.5 bar RO pH: 6-7 Pressure: 12 bar	COD: 96 BOD: 97 TDS: 96 NaCl: 96	(Ali et al., 2016)
9	UF (0.025 µm) tubular Aerobic MBR	SRT: 5-30 day MLSS: 5000-15000 mg/L Pressure: 0.5-1.5 bar F/M: 0.05-1.5	COD: 97 NH_3-N: 70 Color: 72	(Badani et al., 2005)
10	Anaerobic dynami MBR	HRT: 60-120h TMP: 400 mbar MLSSL 10800 mg/L	COD: 98.5 Color: 97.5 TSS: 98.8	(Berkessa et al., 2020)
11	UF (0.05 µm) flat sheet Aerobic MBR	HRT: 40-80 h TMP: 50 mbar MLSS: 12000 mg/L pH: 8-10.5	COD: 90 Red dye: 25-70 Blue dye: 20-50	(Deowan et al., 2013)
12	UF flat sheet Cutoff: 150 KDa Aerobic MBR	HRT: 24-64h MLSS: 5220 mg/L TMP:70-350 mbar Temp: 24-29^{0}C	COD: 98 BOD: 96 SS: 100 Color: 100 Cytotoxicity: 53	(Ben et al., 2015)
13	MF (0.4 µm) hollow fiber and flat sheet Aerobic MBR	MLSS: 8000 mg/L TMP: 40-60 KPa	Color: 99 TOC: 97 By both membrane	(Hai et al., 2005)
14	UF (0.04 µm)	HRT: 24h	COD: 90-	(Grilli et

	hollow fiber NF cutoff: 150-300 Da Anaerobic-biofilm anoxic-aerobic MBR-NF	SRT: 80-100 da NF pressure: 500 KPa	95 Color: 70 NF enhanced the further improvement of COD and Color by 50-80% and 60-70% respectively	al., 2011)
14	MF (0.4 µm) hollow fiber, plyethylene, Submerged MBR	HRT: 15 h MLSS: 10000-55000 mg/L	TOC: 97 Color: 99	(Ibney et al., 2006)
16	MF (0.2 µm) hollow fiber Aerobic MBR	HRT: 6-22.5 h SRT: > 30 day MLSS: 9000-11000 mg/L TMP: 0.05-0.1 bar	COD: 90 NH_3-N: 90-95 Color: 60-75	(Huang et al., 2009)
17	MF (0.2 µm) hollow fiber Aerobic MBR	MLSS: 1000-3000 mg/L pH: 7-8 F/M: 0.1-0.3	COD: 87-96	(A H Konsowa et al., 2013)
18	MF (0.2 µm) plate and frame Aerobic MBR	HRT: 177 h pH: 7-9 TDS: 31-46 MLSS: 1300 mg/L	COD: 90 BOD:80	(Saha et al., 2014)
19	UF (0.02-0.03 µm) Cutoff: 40 Kda Aerobic MBR	Pressure: 1.8 bar Cross-flow velocity of 2.1 m/s.	COD: 93: TSS:99 Ammonia: 96 Anionic surfactants: 92.5 Non-ionic surfactants: 99 Color: 70-80	(Lubello et al., 2004)
20	UF (0.01 µm)	HRT: 8-24 h	COD: 92	(Niren et

	hollow fiber Cutoff: 50 Kda Aerobic MBR	TMP: 0.29-0.58 bar F/M: 0.07-0.14 MLSS: 5500-9100 mg/L	BOD: 93 Color: 91	al., 2011)
21	UF (0.01 µm) tubular Aerobic MBR	HRT: 216h SRT: 9 day MLSS: 840 mg/L F/M: 0.2	COD: 89-92 Color: 70-73	(Lorena et al., 2011)
22	MF (0.1 µm) hollow fiber Aerobic / anoxic MBR-UV-GAC	HRT: 74-124 h TMP: 40 Kpa Air flow: 0.3 m^3/h	COD: 99 Color: 95 Nitrogen: 97 Phosphorus: 73	(Rondon et al., 2015)
23	MF (0.4 µm) tubular Aerobic MBR	HRT: 70-120h MLSS: 4000 mg/L	COD: 93 Color: 80.5	(Schoeberl et al., 2005)
24	MF (0.4 µm) Aerobic MBR	MLSS: 5000 mg/L	COD: 90 TN: 60 TP: 75 Phosphorus: 99.6	(Song et al., 2008)
25	UF (nominal 0.4 µm) flat sheet AnMBR	HRT: 60h SRT: 150-200 day pH: 7	AZO dye: 99 COD: 95	(Spagni et al., 2012)
26	UF (0.04 µm) hollow fiber Aerobic MBR	HRT: 14 h SRT: 25 day MLSS: 13900 mg/L F/M: 0.03-0.07	COD: 97 BOD: 96.7 NH_3-N: 91 NO_3-N: 77 NO_2-N: 62 TKN: 78.5 TN: 78.6 TP: 58.7 TSS: 99 Turbidity: 99 Color: 97	(Yigit et al., 2009)
27	MF (0.4 µm) hollow fiber Aerobic MBR	HRT: 48 h pH: 6.8-7.2	COD: 79 BOD: 99 Color: 54 SS: 100	(You et al., 2007)
28	MF (0.45 µm) flat sheet	HRT AeMBR:24h	COD AeMBR:	(Yurtsever et al.,

	Aerobic/ Anaerobic MBR	AnMBR: 48h MLSS AeMBR 10000 mg/L AnMBR 2000 mg/L Temp: 32-34^{0}C TMP: 0.35-.7 bar	97 AnMBR: 94 Color AeMBR: 30-50 AnMBR: almost 100	2015)
29	MF (0.22 µm) hollow fiber Aerobic MBR with gravity drain	HRT: 6-12 h F/M: 0.24 MLSS: 400-3800 mg/L TMP: 4.4-20.3 KPa	COD: 80 BOD: 95 Turbidity: 99 Color: 58.7	(Zheng et al., 2006)

CHAPTER 2: MATERIALS AND METHOD

2.1 Materials

Commercial grade polysulfone (PSF-4k) was purchased from Sonata Impex, India. Polyethersulfone (PES-58K) was procured from Goodfellow, England. Polyethylene glycol (PEG-6k) and sodium alginate (SA-16k) were purchased from Research-Lab, India and polyvinylpyrrolidone (PVP-40K) was purchased from Sigma-Aldrich. Commercial membrane (NADIR UP150 P) was purchased from Microdyn Nadir, Germany. Dimethylformamide (DMF) was purchased from Daejung Chemicals and Metals Co. Ltd, Korea. Spun bond non-woven fabric, non-woven fusing, and woven polyester fabric were purchased from the local market. Non-woven Holytex-3256 was purchased from TALAS, USA. Fig 2.1 shows the chemical structures of PSF (a), PEG (b), SA (c), PVP (d), and PES (e). Turquoise blue (C.I. Reactive Blue 21) with molecular weight of 1167.5 g/mol was supplied by a local dye supplier. All chemicals and materials were used as received.

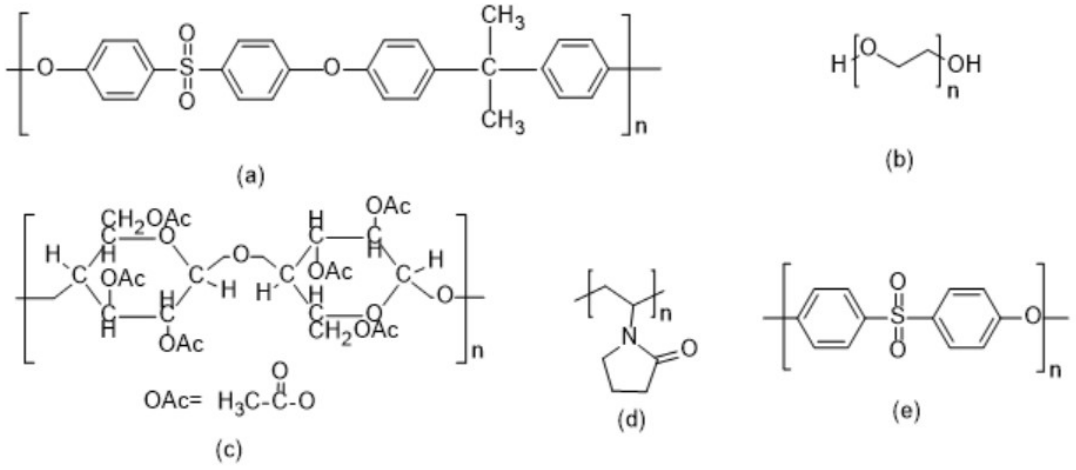

Fig 2.1:Chemical structures of PSF(a), PEG (b), SA (c), (d) PVP, and (e) PES

2.2 Fabrication of membrane by non-solvent induced phase separation (NIPS) method

2.2.1 Preparation of dope or casting solution

To prepare 100.0 gm dope solution a certain amount of PSF (15-23 wt.%), SA (1-10 wt.%), PEG (1-10 wt.%), and DMF (85-67 wt.%) were taken in a glass container and mixed well by stirring in a hotplate magnetic stirrer at 80^{o}C for 4 hours (Moghimifar et al., 2014). The solution was then left overnight under continuous stirring at room temperature followed by sonication for 1 hour to remove air bubbles. The exact composition of the dope solutions is represented in Table

2.1. For PES blended membranes, PES (15-19 wt.%), PVP (1-10 wt.%), PEG (1-10 wt.%), DMF (85-67 wt.%) were taken and their composition of the dope solutions is represented in Table 2.2.

Table 2.1: Composition of dope solutions for PSF blended membranes

PSF (wt.%)	SA (wt.%)	PEG (wt.%)	Solvent (DMF wt. %)
15	-	-	85
17	-	-	83
20	-	-	80
23	-	-	77
23	1	-	76
23	5	-	72
23	10	-	67
23	-	1	76
23	-	5	72
23	-	10	67

Table 2.2: Composition of dope solutions for PES blended membranes

PES (wt.%)	PVP (wt.%)	PEG (wt.%)	Solvent (DMF wt. %)
15	-	-	85
17	-	-	83
19	-	-	81
19	1	-	80
19	3	-	78
19	5	-	76
19	7	-	74
19	-	1	80
19	-	3	78
19	-	5	76
19	-	7	74

2.2.2 Casting of the dope solution

The dope solutions (polymer and solvent) were cast on different membrane support materials (both woven and non-woven fabrics) placed on glass plate (22cm x 27cm) using a casting knife with a clearance of 250μm. Casted films were exposed to ambient atmosphere conditions (26-30^{o} C and relative humidity of 50-65 %) for a duration of 3 to 5 seconds. Subsequently, cast films immersed in a non-solvent bath of distilled water to induce demixing. The membranes thus

formed were submerged in distilled water for a period of 24 hours to thoroughly remove any remaining solvent. A schematic image of membrane fabrication process is shown in Fig 2.2.

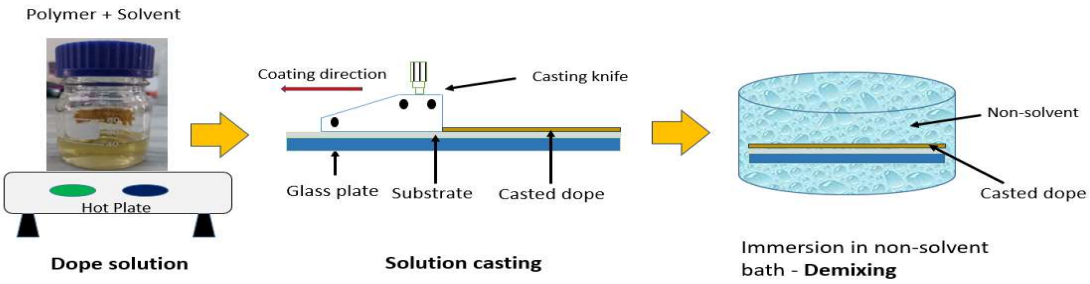

Fig 2.2: Schematic diagram of NIPS process

2.3 Characterization of blended membranes

2.3.1 Effects of polymer concentration and support material on membrane skin formation

Composite membranes were fabricated employing varying amounts of PSF and additives (PEG, SA) and fusing fabric (non-woven), hollytex-3256 (non-woven), spun bond fabric (non-woven), and woven polyester fabric (Fig 2.3) were used as membrane support materials. The fabricated membranes were inspected using tinyscope 1000× mobile microscope (Fig 2.4).

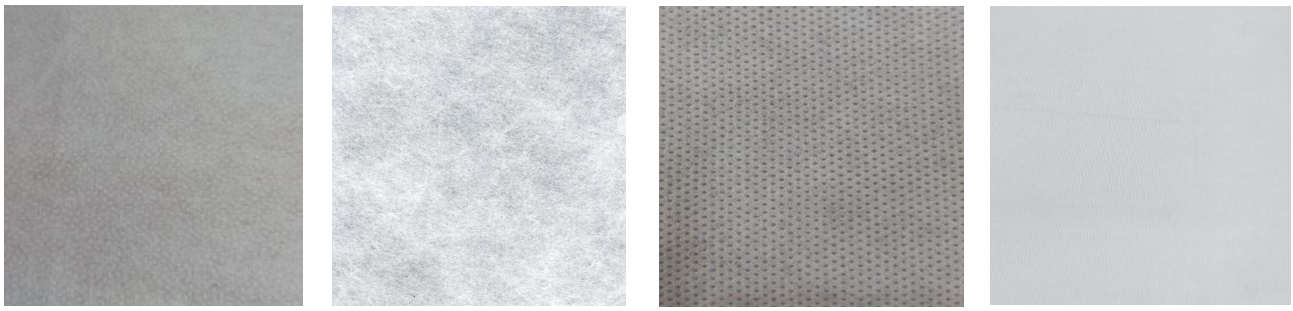

(a) (b) (c) (d)

Fig 2.3: Membrane support materials (a) fusing fabric (non-woven), (b) hollytex-3256 (non-woven), (c) spun bond fabric(non-woven), and (d) woven polyester fabric.

Fig 2.4: Tinyscope 1000× mobile microscope.

2.3.2 Analytical tools

Fourier-transform infrared (FTIR) spectra, conducted with attenuated total reflectance (ATR) were recorded using the IR Prestige-21 model, Shimadzu, Japan to identify the various functional groups within the membranes. Morphology of the membranes were studied by a field-emission scanning electron microscope (FE-SEM) (Model: JSM-7610F, Japan) which directly gives the visible information about the surface morphology of the membranes. For FE-SEM sampling, samples were sputtered with platinum. An atomic force microscope (AFM) (Nanosurf FlexAFM, Switzerland) was utilized for topographic investigations. Measurements were carried out using contact mode in ambient conditions. The cantilever used in this study was XYCONTR manufactured by Nanosensors. For tensile strength (TS), Universal Tensile Testing Machine (SATRA STM 566) was employed following the TM 43:2021 standard. The samples were cut into dumbbell-shaped specimens with an area of 4mm x110mm.

2.3.3 Equilibrium water content (EWC)

Equilibrium water content was measured using 2 cm × 2 cm cut pieces of membrane and weighted in an electronic balance. These cuts were then kept in distilled water for a period of 24 hours. After that the membrane pieces were mopped with tissue paper to remove excess water from the surfaces and weighted again. The percentage of water uptake was calculated using Eq.2.1 (Kumar et al., 2017).

$$\mathrm{EWC}(\%) = \frac{\mathrm{W0}-\mathrm{W1}}{\mathrm{w1}} \times 100 \qquad \text{(Eq. 2.1)}$$

Where, W_0 and W_1 (g) are the masses of the wet membrane and the dry membrane, respectively. The overall porosity of the membranes (ε) was determined by the gravimetric method according to following Eq. 2.2 (Amiri et al., 2020).

$$\varepsilon(\%) = \frac{\mathrm{W0}-\mathrm{W1}}{\mathrm{A}\times\ \mathrm{l}\times \mathrm{dw}} \times\ 100 \qquad \text{(Eq. 2.2)}$$

Where, d_w is the density of water (g/cm^3), A is the membrane effective area (cm^2), and l is the thickness of membranes (cm).

2.3.4 Contact angle measurement.

In this study, a low-cost contact angle measurement equipment was fabricated in-house using smart phone (Samsung A52s), a macro lens (Apexel APL-HB100mm), a mobile phone holder, a sample holder, and a 3.5 cc plastic syringe for producing water drop (Fig 2.5). Sessile drop was regulated with the help of a knob situated on the top of the syringe. For determining the membrane contact angle, a water droplet was put onto the membrane surface, and the contact angle was captured at 10-30 seconds (Peydayesh et al., 2017) (Alkawareek et al., 2018).

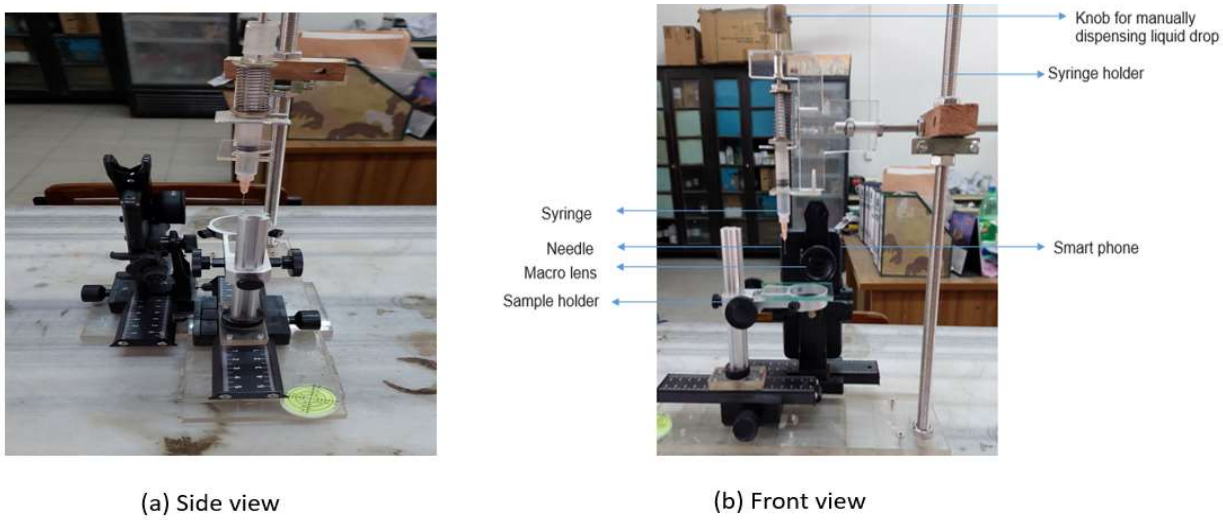

Fig 2.5: Inhouse fabricated contact angle measurement equipment using smartphone.

Multiple images of different points were taken to try and obtain accurate results, and average values were taken. Contact angle of water drops on the membrane surface was measured using ImageJ Software (Fig 2.6).

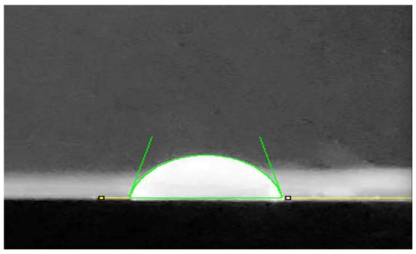

Fig 2.6: Snapshot of the image analysis by ImageJ software

2.3.5 Pure water flux

Crossflow filtration unit (OSMO, Germany) was used to measure the pure water flux of the fabricated membranes where filtration area of a membrane was 0.008 m^2 and operating pressure

was 3 bar to force the distilled water to pass through the membrane (Fig 2.7). The permeate flux (L/m^2h) was determined by the following Eq. 2.3 (Kumar et al., 2017).

$$Jp = \frac{Vp}{A \times \Delta t} \qquad \text{(Eq. 2.3)}$$

Where Jp = permeate flux (LMH), Vp= volume of permeate (L), A= area of the membrane (m^2) and Δt = time (h) required to collect permeates at different transmembrane pressures.

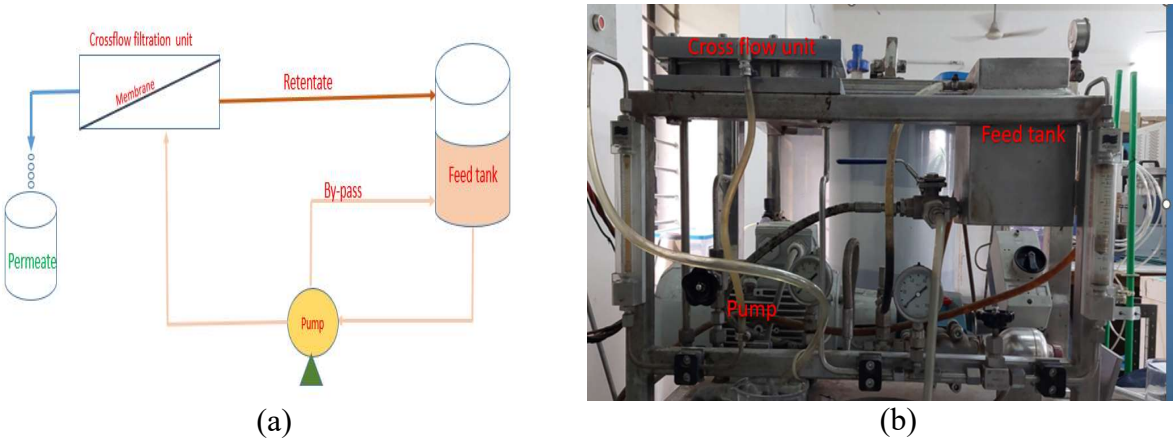

(a) (b)

Fig 2.7: Images of crossflow unit (a) unit diagram and (b) real image

2.4 Membrane bioreactor (MBR) set up

2.4.1 Development of membrane module

A membrane module was designed and fabricated (300 mm × 200 mm) from acrylic sheet, PMMA, (10-12 mm thickness). Design and fabricated membrane module were illustrated in Fig 2.8 and Fig 2.9 respectively.

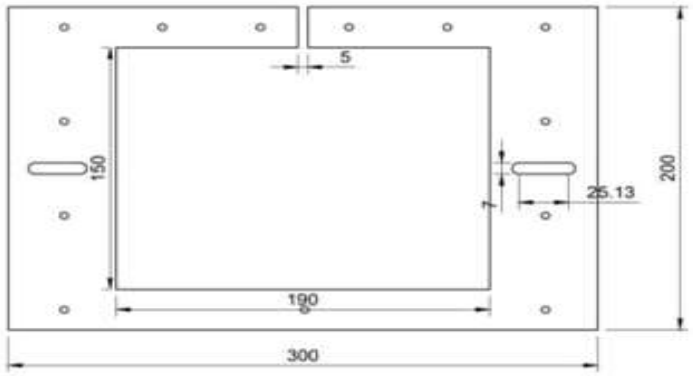

Fig 2.8: Design of membrane module (300 mm × 200 mm)

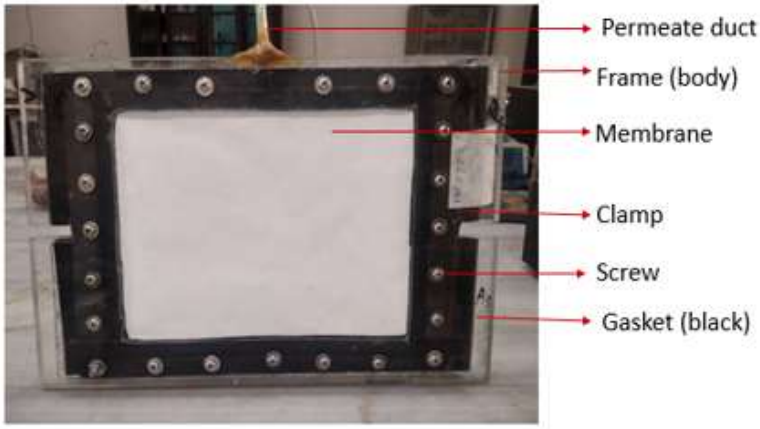

Fig 2.9: Fabricated membrane module using acrylic sheet

Membrane modules were mounted in a membrane holder fabricated by PVC pipes (Fig 2.10)

Fig 2.10: Fabricated flat sheet membrane module

2.4.2 Preparation of synthetic textile wastewater

As the characteristics of real textile effluent change dramatically from day to day, a synthetic textile effluent with composition similar to real effluent was prepared based on the information presented in Table 2.3. Activated sludge was collected from a textile industry and central effluent treatment plant (CETP) located at Savar EPZ, Dhaka, Bangladesh. Preparation of synthetic textile wastewater for this study was based on turquoise blue dye and other auxiliaries such as ammonium chloride, sodium chloride, sodium carbonate, detergent, and glucose. The activated sludge was mixed for acclimatization in such a manner that the concentration of MLSS (Mixed Liquor Suspended Solid) in the prepared wastewater was in the range of 4 - 6 g/L.

Table 2.3: Composition of synthetic textile wastewater

Chemicals	Concentration (mg/L)	References
Turquoise blue dye ($C_{40}H_{21}CuN_9Na_4O_{14}S_5$)	100	(Luong et al., 2016)
Ammonium Chloride (N-source)	300	(Luong et al., 2016)
Sodium Chloride (as electrolyte)	2,500	(Luong et al., 2016)
Sodium bicarbonate (as pH buffer)	1,000	(Işik et al., 2008)
Detergent	50	(Luong et al., 2016)
Glucose (C-source)	2,000	(Luong et al., 2016)

2.4.3 Experimental set up of MBR plant

In an experiment using a pilot plant (Fig 2.11) for membrane bioreactor (MBR), flat sheet membrane modules with dimensions of 14 cm ×14 cm with an active area of 0.025m^2 were submerged in a 50L reactor. To prevent the formation of cake layers on the membrane surfaces and promote aerobic conditions for biological treatment, compressed air (560 L air /m^2 membrane area) was supplied through a diffuser at the base of the membrane modules to create shear stress. Around 2-3 mg/L dissolved oxygen (DO) was maintained throughout the experiment. The pressure sensor recorded the transmembrane pressure (TMP), and two peristaltic pumps were used to control the feed and effluent streams. The flux was measured by collecting permeates over a known period of time.

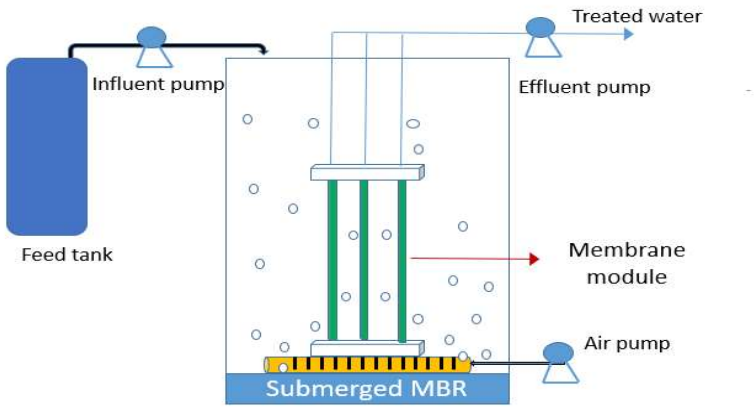

Fig 2.11: Design of plate- and- frame (flat sheet) submerged membrane bioreactor.

As the characteristics of real textile effluent change dramatically from day to day, a synthetic textile effluent with composition similar to real effluent was prepared. The sludge was acclimated using synthetic textile wastewater to get MLSS concentration of 4 to 6 g/L.

2.4.4 Wastewater treatment analysis by MBR

Effluents of commercial and modified membranes from MBR plant were collected and analyzed immediately. Chemical oxygen demand (COD), and Biochemical oxygen demand (BOD_5), were analyzed based on the Standard Methods (APHA, 2017). Color was measured by spectrophotometric method by measuring absorbance at 592 nm which is the λ_{max} of the used dye. The dye concentration was estimated by calibration method where a calibration curve was constructed in advance.

2.4.5 Bacteriological analysis

The permeate samples were collected from the MBR plant and poured into sterile tubes. All the samples were brought to the laboratory by maintaining temperature (4-8ºC) using a cool box within 2 hours of collection. Microbiological analyses were done according to USFDA Bacteriological Analytical Methods (2001). The bacteriological analysis was carried out by serially diluting the samples and plating 1.0 mL of the appropriate dilution onto Tryptic Soy Agar (Fluka, USA) microbial culture media for total aerobic bacterial count; Hichrome™ Coliform Agar (Fluka, USA) media for total coliform bacterial count; Sorbitol MacConkey Agar (Oxoid, UK) medium for enumerating fecal coliform bacterial count; NGKG agar: Kim and Goepfert agar with NaCl and Glycine for *Bacillus* spp. and Cetrimide selective agar for *Pseudomonas* sp 37ºC for 24 hours and Dichloran Rose Bengal Chloramphenicol Agar for total yeast and mold count. After inoculating the samples, all culture media plates were incubated for 24-48 hours at 37ºC before being counted. All the plate count data represent the mean values obtained from three individual trials, with each of these values being obtained from duplicated samples.

CHAPTER 3: RESULTS AND DISCUSSION

Part 1 PSF based membranes

3.1 Fabrication and characteristics of PSF blended membranes

A uniform membrane film was obtained only when 23 wt.% commercial PSF polymer solution was cast on Hollytex-3256 (non-woven) support material. However, when other supports materials were used, double layered film was formed on both sides of the support materials. Fig 3.1 displays the different membranes that were produced using 23 wt.% PSF concentration with various support materials. Table 3.1 demonstrates the impact of polymer concentrations on different membrane supports. The data indicated that support materials, except for Hollytex-3256, possessed larger pore sizes which resulted in the seepage of the dope solutions through the support materials, creating double layers. Additionally, the capillary forces of support materials drew the dope solution into the bulk support materials (Pinnau et al., 2000) and formed double layer.

Magnified view of membrane surface

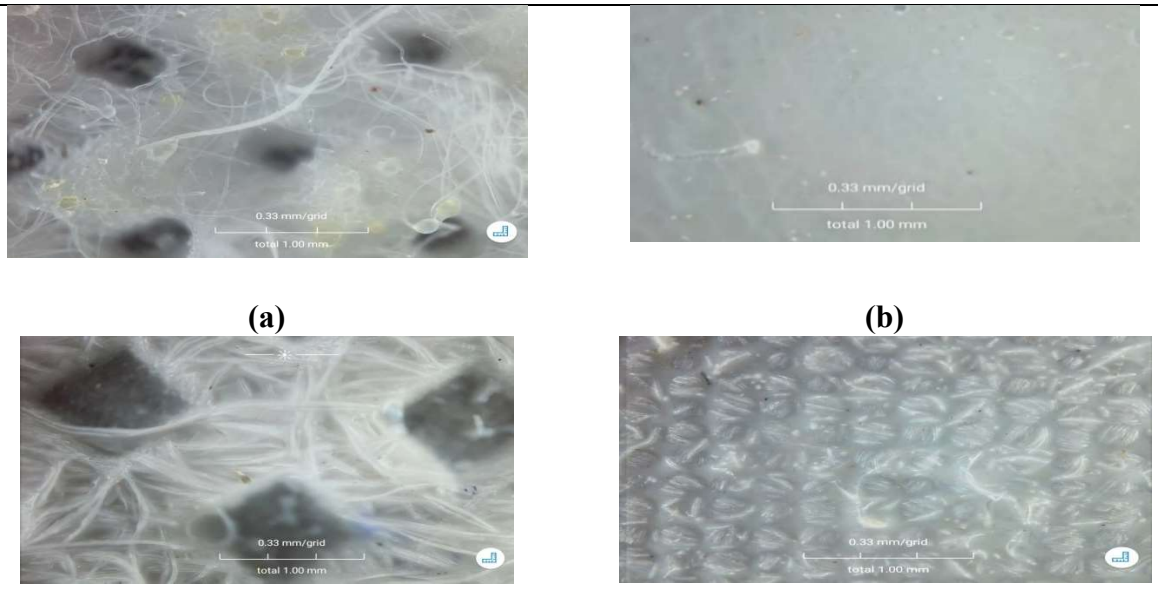

(a) **(b)**

(c) **(d)**

Fig 3.1: Membrane with 23% PSF concentration on various support materials: (a) Fusing fabric (non-woven), (b) Hollytex-3256 (non-woven), (c) Spun bond fabric (non-woven), and (d) Woven fabric. (Magnification done by tinyscope 1000x mobile microscope)

Table 3.1 clearly shows that a uniform membrane was only obtained when non-woven Holletex-3256 support material and 23 wt.% PSF were used. Therefore, throughout the research, membranes were fabricated using 23 wt. % PSF and Holletex-3256 support material (Table 3.2).

Table 3.1: The effect of PSF concentrations on various membrane supports materials

PSF (wt. %)	Support material	Solvent (DMF wt. %)	Membrane condition
15	Fusing fabric	85	Formed double layers.
15	Hollytex-3256		
15	Spun bond fabric		
15	Woven fabric		
17	Fusing fabric	83	Formed double layers.
17	Hollytex-3256		
17	Spun bond fabric		
17	Woven fabric		
20	Fusing fabric	80	Formed double layers.
20	Hollytex-3256		
20	Spun bond fabric		
20	Woven fabric		
23	Fusing fabric	77	Formed double layers.
23	Hollytex-3256		No formation of double layers.
23	Spun bond fabric		Formed double layers.
23	Woven fabric		Formed double layers.

The study was also designed to evaluate the impact of additives such as SA and PEG on membrane performance in comparison to the control membrane (without additives).

Table 3.2: Effect of additive concentration on PSF blended membrane performance

Sl. No.	Code	PSF (wt. %)	Support material	SA (wt.%)	PEG (wt.%)	Solvent (DMF, wt. %)	Membrane performance
1	PSF-1SA	23	Hollytex-3256 (non-woven)	1	-	76	1.40 × water flux than control membrane
2	PSF-5SA	23	Hollytex-3256 (non-woven)	5	-	72	2.10 × water flux than control membrane
3	PSF-10SA	23	Hollytex-3256 (non-woven)	10	-	67	1.60 × water flux than control membrane
4	PSF-1PEG	23	Hollytex-3256 (non-woven)	-	1	76	2.65 × water flux than control membrane
5	PSF-5PEG	23	Hollytex-3256 (non-woven)	-	5	72	4.80 × water flux than control membrane
6	PSF-10PEG	23	Hollytex-3256 (non-woven)	-	10	67	3.46 × water flux than control membrane

3.2 FTIR Analysis of PSF blended membranes

FTIR analysis of the fabricated membranes and pure additives was carried out using ATR technique and the spectra are presented in Fig 3.2. It is an important characterization technique for determining the existence of different functional groups in the membranes.

For the PSF-PEG blended membrane (Fig.3.2d), the characteristic peaks at around 3700-3471cm^{-1} (-OH), 3066 cm^{-1} (aromatic C-H stretching), 2893 cm^{-1} (aliphatic C-H stretching), 1408 cm^{-1} (-CH_2 bending), 1265 cm^{-1} (C-O of alcohol), 1053 cm^{-1} (C-O-C stretching) were present.

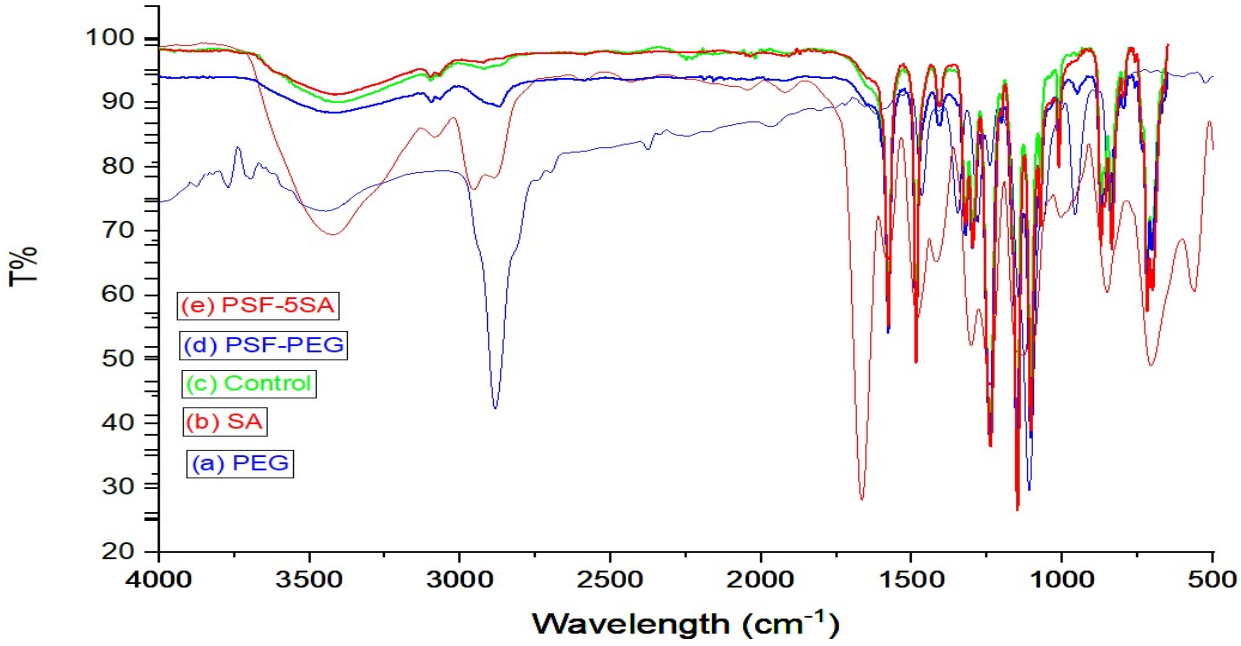

Fig 3.2: FTIR/ATR spectra of (a) PEG, (b) SA, (c) control membrane, (d) PSF-PEG membrane and (e) PSF-SA membrane

For the PSF-SA blended membrane (Fig. 3.2e), the peaks were found at around 3700-3414cm^{-1} (-OH), 3066 cm^{-1} (aromatic C-H stretching), 2897 cm^{-1}(aliphatic C-H stretching), 1674 cm^{-1}(C=O stretching),1593 cm^{-1} (C-C stretching in aromatic ring), 1319 cm^{-1} (C-O of COO^- group), and 1053 cm^{-1} (C-O-C group). The peaks at 1319 cm^{-1} and 1674cm^{-1} confirmed the presence of SA in the blended membrane.

3.3 SEM Analysis of PSF blended membranes

The images of field-emission scanning electron microscope (FE-SEM) of membrane surface and cross-section were captured to investigate the morphology of the membranes (Fig 3.3 and Fig 3.4). PSF-PEG membranes exhibited an asymmetrical structure comprising of a dense top layer and a porous sublayer. The sublayer contained cellular or sponge-like pores, as well as finger-like macrovoids. In contrast, the control membrane was a less porous, non-uniform dense membrane with an average pore size of 0.12 μm. As the PEG additive was increased, the number of pores and pore size increased, reaching a maximum at 5 wt.% PEG in the dope solution. Beyond 5% wt. of PEG, the number of surface pores were decreasing due to the increased viscosity of dope solution (Mulyati et al., 2017).

The impact of PEG can be attributed to the fact that increased the concentration of the water-soluble additive in the casting solution increased the likelihood of coagulation accelerating the rate of solvent and non-solvent interchange, leading to faster separation which created larger pores (Khorsand-Ghayeni et al., 2017). Additionally, PEG might modify the rheology of the casting solution, which in turn changes the precipitation kinetics during phase separation (Feng et al., 2017).

Regarding the SA blended membranes (Fig 3.4), both the surface and cross-sectional images displayed the dense structure of the membranes. Increasing the SA concentration did not result in a significant improvement in porosity. Therefore, it was concluded that PEG has a greater ability to form pores compared to SA. Additionally, PEG served as a plasticizer, leading to the expansion of the polymer matrix and the subsequent formation of pores (Tomietto et al., 2020).

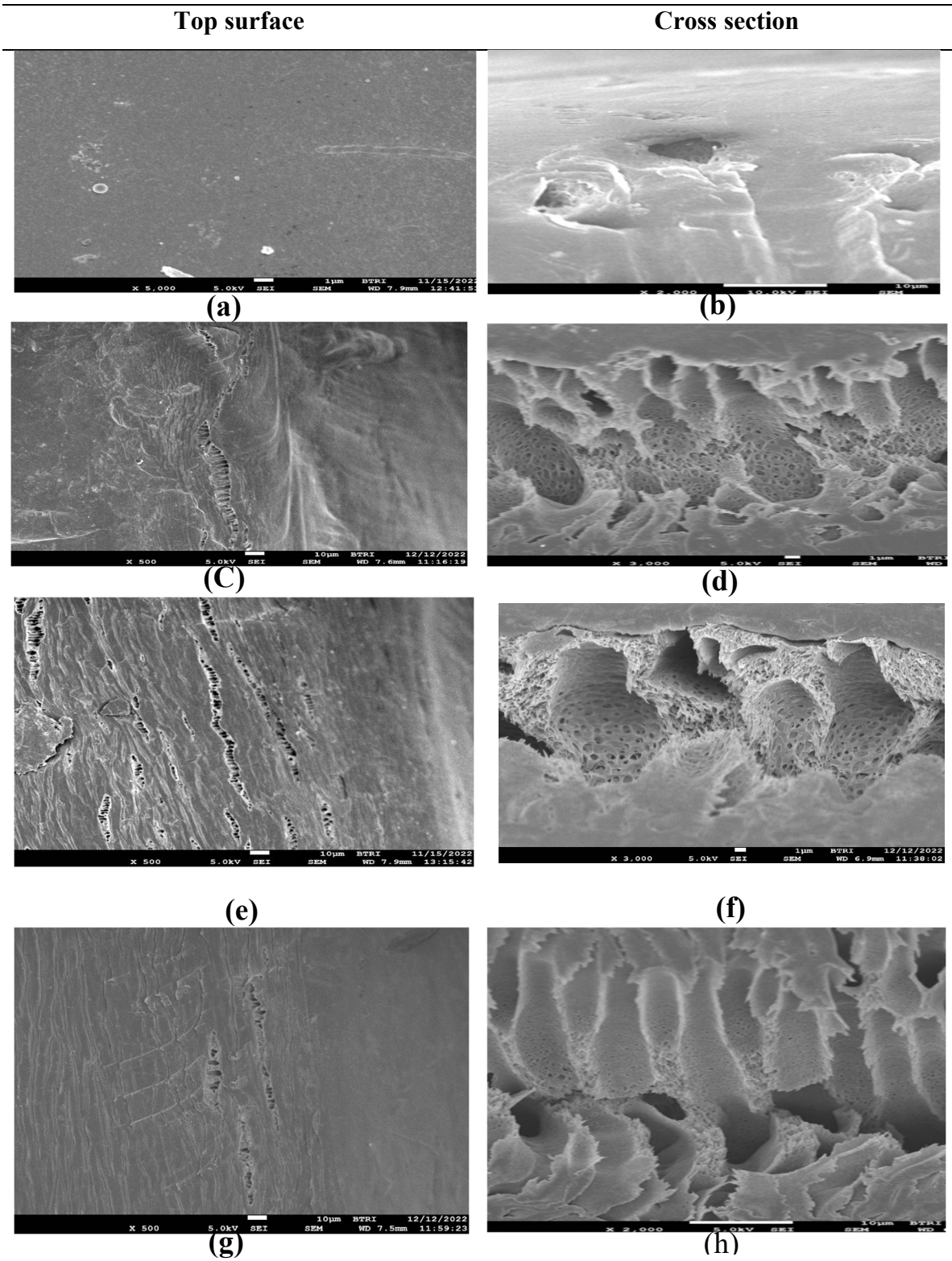

Fig 3.3: Surface (Left) images of membranes: (a) Control, (c) PSF-1PEG, (e) PSF-5PEG, and (g) PSF-10PEG and Cross-section (right) images of membranes: (b) Control, (d) PSF-1PEG, (f) PSF-5PEG, and (h) PSF-10PEG

Top surface	Cross section

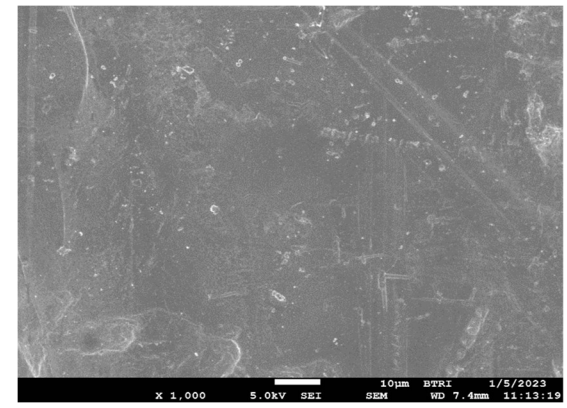

(a)

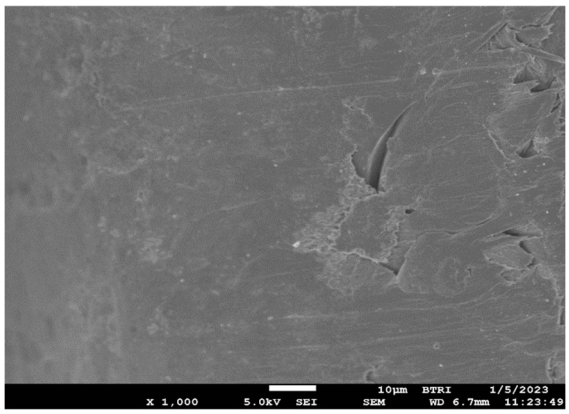

(b)

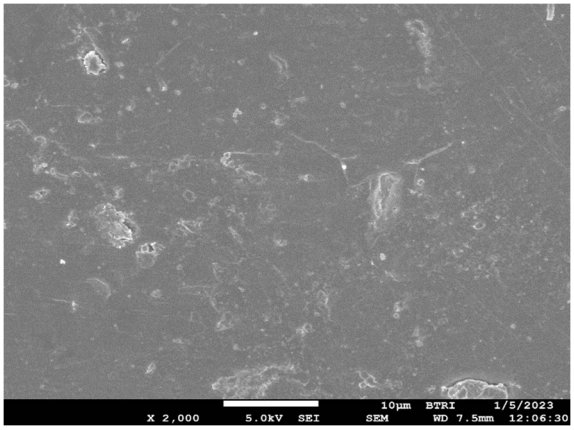

(c)

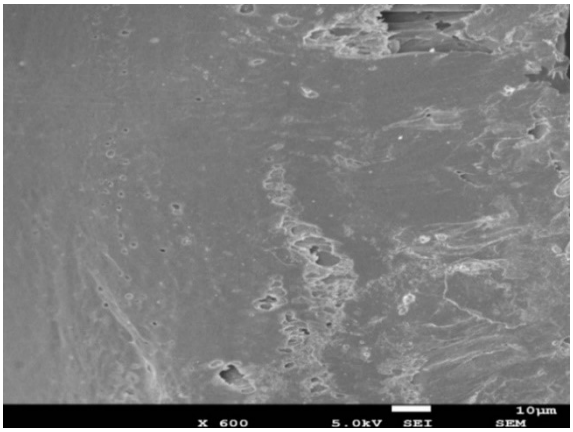

(d)

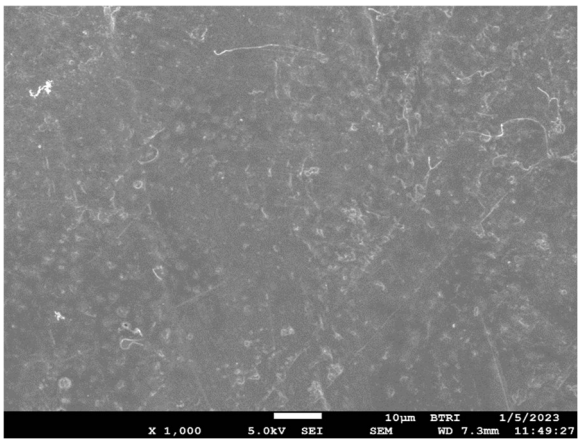

(e)

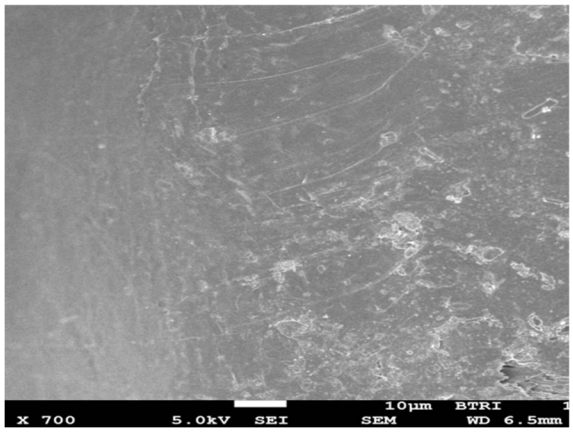

(f)

Fig 3.4: Surface (Left) images of membranes: (a) PSF-1SA, (c) PSF-5SA, and (e) PSF-10SA and Cross-section (right) images of membranes: (b) PSF-1SA, (d) PSF-5SA, and (f) PSF-10SA

3.4 Pore size measurement of PSF blended membranes

Pore sizes of various fabricated membranes (Fig 3.5 and Table 3.3) were measured by gravimetric method. The average pore size of the control membrane was 0.12 µm, which increased with the addition of PEG, and the highest pore size of 3.1 µm was obtained at 5 % wt. PEG addition. However, increasing the PEG concentration beyond this point resulted in smaller pore sizes because it slowed down the exchange of solvent and non-solvent during the demixing process (Mulyati et al., 2017). The same trend in pore size was observed with the addition of SA in the current study.

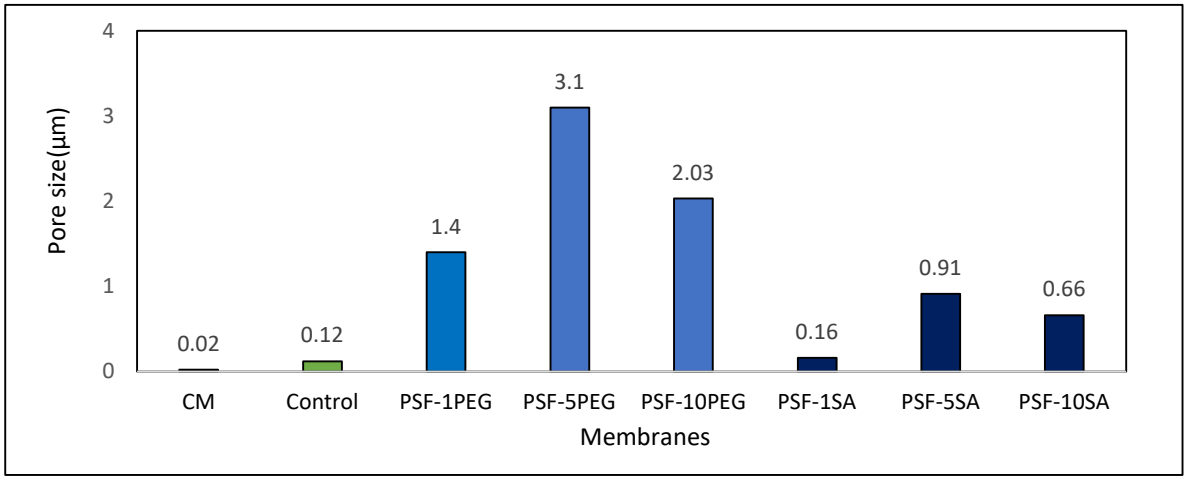

Fig 3.5: Pore size of PSF blended membranes

SA molecule having higher molecular weight and more complex structure than the PEG molecule might have a slower diffusion rate. This could result in the formation of a denser membrane (Chakrabarty et al., 2008). Therefore, it was hypothesized that PEG has a greater ability to form pore than SA.

Table 3.3: Pore size data of PSF blended membranes

Sl. No.	Membrane	Pore size (µm)
1	CM	0.02
2	Control	0.12
3	PSF-1PEG	1.4
4	PSF-5PEG	3.1
5	PSF-10PEG	2.03
6	PSF-1SA	0.16
7	PSF-5SA	0.91
8	PSF-10SA	0.66

3.5 Atomic force microscopy (AFM) of PSF blended membranes

Fig 3.6 displays the 3D AFM images of the membrane surfaces, with topographical features studied across an image area of 10.30µm x 10.30µm. The surface roughness of control and composite membranes were determined by analyzing the AFM images with SPM control software version 3.1 throughout the scanned area of the film surface. The addition of PEG decreased the surface roughness, whereas the addition of SA increased the roughness. The reason for the increased roughness of the SA-blended membrane could be due to the uneven mixing of SA with the PSF solution, as shown in Fig 3.7.

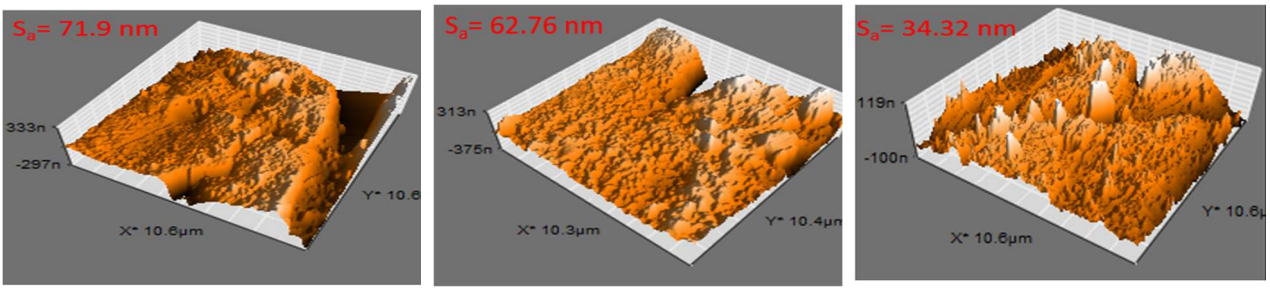

PSF-5SA Control PSF-5PEG

Fig 3.6: AFM images of PSF blended membranes

When fabricating the PSF-SA dope solution, dispersion of small particles were obtained whereas a homogeneous solution was obtained for the PSF-PEG dope solution. It was concluded that PEG created a smoother surface on the membrane.

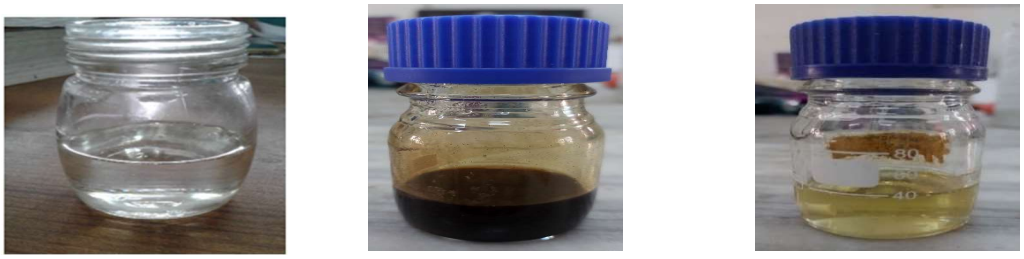

a. PSF solution b. PSF-5SA dope solution c. PSF-5PEG dope solution

Fig 3.7: Images of dope solutions using DMF as solvent

The homogeneity of a solution is dependent on the solubility parameters (Hołda et al., 2015). If the solubility parameters of two materials are similar, they tend to exhibit a strong attraction or

affinity towards each other. Table 3.4 lists the solubility parameters of PSF, PEG, SA, DMF, and water.

Table 3.4: Solubility parameters of PSF, PEG, SA, DMF, and water

Sl. No.	Material	Solubility parameter ($MPa^{1/2}$)
1	PSF	21.2
2	PEG-6k	35.3
3	SA	37
4	DMF	24.8
5	Water	47.8

Table 4.4 indicated that PSF-PEG can be dissolved more easily in DMF than PSF-SA due to their closer solubility parameters to DMF. Therefore, the PSF-PEG mixture produced a more homogeneous dope solution than the PSF-SA dope solution (Fig 3.7).

3.6 Equilibrium water content (EWC) and membrane porosity of PSF blended membranes

Equilibrium water content is a method for characterizing membranes that measures how much water the membrane can hold compared to its total volume. It states the fraction of void space relative to the apparent total bulk volume of the material (Espinal, 2012). Equilibrium water content of different membranes (Table 3.5) was determined by the percentage of water uptake. When PEG and SA were added to the membranes, their equilibrium water content (EWC) increased compared to the control membrane. This indicated that the modified membranes had more pores. The porosity of the different composite membranes was shown in Fig 3.8, and it was clear that porosity increased as the additive concentration increased up to 5 %. However, increasing the amount of additive beyond 5% resulted in a decrease in porosity.

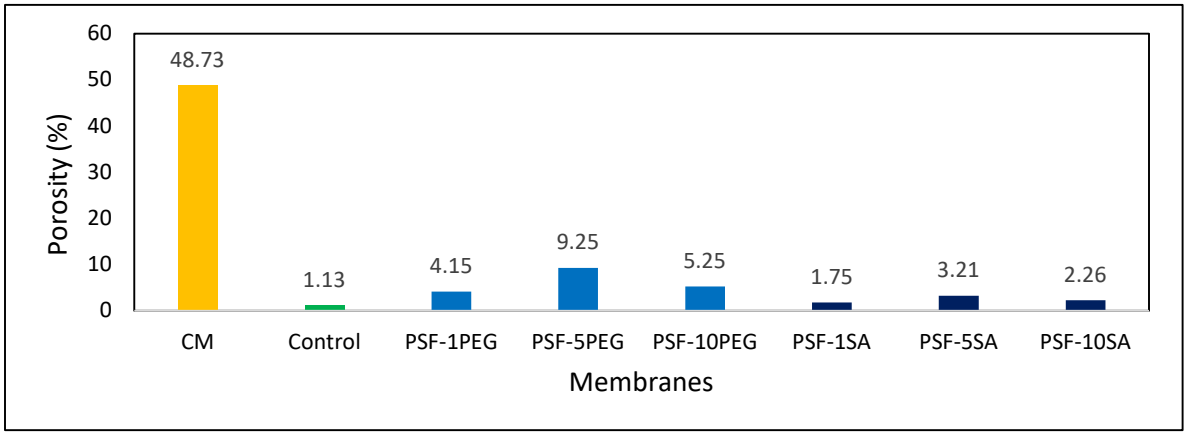

Fig 3.8: Percentage of porosity of different membranes

It was assumed that due to their hydrophilic nature PEG and SA accelerated the solvent/non-solvent mass transfer that led to the formation of highly porous structures. However, after certain concentration of additives, porosity was declined due to the increasing viscosity that slowed down the coagulation process and afforded less porosity (Rashid et al., 2022).

Pore forming agents work by interacting with water vapors during membrane casting that leads to the nucleation of emulsion drops, which grow and coalesce to create pores on the membrane surface. The hydrophilic additives in the dope solution are responsible for this process (Malik et al., 2019). PEG, having a low molecular weight than SA, easily washes out with the solvent from the membrane film in the coagulation bath. In contrast, SA takes more time to reach the surface providing enough time for polymer aggregates on top layer to form a thicker layer (Aminudin et al., 2013).

Table 3.5: Percentage of porosity and EWC of different membranes of PSF blended membranes

Sl. No.	Membrane	Porosity (%)	Equilibrium water content (EWC, %)
1	CM	48.73	39
2	Control	1.13	1.48
3	PSF-1PEG	4.15	5.45
4	PSF-5PEG	9.25	9.78
5	PSF-10PEG	5.25	7.67
6	PSF-1SA	1.75	2.34
7	PSF-5SA	3.21	4.23
8	PSF-10SA	2.26	2.92

3.7 Pure water flux of PSF blended membranes

The pure water flux of fabricated membranes (Fig 3.9 and Table 3.6) was measured by crossflow filtration and were performed at 3 bar pressure which showed that flux was affected by the concentration of additives to the casting solution.

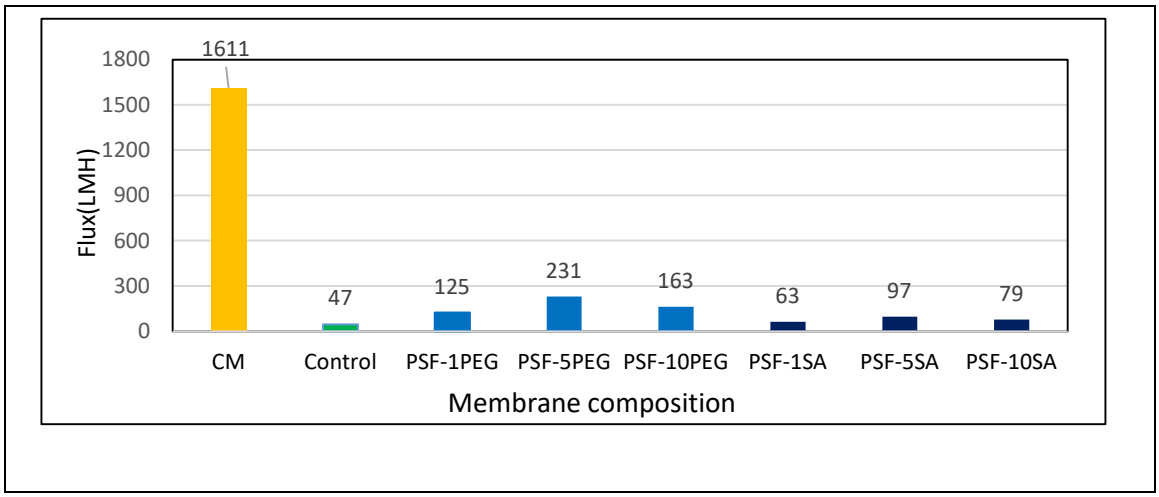

Fig 3.9: **Pure water fluxes of PSF blended membranes at 3 bar**

Table 3.6: Pure water fluxes data of PSF blended membranes

Sl. No.	Membrane	Flux (L/m^{2}h) @ 3 bar
1	CM	1611
2	Control	47
3	PSF-1PEG	125
4	PSF-5PEG	231
5	PSF-10PEG	163
6	PSF-1SA	63
7	PSF-5SA	97
8	PSF-10SA	79

At each pressure, the flux increased for membrane containing 5% for each additive, indicating instantaneous demixing due to the increased thermodynamic instability of the dope solution. However, beyond this additive concentration, the fluxes of both types of blended membranes decreased which could be attributed to the increased viscosity of the casting solution that in turn decreased the rate of solvent and non-solvent interchange in the demixing process and caused delayed demixing. This phenomenon resulted a dense top layer (SEM Fig 3.3 and Fig 3.4) with suppressed pore sizes (Mulyati et al., 2017). It was also observed that the pure water flux of PSF-PEG membranes was higher than the PSF-SA membranes, which may be attributed to the higher porosity of the PEG blended membranes.

3.8 Contact angle of PSF blended membranes

The contact angle of a liquid droplet on a surface is a way to measure the surface tension between the liquid and solid surface. A high contact angle indicates a high surface tension between the two surfaces, while a low contact angle indicates a low surface tension. Contact

angles of control and composite membranes (Fig 3.10) were measured using the in-house built contact angle device. A comparison between contact angle measurements between an in-house built device and a commercial device is presented in Table 3.7, revealing a high degree of comparability between the two measurements. The control membrane (23 wt.% PSF) had an average contact angle of 79±2°.

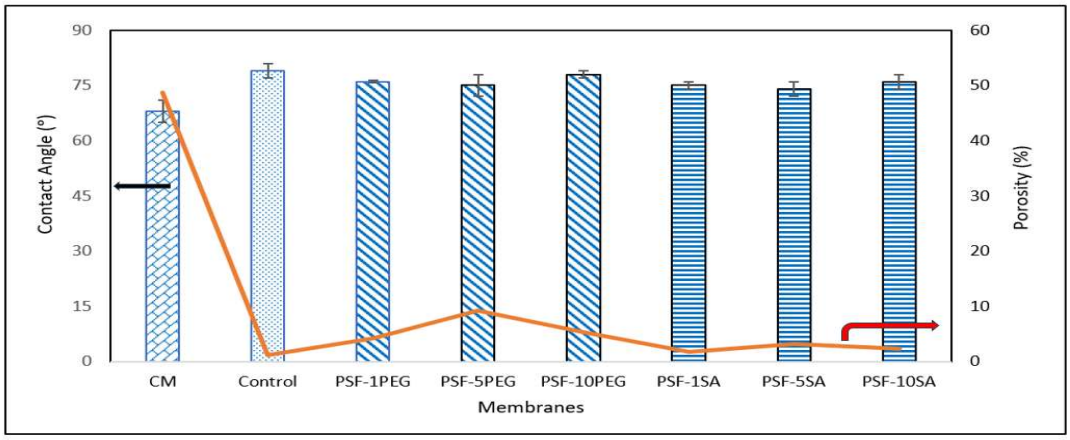

Fig 3.10: Contact angle of PSF blended membranes (average contact angle of three replicates are reported)

For the PSF-PEG membranes, the contact angle decreased as the PEG concentration increased from 1 to 5 wt.% and then increased as the PEG concentration went up from 5 to 10 wt.%. This increase in contact angle values was linked to the decrease in porosity, which was achieved at higher dope solution viscosity (Aljanabi et al., 2022).

Table 3.7: Comparison of contact angles (°) measured with inhouse device and commercial device for PSF blended membranes

Sl. No.	Membrane	Inhouse Contact angle (°)	Goniometer KYOWA Dme-211plus
1	Control	79±2	77±2
2	PSF-1PEG	76±0.35	78±3
3	PSF-5PEG	75±3	76±1
4	PSF-1SA	75±1	73±3
5	PSF-5SA	74±2	75±3

Similar trends in contact angle for PSF-SA membranes were observed. In comparison, membranes blended with SA showed slightly more hydrophilicity than those blended with PES due to the hydroxyl groups present in the SA structure.

3.9 Tensile strength of PSF blended membranes

Fig. 3.11 shows the tensile strength (N/mm^2) of PSF blended membranes. Control PSF membrane had tensile value of 34 N/mm^2. After addition of PEG and SA up to 5 wt.%, the tensile values decreased due to increased porosity (Wang et al., 2017). However, beyond 5 wt.% of PEG and SA, the porosity of the fabricated membranes decreased because of the increased viscosity of the casting solution, resulting in an increase in tensile strength.

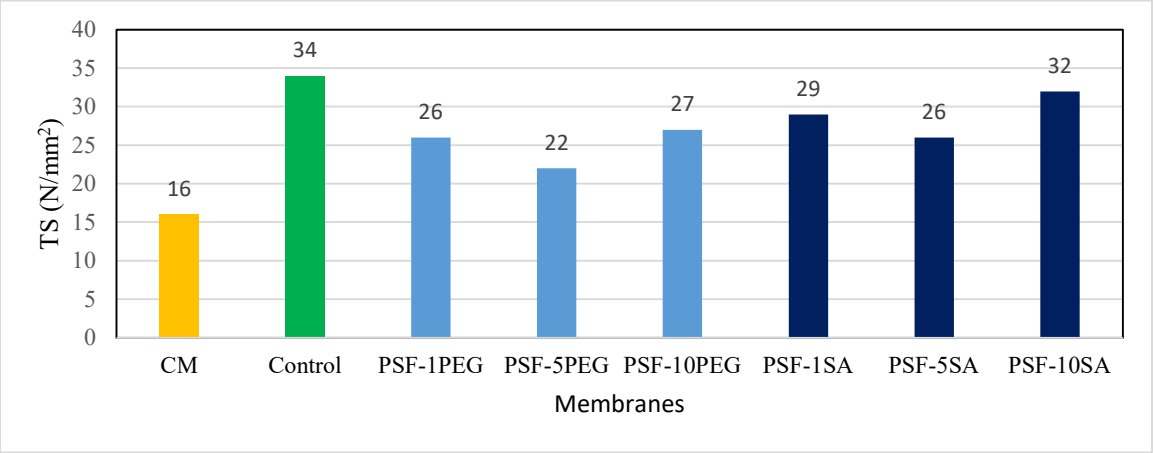

Fig 3.11: Tensile strengths of PSF blended membranes

3.10 Wastewater treatment by MBR using PSF blended membranes and PES based commercial membrane (CM)

3.10.1 Characteristics of synthetic textile wastewater

Synthetic wastewater was prepared following the literatures ((Luong et al., 2016) and (Işik et al., 2008)) and shown in Fig 3.12. The characteristics of synthetic textile wastewater are presented in Table 3.8. Activated sludge was collected from a textile industry located at Savar EPZ, Dhaka, Bangladesh, mixed with the synthetic textile wastewater to attain a MLSS concentration within the range of 4-6 g/L.

Fig 3.12: Color of the synthetic textile dye

Table 3.8: Characteristics of synthetic textile wastewater in the MBR tank

Parameter	Value
Turquoise blue dye ($C_{40}H_{21}CuN_9Na_4O_{14}S_5$) (mg/L)	100
pH	8.04
COD (mg/L)	6300
BOD_5 (mg/L)	3024
Conductivity (ms/cm)	8.1
MLSS (g/L)	4-5

3.10.2 pH change of permeate of CM and PSF blended membranes

Fig 3.13 and Table 3.9 show the variation of pH during the MBR process employing fabricated PSF-based and commercial membranes (CM). The pH of the permeate of all membranes during MBR treatment showed a decreasing trend up to 30 days after that the pH again increased.

This was due to the production of CO_2 by aerobic degradation of organic matters in the MBR which reacted with the water and formed H_2CO_3 acid that was responsible for gradual decreased of pH. However, after 30 days, as the biological activities of the biomass decreased (H.-D. Park et al., 2015), the aerobic process also decreased. This leading to a decline in the production of H_2CO_3 acid and subsequently pH increased.

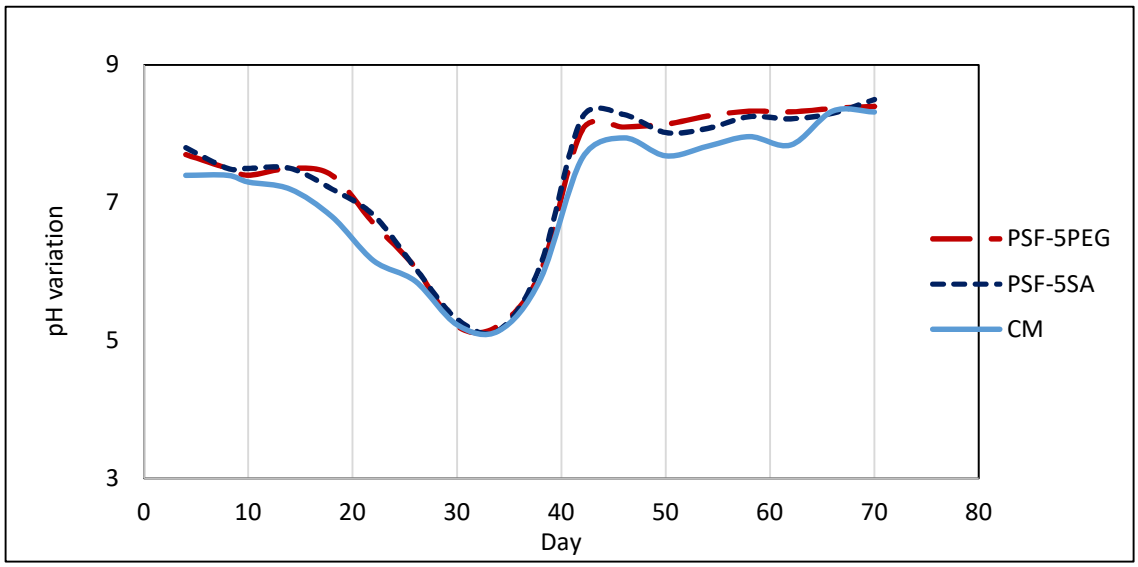

Fig 3.13: Variations of pH of permeate from CM and PSF blended membranes

Table 3.9: pH variations data of permeate from CM and PSF blended membranes

Day	Raw pH of synthetic wastewater	pH of permeate		
		PSF-5PEG	PSF-5SA	CM
4	8.04	7.7	7.8	7.4
8	8.04	7.5	7.5	7.4
10	8.04	7.4	7.5	7.3
14	8.04	7.5	7.5	7.2
18	8.04	7.4	7.2	6.8
22	8.04	6.7	6.82	6.16
26	8.04	6.06	6.05	5.86
30	8.04	5.21	5.31	5.23
34	8.04	5.22	5.15	5.14
38	8.04	6	6.1	5.9
42	8.04	8.06	8.24	7.65
46	8.04	8.1	8.28	7.94
50	8.04	8.14	8.02	7.68
54	8.04	8.26	8.08	7.82
58	8.04	8.33	8.25	7.96
62	8.04	8.32	8.22	7.84
66	8.04	8.37	8.3	8.33
70	8.04	8.4	8.5	8.32

3.10.3 COD removal of permeate from CM and PSF blended membranes

Fig 3.14 and Table 3.10 show the comparison of the performance of commercial (CM) and blended membranes (PEG and SA based PSF membranes) regarding COD removal efficiency throughout the entire experimental study.

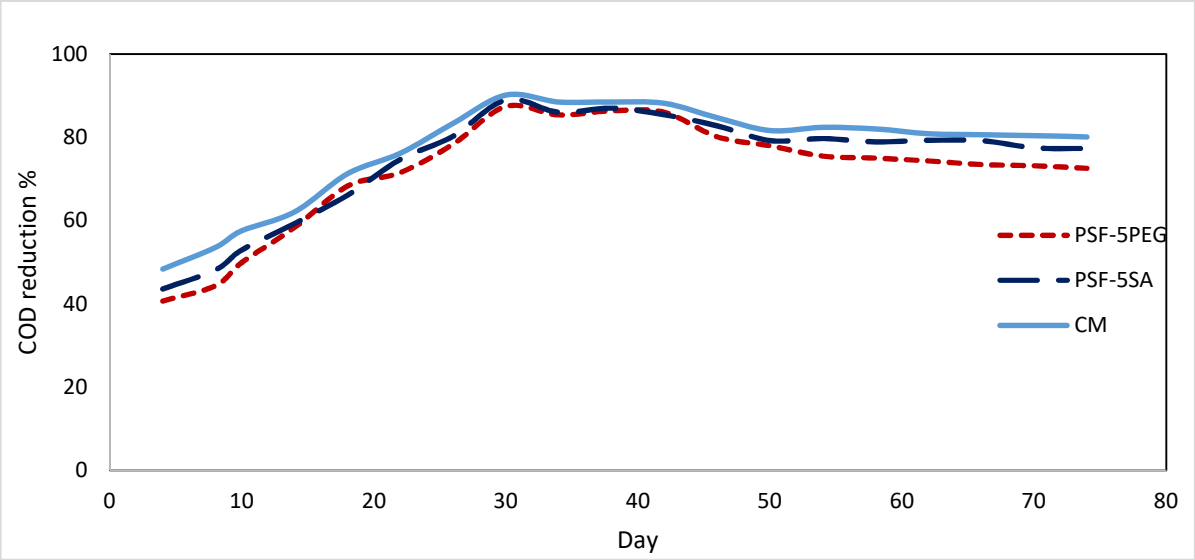

Fig 3.14: COD removal of permeate from CM and PSF blended membranes

After 30 days of operation, the highest percentage of COD removal were consistently observed for all membranes, demonstrating excellent agreement reaching up to 87.48%, 89.05%, and 90.21% COD removal by PSF-PEG, PSF-SA, and CM membranes, respectively. The reason behind this is that MBR operated longer than 30 days and cannot take advantages of long SRT due to decrease of biological activity of biomass (H.-D. Park et al., 2015).

Table 3.10: COD data of permeate from CM and PSF blended membranes

Day	Raw COD of synthetic (mg/l)	COD of permeate					
		PSF-5PEG (mg/l)	PSF-5PEG Reduction %	PSF-5SA (mg/L)	PSF-5SA Reduction %	CM (mg/L)	CM Reduction %
4	6300	4366	30.70	4183	33.60	3881	38.40
8	6300	4133	34.40	4082	35.21	3553	43.60
10	6300	3780	40.00	3591	43.00	3301	47.60
14	6300	3250	48.41	3190	49.37	3017	52.11
18	6300	2626	58.32	2321	63.16	2441	61.25
22	6300	1790	71.59	1591	74.75	1625	74.21
26	6300	1360	78.41	1240	80.32	1045	83.41
30	6300	789	87.48	690	89.05	617	90.21
34	6300	919	85.41	879	86.05	723	88.52
38	6300	856	86.41	816	87.05	723	88.52
42	6300	879	86.05	915	85.48	743	88.21
46	6300	1250	80.16	1084	82.79	961	84.75

50	6300	1386	78.00	1307	79.25	1154	81.68
54	6300	1542	75.52	1276	79.75	1108	82.41
58	6300	1572	75.05	1326	78.95	1131	82.05
62	6300	1615	74.37	1303	79.32	1204	80.89
66	6300	1670	73.49	1307	79.25	1217	80.68
70	6300	1688	73.21	1416	77.52	1232	80.44

3.10.4 BOD_5 removal of permeate from CM and PSF blended membranes

The BOD_5 removal percentage of effluent by MBR is illustrated in Fig 3.15 with corresponding data provided in Table 3.11.

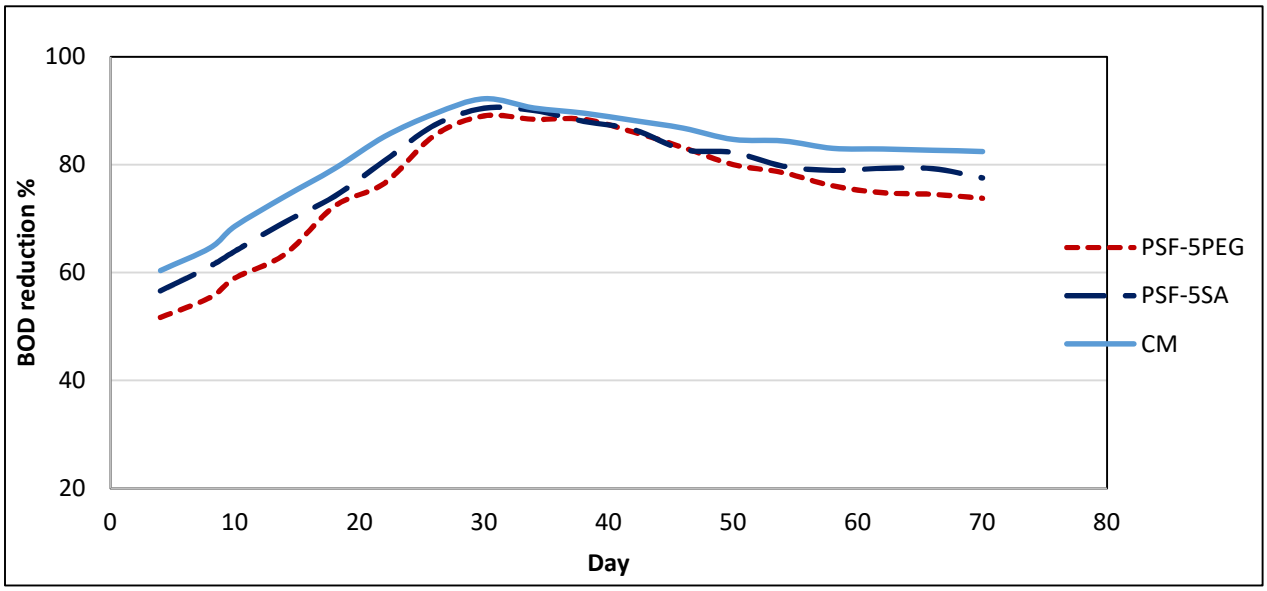

Fig 3.15: **BOD_5 removal of permeate from CM and PSF blended membranes**

Following a 30-day operational period, remarkable consistency was observed in achieving the highest BOD_5 removal for all membranes exhibiting notable BOD_5 removal percentage of 89.05%, 90.48%, and 92.20%, by PSF-PEG, PSF-SA, and CM membranes, respectively.

Table 3.11: BOD_5 data of permeate from CM and PSF blended membranes

Day	Raw BOD_5 of synthetic wastewater (mg/L)	BOD_5 of permeate					
		PSF-5PEG (mg/L)	PSF-5PEG Reduction %	PSF-5SA (mg/L)	PSF-5SA Reduction %	CM (mg/L)	CM Reduction %
4	3024	1461	51.69	1312	56.61	1198	60.38
8	3024	1349	55.39	1174	61.18	1071	64.58
10	3024	1240	58.99	1089	63.99	950	68.58
14	3024	1106	63.43	926	69.38	783	74.11
18	3024	837	72.32	781	74.17	627	79.27
22	3024	708	76.59	582	80.75	447	85.22
26	3024	441	85.42	383	87.33	320	89.42
30	3024	331	89.05	288	90.48	236	92.20
34	3024	350	88.43	301	90.05	286	90.54
38	3024	350	88.43	362	88.03	317	89.52
42	3024	422	86.04	409	86.47	357	88.19
46	3024	509	83.17	520	82.80	400	86.77
50	3024	604	80.03	536	82.28	463	84.69
54	3024	649	78.54	613	79.73	471	84.42
58	3024	724	76.06	637	78.94	513	83.04
62	3024	762	74.80	625	79.33	517	82.90
66	3024	771	74.50	627	79.27	523	82.71
70	3024	793	73.78	679	77.55	530	82.47

3.10.5 Color removal of permeate from CM and PSF blended membranes

The color removal efficiencies of PSF-PEG, PSF-SA, and commercial (CM) membranes are demonstrated in Fig 3.16 and Table 3.12. The highest color removal was observed after 30 days of operation exceeding more than 70% by PSF-PEG and PSF-SA fabricated membranes whereas, about 90% was achieved by the CM membrane. However, the efficiencies gradually decreased due to declining biological activities of biomass since MBR system cannot take advantage of SRT longer than 30 days (H.-D. Park et al., 2015). As the CM membrane has a lower pore size than the fabricated membranes, it exhibited higher color removal.

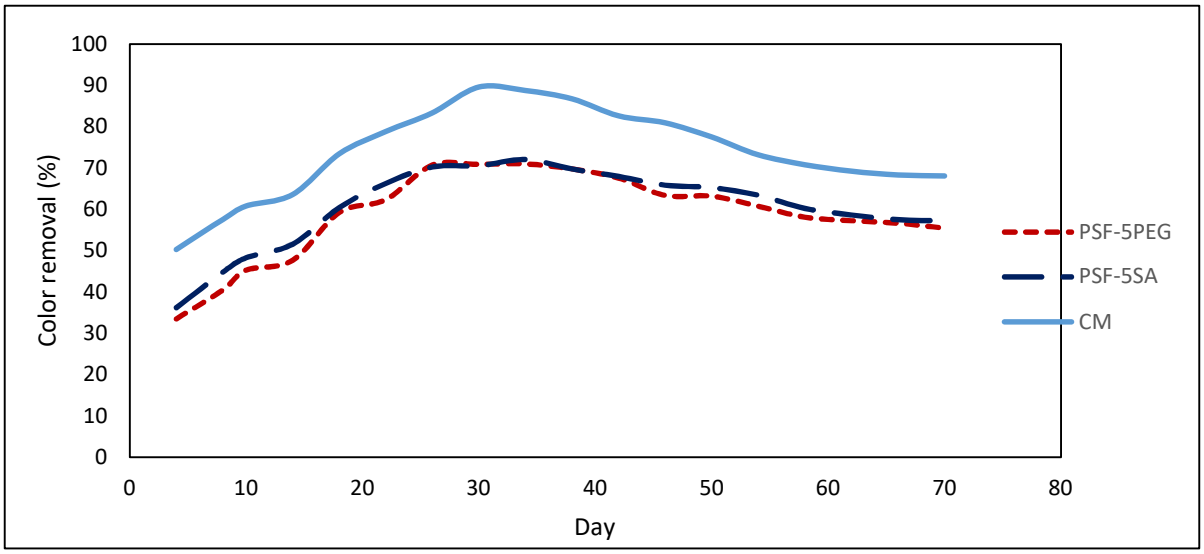

Fig 3.16: Color removal efficiencies of permeate of CM and PSF blended membranes

Table 3.12: Color removal data of permeate from CM and PSF blended membranes

Day	Dye concentration (mg/L)	Dye concentration in permeate					
		PSF-5PEG (mg/L)	Reduction %	PSF-5SA (mg/L)	Reduction %	CM (mg/L)	Reduction %
4	100	67	33	64	36	50	50
8	100	60	40	55	45	42	58
10	100	55	45	52	48	39	61
14	100	52	48	48	52	36	64
18	100	41	59	40	60	27	73
22	100	38	62	34	66	21	79
26	100	29	71	30	70	17	83
30	100	29	71	29	71	10	90
34	100	29	71	28	72	11	89
38	100	30	70	30	70	13	87
42	100	32	68	32	68	17	83
46	100	37	63	34	66	19	81
50	100	37	63	35	65	22	78
54	100	39	61	37	63	27	73
58	100	42	58	40	60	29	71
62	100	43	57	41	59	31	69
66	100	43	57	42	58	32	68
70	100	45	55	43	57	32	68

Fig 3.17 shows the color of permeate from fabricated and commercial membranes.

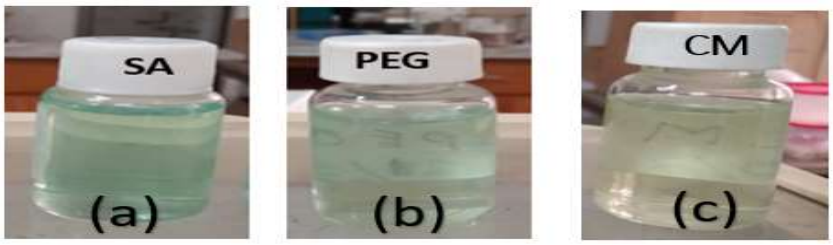

Fig 3.17: Visual representation of color removal by using (a) PSF-SA membrane (b) PSF-PEG membrane, and (c) commercial membrane

3.10.6 MBR Fluxes of CM and PSF blended membranes

In Fig 3.18 and Table 3.13, the fluxes of PSF-PEG, PSF-SA, and commercial membranes (CM) are presented. The fabricated membranes exhibited lower permeate fluxes compared to the commercial one due to their reduced porosity. On average, membranes blended with PEG and SA demonstrated fluxes of 14% and 8% of that observed for commercial membrane (CM).

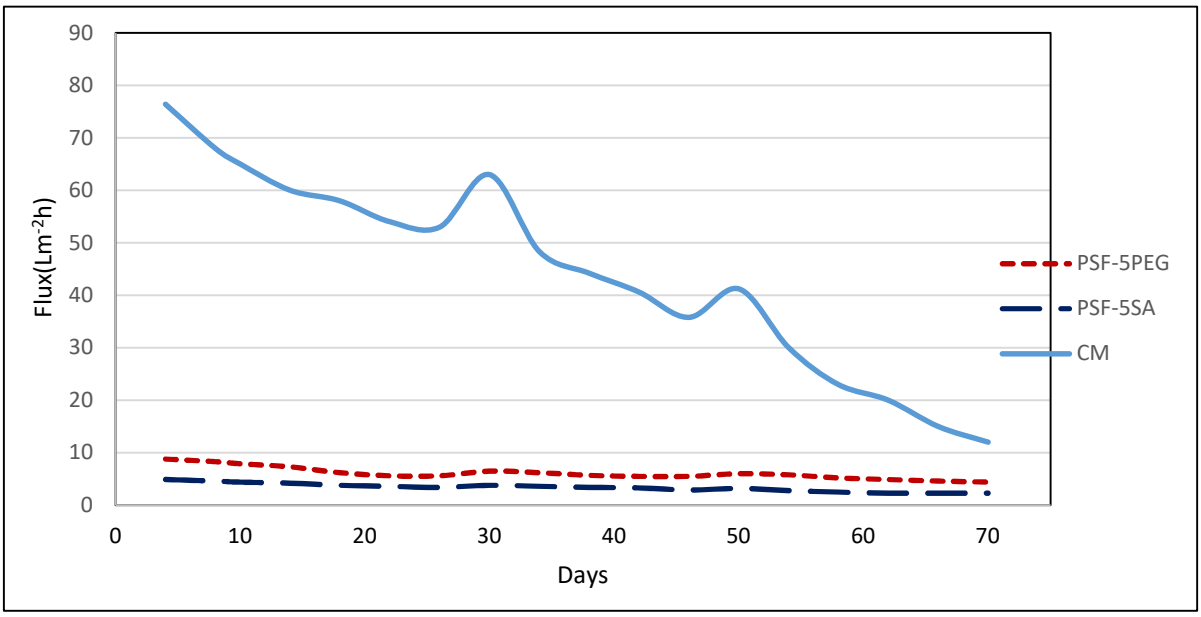

Fig 3.18: Fluxes of MBR permeate of CM and PSF blended membranes

At 30 and 50 days, the fluxes of all the membranes exhibited improved fluxes which was attributed to the physical cleaning by backflushing and washing.

Table 3.13: MBR fluxes data of CM and PSF blended membranes

Day	PSF-5PEG (L/m^2h)	PSF-5SA (L/m^2h)	CM (L/m^2h)
4	8.8	4.9	76.4
8	8.3	4.6	68
10	7.9	4.4	65
14	7.32	4.2	60
18	6.2	3.8	58
22	5.6	3.6	54
26	5.6	3.4	53
30	6.5	3.8	63
34	6.2	3.6	48.3
38	5.7	3.4	44.2
42	5.5	3.3	40.6
46	5.5	2.9	35.8
50	6	3.2	41.2
54	5.8	2.8	30
58	5.2	2.5	23
62	4.9	2.3	20
66	4.6	2.3	15
70	4.4	2.3	12

A membrane before and after MBR running was illustrated in Fig 3.19 and showed that membranes also adsorbed color.

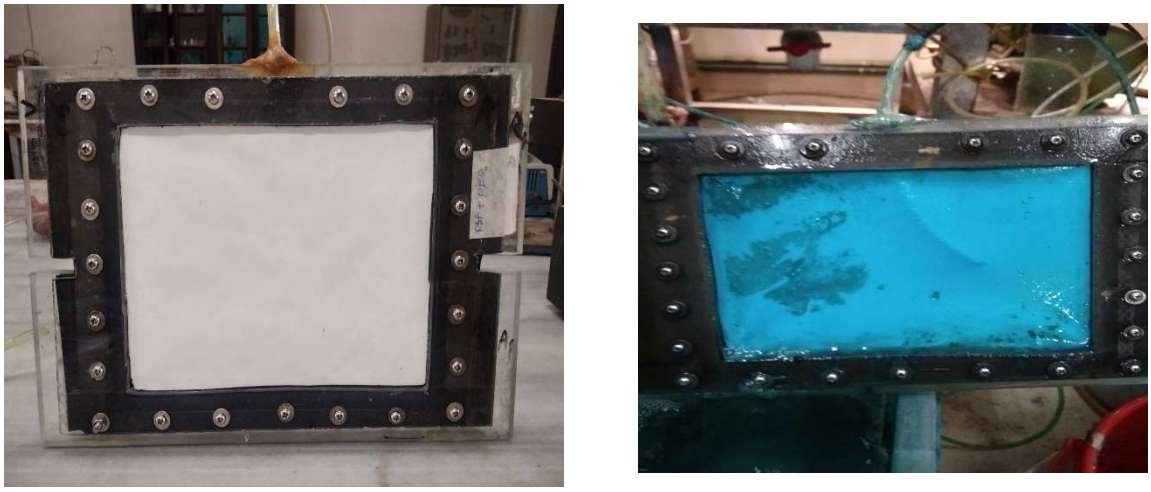

Fig 3.19: Membrane (a) before and after treatment (b)

Part 2 PES based membranes

In part 2, Polyethersulfone (PES) based polymeric membranes were fabricated incorporating polyethylene glycol (PEG) and polyvinylpyrrolidone (PVP) as additives using dimethylformamide (DMF) as solvent and water as non-solvent.

3.11 Effects of PES concentration on membrane skin formation

Dope solutions of PES concentrations ranging from 15 to 19 wt.% were applied onto the support material. Remarkably, it was noted that only the 19 wt.% polymer concentration resulted in a consistently uniform skin on the support material, as illustrated in Fig 3.20a and detailed in Table 3.14. On the other hand, a membrane with a 15 wt.% concentration exposed the fibers of the support material, as depicted in the magnified image of Fig 3.20c.

(a) 15 wt.% PES

(b) 17 wt.% PES

(c) 19 wt.% PES

Fig 3.20: **Effect of PES concentration on membrane skin formation (magnification was done by a tinyscope 1000x mobile microscope)**

At 19 wt.%, the viscosity of the cast solution was enough to form a uniform film on the support material while below this concentration, it is evident that the cast solution did not cover the support material efficiently.

Table 3.14: Effect of PES concentration on membrane skin formation

Sl. No.	PES (wt.%)	PEG (wt.%)	PVP (wt.%)	Solvent (DMF wt. %)	Membrane condition
1	15	-	-	85	Formed double layer
2	17	-	-	83	Formed double layer
3	19	-	-	81	No formation of double layer

The influence of additive concentration on pure water flux is outlined in Table 3.15, indicating the addition of PEG resulted in a flux increase of at least 2.7-fold, while the inclusion of PVP led to a flux enhancement of at least 1.3-fold compared to the control membrane.

Table 3.15: Effect of additive concentration on PES blended membrane performance

Sl. No.	Code	PES (wt.%)	PEG (wt.%)	PVP (wt.%)	Solvent (DMF wt. %)	Membrane performance
1	PES-1PEG	19	1	-	80	2.7 × water flux than control membrane
2	PES-3PEG		3	-	78	5.9 × water flux than control membrane
3	PES-5PEG		5	-	76	4.1 × water flux than control membrane
4	PES-7PEG		7	-	74	3.3 × water flux than control membrane
5	PES-1PVP		-	1	80	1.3 × water flux than control membrane
6	PES-3PVP		-	3	78	2.4 × water flux than control membrane
7	PES-5PVP		-	5	76	2.9 × water flux than control membrane
8	PES-7PVP		-	7	74	1.9 × water flux than control membrane

3.12 FTIR Analysis of PES blended membranes

FTIR/ATR spectra of PES-control membrane, PES-PEG, and PES-PVP blended membranes are illustrated in Fig. 3.21 and found that PES-control membrane exhibited distinct peaks. Peaks at 1577 cm^{-1} and 3068 cm^{-1} corresponds to the presence of aromatic ring, while the peak at 1247 cm^{-1} represented ether group. The sulfonyl group is identified through two stretching vibration at 1153 and 1105 cm^{1}. These spectral features of PES is aligned well with the previous studies on PES FTIR (Qu et al., 2010; Şimşek et al., 2016; Alenazi et al., 2018).

For PES-control and PES-PEG, weak vibration at 1670 cm^{-1} may be attributed to the C=O group of the polyester material of Hollytex-3256 support material. Similar to PES-control membrane,

the presence of aromatic rings in PES-PEG (Fig. 3.21b) and PES-PVP (Fig. 3.21c) membranes were identified by peaks around 3030-3100 cm^{-1}, corresponding to aromatic C-H stretching vibrations and characteristics stretching vibrations of aliphatic C-H bond were observed in all the membranes at around 2800 to 3000 cm^{-1}. For PES-PVP membrane a strong C=O stretching group was observed at 1668 cm [1] (Fig. 3.21c).

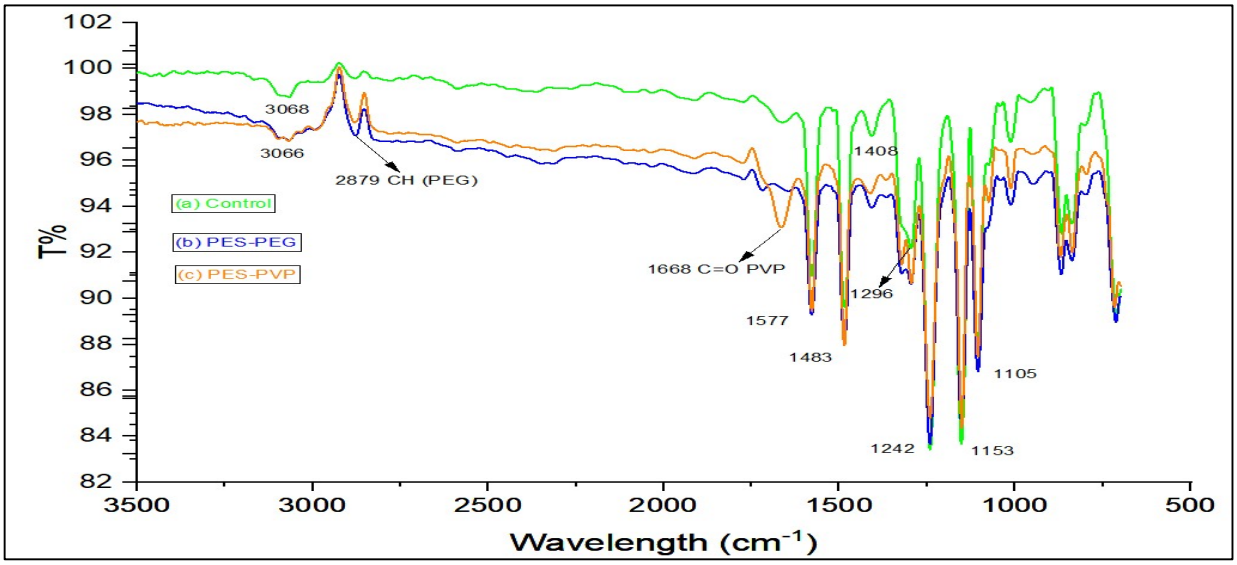

Fig 3.21: FTIR/ATR spectra of (a) control membrane, (b) PES-PEG membrane (e) PES-PVP membrane.

A distinct peak at 1670 cm^{-1} was identified in the control membrane (Fig 3.21 a), corresponding to the C=O group of the support material, which is composed of polyester fabric.

3.13 SEM Analysis of PES blended membranes

In Fig 3.22, the FE-SEM images depict the control and PES-PEG blended membranes. The control membrane reveals a top dense layer (Fig 3.22b) characterized by a nonporous surface (Fig 3.221a). Introducing PEG as an additive enhances membrane porosity, reaching its maximum at a PEG concentration of 3 wt.%. However, beyond this concentration, porosity diminishes due to the increasing viscosity of the dope solution. This infers that up to a 3 wt.% concentration of PEG, the diffusion rate of non-solvent and solvent exchange is optimized, facilitating instantaneous demixing and the formation of a porous membrane. Conversely, at higher additive concentrations, the elevated viscosity impedes the process, leading to delayed demixing and a subsequent reduction in membrane porosity (Mulyati et al., 2017).

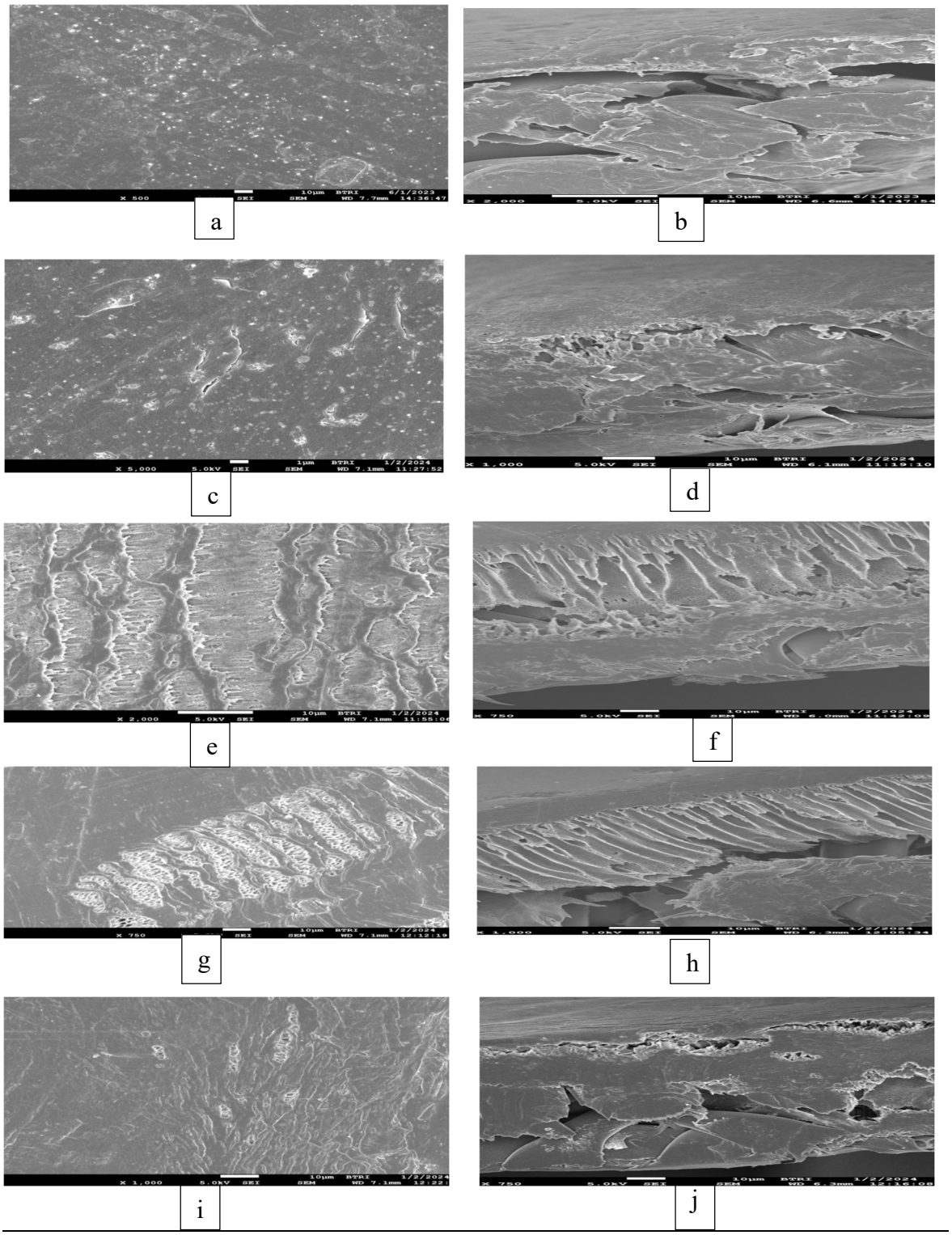

Fig 3.22: Surface (Left) images of membranes: (a) Control, (c) PES-1PEG, (e) PES-3PEG, (g) PES-5PEG, and (i) PES-7PEG and Cross-section (right) images of membranes: (b) Control, (d) PES-1PEG, (f) PES-3PEG, (h) PES-5PEG and (j) PES-7PEG

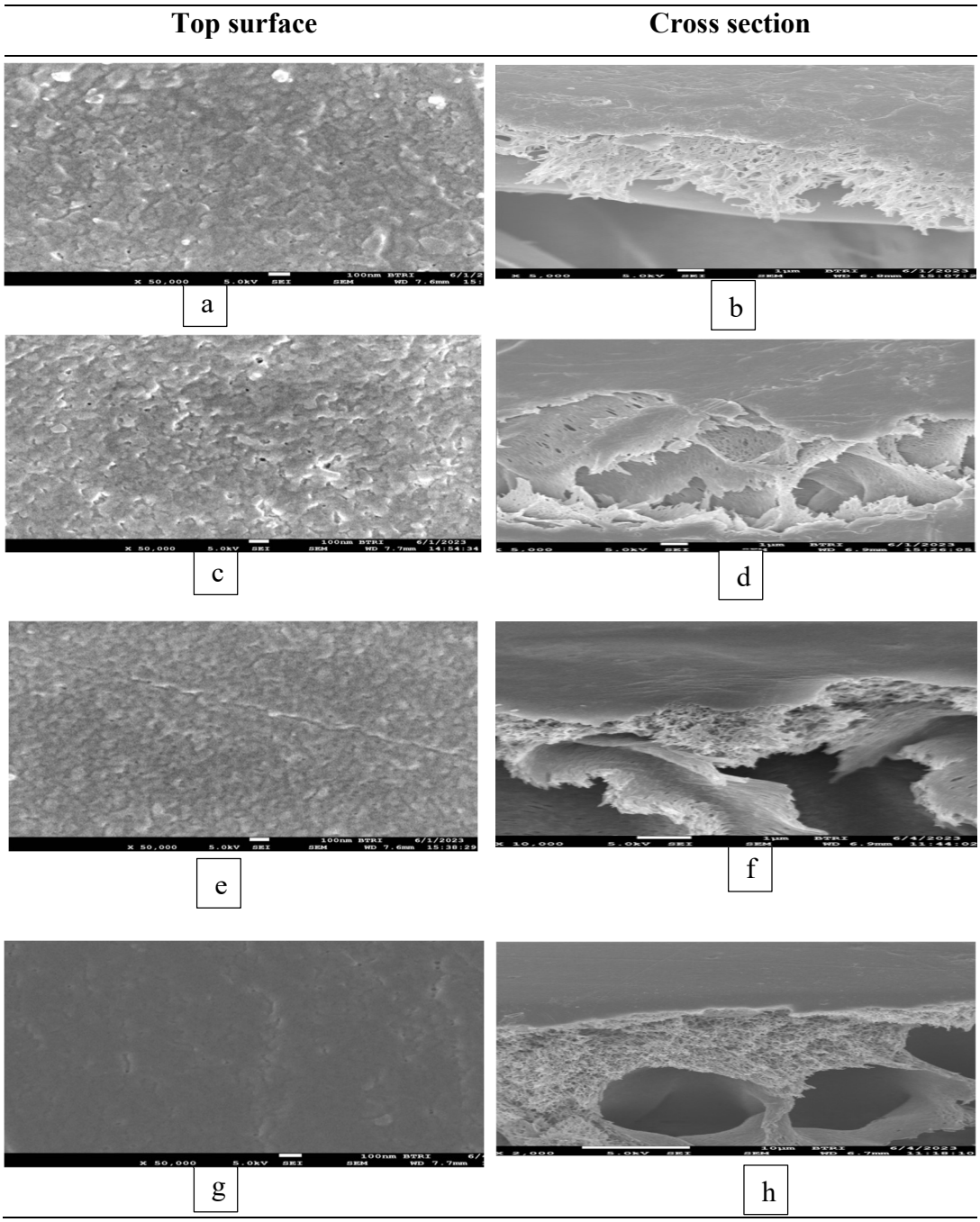

Fig 3.23: Surface (Left) images of membranes: (a) PES-1PVP, (c) PES-3PVP, (e) PES-5PVP, and (g) PES-7PVP and Cross-section (right) images of membranes: (b) PES-1PVP, (d) PES-3PVP, (f) PES-5PVP and (h) PES-7PVP

The FE-SEM images presented in Fig 3.23 illustrates the characteristics of PES-PVP blended membranes. In these membranes, both the surface and cross-section images display dense membrane structures. Owing to its higher molecular weight compared to the PEG molecule, PVP is less easily washed out during the demixing process, necessitating an extending duration for the

effective removal of the additive from the membrane film. This prolong duration allows polymer aggregates to accumulate on the top layer, resulting in the formation of a non-porous membrane (Nabilah Aminudin et al., 2013).

3.14 Pore size measurement of CM and PES blended membranes

Fig 3.24 and Table 3.16 provide insight into the pore sizes (μm) of variously fabricated membranes, including commercial ones. CM and PES-control membranes had average pore size of 0.02 μm and 0.2 μm, respectively while PES-PEG membranes showed increased pore size reaching its maximum of 0.51 μm at 3 wt.% PEG concentration. However, a further increase in PEG concentration had a minimal impact, as it led to an elevation in dope solution viscosity that consequently producing a membrane with suppressed pores (Mulyati et al., 2017).

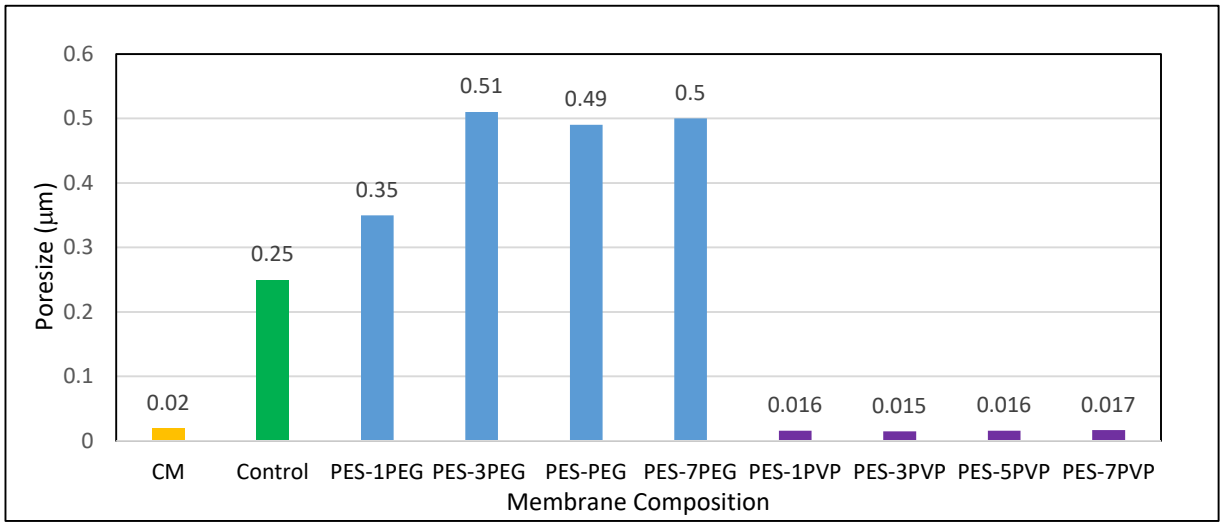

Fig 3.24: Percentage of pore size of CM and PES blended membranes

For PES-PVP membranes, the pore sizes were in the range of 0.015 to 0.017 μm closed to the commercial membrane (CM). At respective optimum concentrations, the average pore size of PES-PEG blended membrane was approximately 3000 times larger than that of PES-PVP blended membrane. It was assumed that PEG functioned as a more efficient pore-forming agent compared to PVP which may be achieved through PEG's role as a plasticizer that facilitated the expansion of the polymer matrix and the subsequent formation of pores (Tomietto et al., 2020).

Table 3.16: Pore sizes (μm) data of CM and PES blended membrane

Sl. No.	Membrane	Pore size (μm)
1	CM	0.02
2	Control	0.25
3	PES-1PEG	0.35
4	PES-3PEG	0.51
5	PES-5PEG	0.49
6	PES-7PEG	0.50
7	PES-1PVP	0.016
8	PES-3PVP	0.015
9	PES-5PVP	0.016
10	PES-7PVP	0.017

3.15 Equilibrium water content (EWC) and membrane porosity of PES blended membranes

The equilibrium water content (EWC) stands as a crucial parameter for membrane characterization, evaluating the membrane's hydrophilicity, which, in turn, influences water flux and porosity. It signifies the fraction of void space relative to the apparent total bulk volume of the material (Espinal, 2012). The EWC of various membranes (Fig 3.25 and Table 3.17) indicates that the inclusion of PEG and PVP led to an increase in EWC compared to the PES-control membrane. This elevation in water content affirms the presence of a greater number of pores in the fabricated blended membranes than that of PES-control membrane due to the incorporation of these additives.

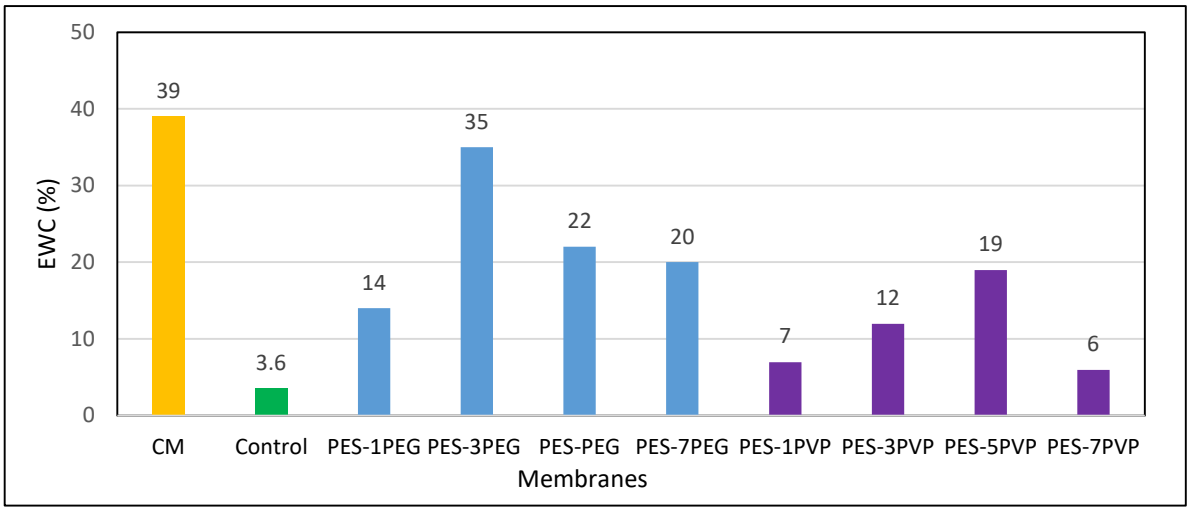

Fig 3.25: Equilibrium water content of CM and PES blended membranes

Table 3.17: Equilibrium water content data of CM and PES blended membranes

Sl. No.	Membrane	EWC (%)
1	CM	39
2	Control	3.6
3	PES-1PEG	14
4	PES-3PEG	35
5	PES-5PEG	22
6	PES-7PEG	20
7	PES-1PVP	7
8	PES-3PVP	12
9	PES-5PVP	19
10	PES-7PVP	6

The membrane porosity is illustrated in Fig 3.26 and detailed in Table 3.18. In the case of PEG and PVP blended membranes, porosity exhibited a steady increase up to 3% PEG and 5% PVP additive concentration. This improvement was ascribed to the hydrophilic nature of PEG and PVP, facilitating solvent/non-solvent mass transfer and resulting in a highly porous structure. However, beyond these additive concentrations, porosity declined due to increased viscosity which hindered the coagulation process, ultimately leading to a reduction in membrane porosity (Rashid et al., 2022).

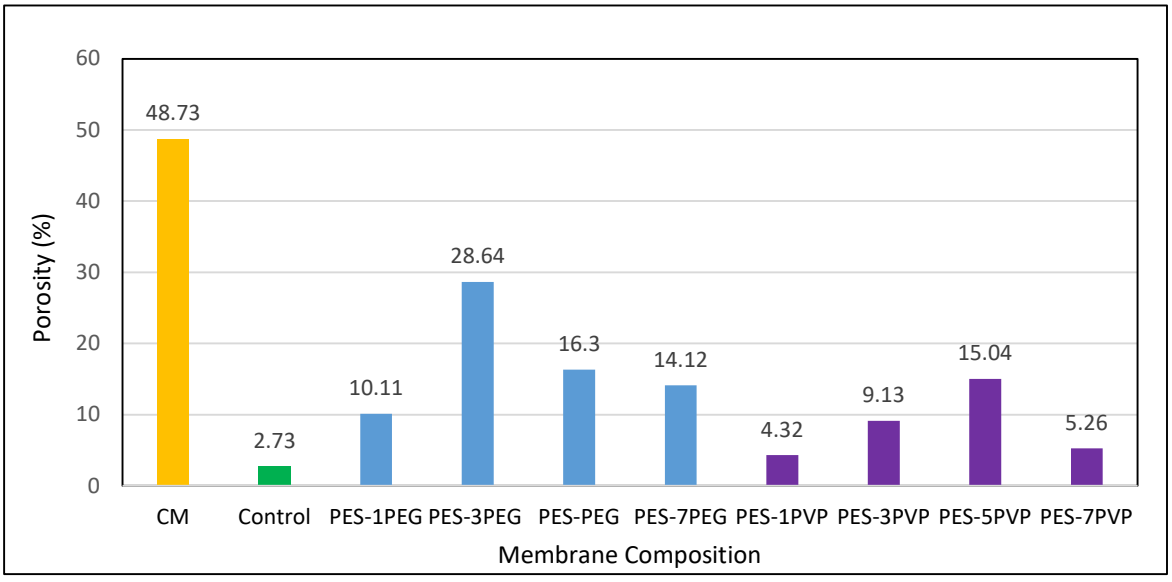

Fig 3.26: Porosity of CM and PES blended membranes.

Table 3.18: Porosity data of CM and PES blended membranes

Sl. No.	Membranes	Porosity (%)
1	CM	48.73
2	Control	2.73
3	PES-1PEG	10.11
4	PES-3PEG	28.64
5	PES-5PEG	16.3
6	PES-7PEG	14.12
7	PES-1PVP	4.32
8	PES-3PVP	9.13
9	PES-5PVP	15.04
10	PES-7PVP	5.26

Water-soluble additives such as PEG and PVP etc., have demonstrated their efficacy as pore formers in phase separation membrane fabrication processes. The underlying assumption is that these water-soluble additives can be leached out from the casting film, creating microporous in the spaces they previously occupied (Jung et al., 2004; Zhao et al., 2011). Notably, the hydrodynamic radius of PEG and PVP is 1.8 nm and 5.2 nm, respectively (Chibowski et al.; Armstrong et al., 2004). Consequently, the PEG molecule can readily leach out during the demixing process, resulting in the formation of more porous structures compared to PVP-blended membranes. The higher porosity percentage in PEG-blended membranes can also be elucidated through the solubility parameter, as presented in Table 3.19.

Table 3.19: Solubility parameters of polymers (Tsakiridou et al., 2019; Chen et al., 2020)

Sl. No	Material	Solubility parameter δ ($MPa^{1/2}$)
1	Polyethylene glycol (PEG-6K)	35.3
2	Polyvinylpyrrolidone (PVP-40K)	19.4
3	Polyethersulfone (PES)	23
4	DMF	24.8
5	Water	47.8

The data from Table 3.19 inferred that PEG exhibits a higher propensity to dissolve in water compared to PVP, primarily attributed to its closer solubility parameter to that of water. Hence, in the demixing process, PEG can be easily washed out or leached into the non-solvent water

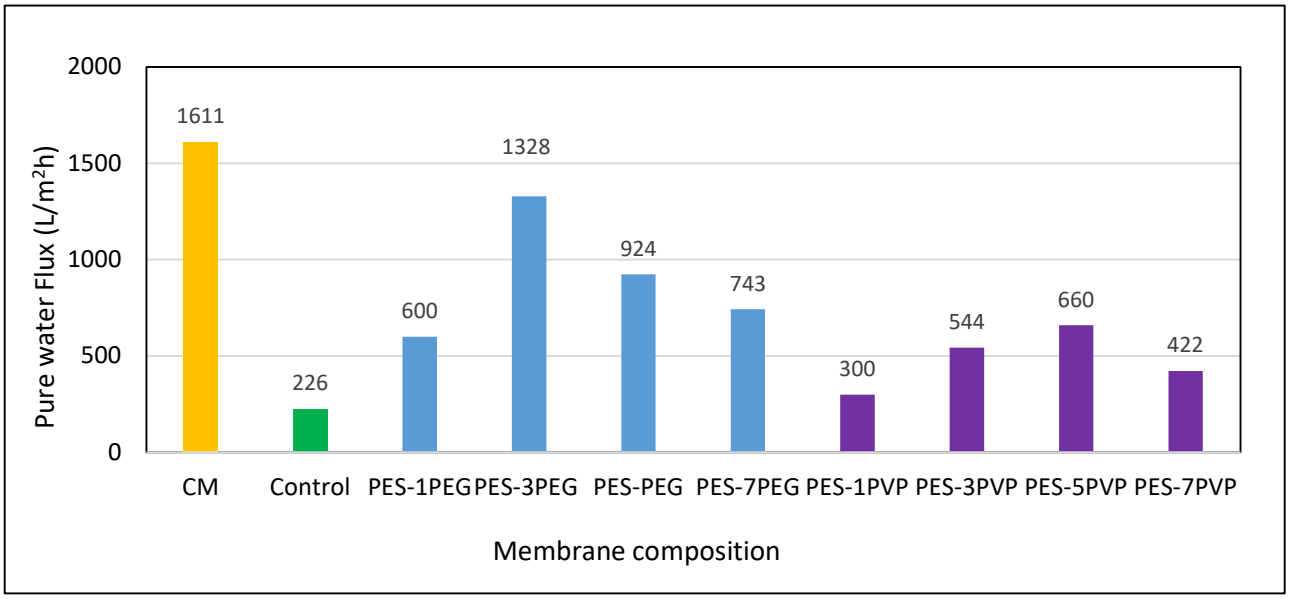

Fig 3.27: Pure water fluxes of PES blended membranes at 3 bar

bath, facilitating the creation of pores in the membrane. This phenomenon significantly accelerates the phase separation, ultimately leading to the rapid formation of a porous membrane.

3.16 Pure water flux of PES blended membranes

The pure water flux (L/m^{2}h) of CM and PES fabricated membranes (Fig 3.27 and Table 3.20) was assessed through crossflow filtration under a pressure of 3 bar. The findings revealed a noticeable influence of additive concentration in the casting solution on the water flux. The pure water fluxes demonstrated an increase up to 3% for PEG additive concentration and 5% for PVP additive concentration. Membranes prepared with these additive concentrations displayed higher porosity indicating instantaneous demixing process attributed to the increased thermodynamic instability of casting solution.

However, beyond these additive concentrations, the water fluxes of both types of blended membranes experienced a decline. This can be attributed to the increased viscosity of the casting solution, resulting in a reduced rate of interchange between solvent and non-solvent during the demixing process. Consequently, delayed demixing occurred leading to the formation of a dense top layer (SEM Fig.3.22 and 3.23) with suppressed pore sizes (Mulyati et al., 2018). It was also observed that the pure water flux of PES-PEG membranes was higher (1328 L/m^{2}h) than the PES-PVP membranes (975 L/m^{2}h). This difference was attributed to the higher porosity exhibited by the PES-PEG blended membrane.

Table 3.20: Pure water fluxes data of PES blended membranes

Sl. No.	Membrane	Flux (L/m^{2}h) @ 3 bar
1	CM	1611
2	Control	226
3	PES-1PEG	600
4	PES-3PEG	1328
5	PES-PEG	924
6	PES-7PEG	743
7	PES-1PVP	300
8	PES-3PVP	544
9	PES-5PVP	660
10	PES-7PVP	422

3.17 Contact angle of PES blended membranes

The contact angle **(°)**, serving as a visual indicator of a liquid droplet on a surface, plays a crucial role in evaluating the surface tension between the liquid and the solid substrate. A higher contact angle signifies increased surface tension between the solid and liquid, while a lower angle suggests the opposite. If the contact angle measures below 90 degrees, the membrane exhibits hydrophilic characteristics, whereas a contact angle surpassing 90 degrees indicates hydrophobic characteristics of membrane (Hussein et al., 2023). Contact angles of CM, PES-control, and PES composites membranes were determined using an in-house built contact angle device as illustrated in Fig 3.28 and detailed in Table 3.21.

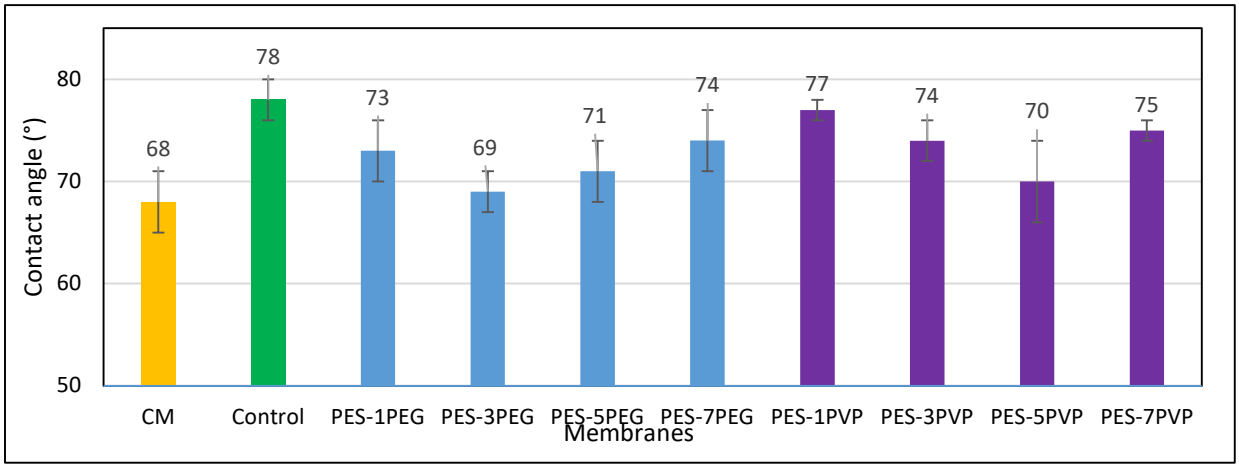

Fig 3.28: Contact angle of CM and PES blended membranes (average contact angle of five replicates are reported)

The figure illustrates that the addition of PEG and PVP additives to the dope solution led to a notable decline in the contact angles of the manufactured membranes in comparison to the PES-

control membrane. Both the PEG and PVP additives are hydrophilic in nature and contributed to the reduction in contact angles for the blended membranes, showing similar trends. However, after the addition of 3 wt.% of PEG and 5 wt.% of PVP, the contact angles of the PES-PEG and PES-PVP membranes increased. This increase was due to a decrease in porosity which resulted from the higher viscosity of the dope solution (Aljanabi et al., 2022).

Comparison of contact angle of in-house device with commercial device: From the Table 3.22, it is shown that results of inhouse developed contact device is closely related to the commercial device (Goniometer KYOWA Dme-211plus).

Table 3.21: Contact angle data of CM and PES blended membranes

Sl. No.	Membrane	Contact angle (°)
1	CM	68±3
2	Control	78±2
3	PES-1PEG	73±3
4	PES-3PEG	69±2
5	PES-PEG	71±3
6	PES-7PEG	74±3
7	PES-1PVP	77±1
8	PES-3PVP	74±2
9	PES-5PVP	70±4
10	PES-7PVP	75±1

Table 3.22: Comparison of inhouse device contact angle measurements with commercial device for PES blended membranes

Sl. No.	Membrane	Inhouse device (°)	Commercial device (°)
1	Control	78±2	77±3
2	PES-1PEG	73±3	70±3
3	PES-3PEG	69±2	73±3
4	PES-1PVP	77±1	76±4
5	PES-5PVP	70±4	74±3

3.18 Tensile strength of PES blended membranes

Fig. 3.29 shows the tensile strength (N/mm^2) of PES blended membranes. Control PES membrane had tensile value of 29 N/mm^2. After addition of PEG up to 3 wt.% and PVP up to 5 wt.%, the tensile values decreased due to increased porosity (Wang et al., 2017). However, beyond 3 wt.% PEG and 5 wt.% of PVP, the porosity of the fabricated membranes decreased because of the increased viscosity of the casting solution, resulting in an increase in tensile strength.

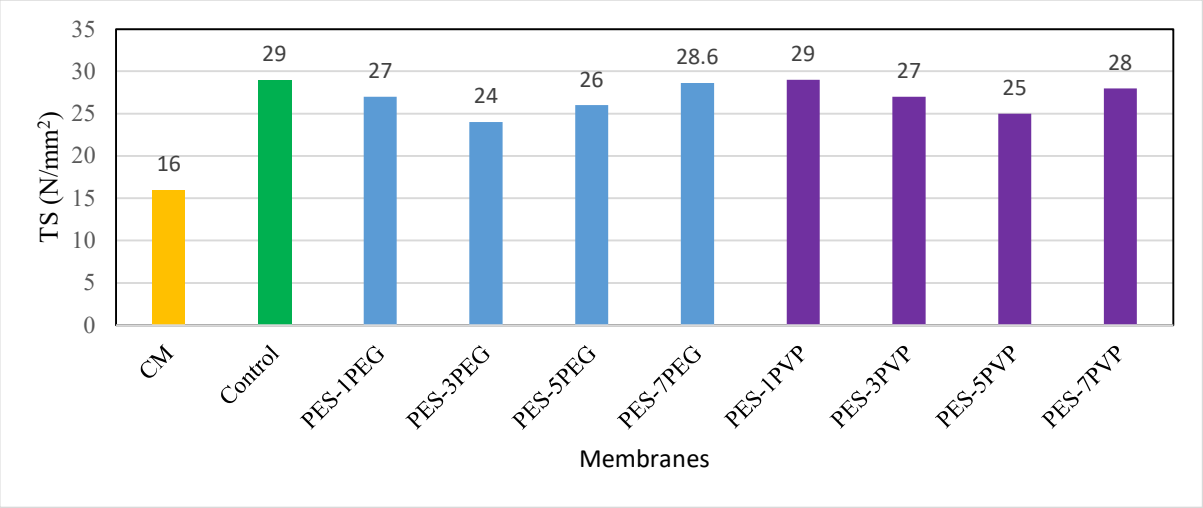

Fig 3.29: Tensile strengths of PES blended membranes

3.19 Wastewater treatment by MBR using PES blended membranes and PES based commercial membrane (CM)

A membrane bioreactor was equipped with three flat sheets modules, one was commercially available membrane (CM) and two were fabricated membranes based on their pure water fluxes. Sludge was collected from Flagship Dhaka CETP (BD), DEPZ, Savar.

Table 3.23: Characteristics of synthetic textile wastewater (with activated sludge)

Parameter	Value
Dye concentration (mg/L)	100
pH	7.66
COD (mg/L)	6500
BOD_5 (mg/L)	3100
Conductivity (ms/cm)	7.8
MLSS (g/L)	4-6

The treatment of synthetic textile wastewater continued for around 70 days. Table 3.23 showed the characteristics of synthetic textile wastewater.

3.19.1 pH variation of permeate of CM and PES blended membranes

In the context of biological wastewater treatment, aerobic bacteria engage in the consumption of organic pollutants in the presence of oxygen, transforming them into carbon dioxide, water, and new cells. This carbon dioxide can dissolve in water in the MBR tank leading to the formation of carbonic acid and subsequently causing a decrease in pH. Since MBR system cannot take advantage of SRT longer than 30 days (H.-D. Park et al., 2015), the lowest pH levels are typically observed days between 20 and 30. This period is presumed to align with optimal biological activity, fostering enhanced biodegradation and increased carbon dioxide production.

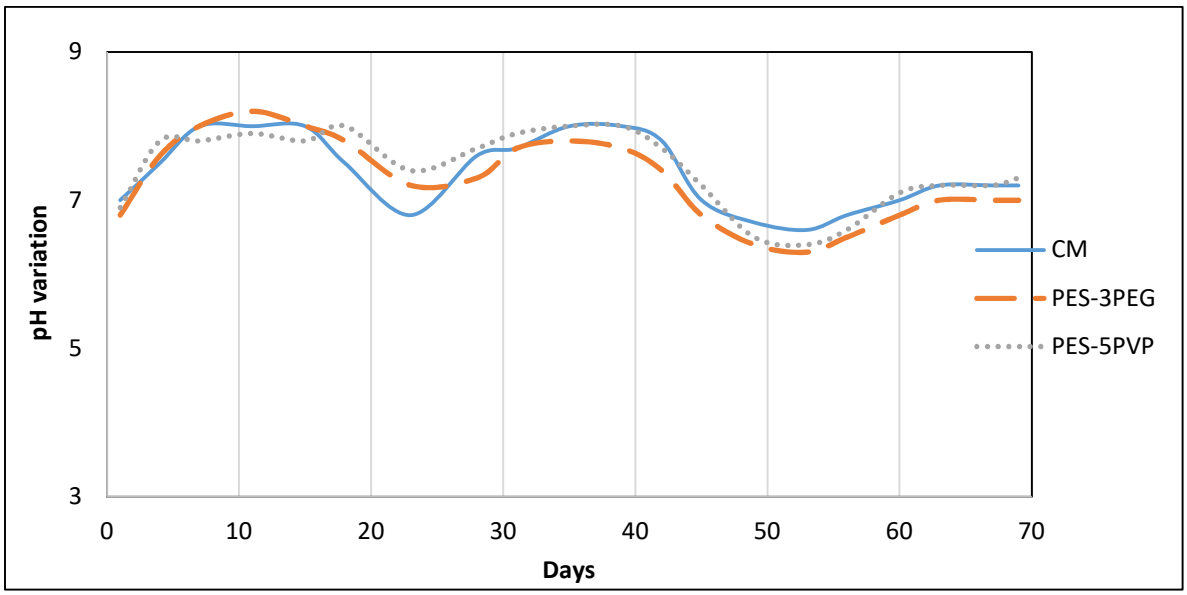

Fig 3.30: Variations of pH of permeates from CM and PES blended membranes

Fig 3.30 depicts the pH variations over time, revealing similar trends for both the commercial and fabricated membranes and details are presented in Table 3.24. Incorporation of new sludge after 30 days of operation, pH was again dropped which was between 45 and 50 days.

Table 3.24: pH variations data of permeates from CM and PES blended membranes

Day	Raw pH	pH of permeate		
		CM	PES-3PEG	PES-5PVP
1	7.66	7	6.8	6.9
4	7.66	7.5	7.6	7.8
7	7.66	8	8	7.8

11	7.66	8	8.2	7.9
15	7.66	8	8	7.8
18	7.66	7.5	7.8	8
23	7.66	6.8	7.2	7.4
28	7.66	7.6	7.3	7.7
31	7.66	7.7	7.7	7.9
35	7.66	8	7.8	8
39	7.66	8	7.7	8
42	7.66	7.8	7.4	7.7
45	7.66	7	6.8	7.2
49	7.66	6.7	6.4	6.5
53	7.66	6.6	6.3	6.4
56	7.66	6.8	6.5	6.6
60	7.66	7	6.8	7.1
63	7.66	7.2	7	7.2
67	7.66	7.2	7	7.2
69	7.66	7.2	7	7.3

3.19.2 BOD_5 and COD removal of permeate from CM and PES blended membranes

Fig 3.31 and Fig 3.32 depict the BOD_5 and COD removal results for synthetic textile wastewater. It was found that the MBR exhibited remarkably high efficiency in organic matter removal for all the utilized membranes, achieving approximately 93-94% removal for BOD_5 and 95-96% for COD after 25 days of operation, then dropped a bit, due to loss of activity of microorganisms. The addition of new sludge again increased the BOD_5 and COD removal. MBR does not benefit from prolonged SRT exceeding 30 days in terms of active biomass. Instead, the heightened concentration of solids may exacerbate the fouling tendency of the membranes (H.-D. Park et al., 2015). Therefore, following 30 days of continuous operation, fresh active sludge was introduced into the MBR tank that provided active microorganisms for the organic matters and a renewed increase of BOD_5 and COD removal was achieved.

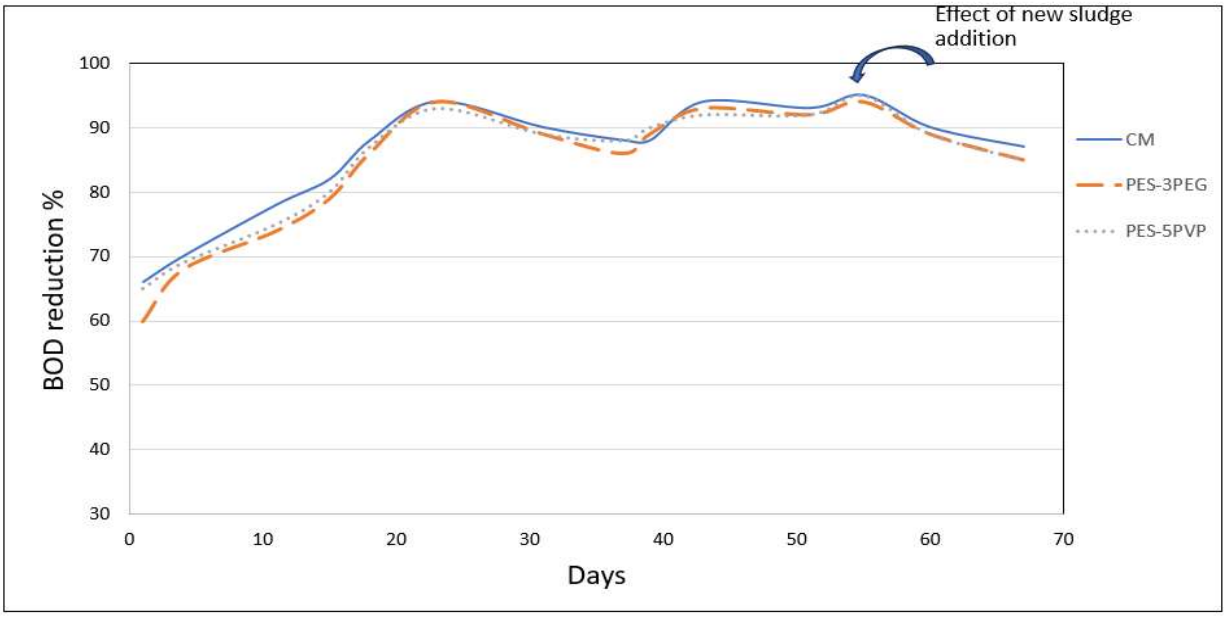

Fig 3.31: BOD_5 removal of permeate of CM and PES blended membranes

Table 3.25: BOD_5 data of permeate from CM and PES blended membranes

Day	Raw BOD_5 of synthetic wastewater (mg/L)	BOD_5 of permeate					
		CM (mg/L)	CM removal %	PES-3PEG (mg/L)	PES-3PEG removal %	PES-5PVP (mg/L)	PES-5PVP removal %
1	3100	1054	66	1240	60	1085	65
4	3100	930	70	992	68	961	69
11	3100	682	78	806	74	775	75
15	3100	558	82	651	79	620	80
18	3100	372	88	434	86	403	87
23	3100	186	94	186	94	217	93
31	3100	310	90	341	89	341	89
37	3100	372	88	434	86	372	88
39	3100	372	88	341	89	310	90
43	3100	186	94	217	93	248	92
51	3100	217	93	248	92	248	92
55	3100	149	95	171	95	158	95
60	3100	310	90	341	89	341	89
67	3100	403	87	465	85	465	85

It was noteworthy that fabricated membranes demonstrated equivalent efficiencies to commercial membrane in removing organic matter from wastewater using MBR. Moreover, in MBR

operation, mixed liquor suspended solid (MLSS) and solid retention time (SRT) play vital role in degradation of organic matters and thus high MLSS and high SRT are generally maintained. In this study, MLSS of 4-5 g/L and SRT of 30 days were maintained. Apart from biodegradation, it was reported that filtration alone contributes approximately 30% to the overall BOD_5 and COD removal process (Matošić et al., 2009). Table 3.25 and Table 3.26 are showing the detail data of COD and BOD_5 removal, respectively.

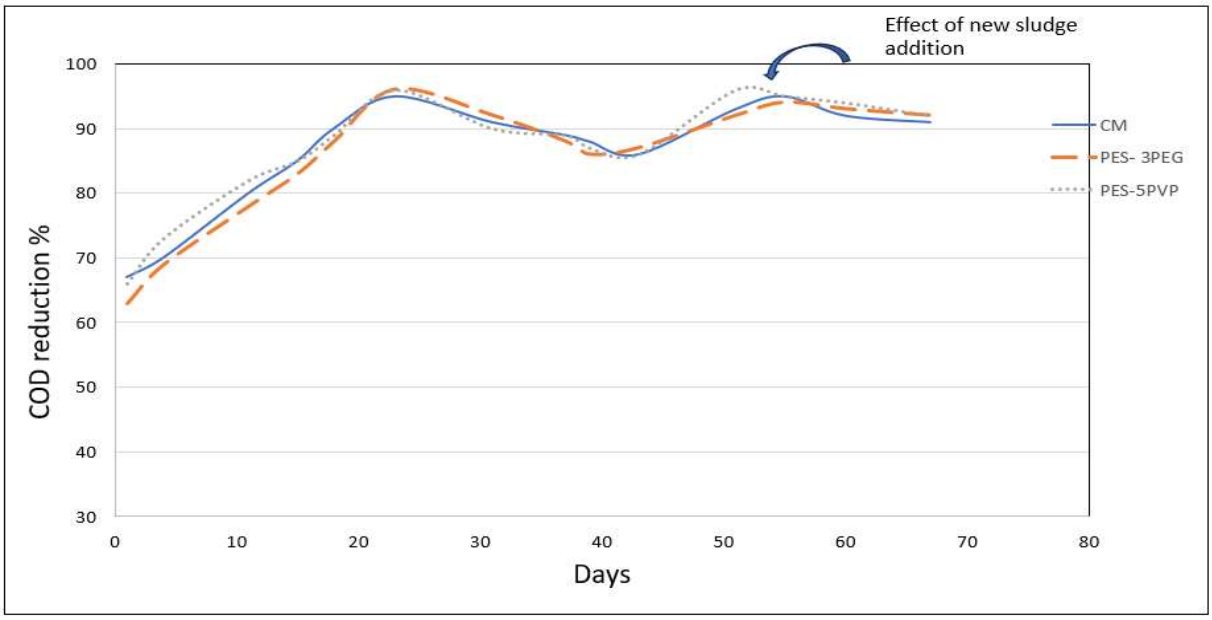

Fig 3.32: COD removal of permeate of CM and PES blended membranes

Table 3.26: COD data of permeate from CM and PES blended membranes

Day	Raw COD of synthetic wastewater (mg/L)	COD of permeate					
		CM (mg/L)	CM removal %	PES-3PEG (mg/L)	PES-3PEG removal %	PES-5PVP (mg/L)	PES-5PVP removal %
1	6500	2145	67	2405	63	2210	66
4	6500	1950	70	2015	69	1755	73
11	6500	1300	80	1430	78	1170	82
15	6500	975	85	1105	83	975	85
18	6500	650	90	780	88	715	89
23	6500	325	95	260	96	260	96
31	6500	585	91	520	92	650	90
37	6500	715	89	780	88	715	89
39	6500	780	88	910	86	845	87

43	6500	910	86	845	87	910	86
51	6500	455	93	520	92	260	96
55	6500	325	95	364	94	351	95
60	6500	520	92	455	93	390	94
67	6500	585	91	520	92	520	92

3.19.3 Color removal of permeate from CM and PES blended membranes

In Fig 3.33, the graph depicts the evolution of removal (%) with operation days and details are presented in Table 3.27. It was evident that PES-PVP blended membrane exhibited outstanding performance, achieving the highest color removal rate at 94% while CM and PES-PEG blended membranes exhibited 93% color removal after 39 days of operation.

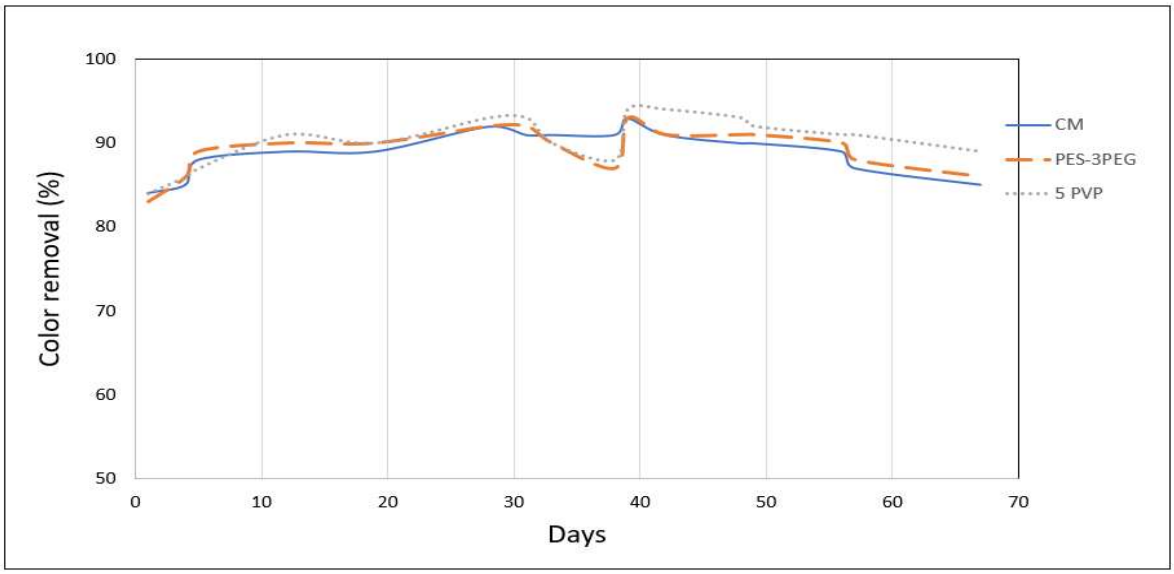

Fig 3.33: Color removal of permeate of CM and PES blended membranes

Table 3.27: Color removal data of permeate of CM and PES blended membranes

Day	Dye concentration (mg/L)	Dye concentration in permeate					
		CM (mg/L)	CM removal (%)	PEG (mg/L)	PEG removal (%)	PVP (mg/L)	PVP removal (%)
1	100	16	84	17	83	16	84
4	100	15	85	14	86	14	86
8	100	12	88	11	89	13	87
12	100	11	89	10	90	9	91
19	100	11	89	10	90	10	90
28	100	8	92	8	92	7	93
31	100	9	91	8	92	7	93

33	100	9	91	10	90	10	90
38	100	9	91	13	87	12	88
39	100	7	93	7	93	6	94
42	100	9	91	9	91	6	94
48	100	10	90	9	91	7	93
49	100	10	90	9	91	8	92
56	100	11	89	10	90	9	91
57	100	13	87	12	88	9	91
67	100	15	85	14	86	11	89

The primary mechanism assumed to drive color removal is the adsorption onto biomass, however, biodegradation appears to have a limited impact on color removal due to the persistent nature of textile dyes in activated sludge systems (Brik et al., 2006). As MBR typically operates with higher MLSS concentrations in comparison to conventional activated sludge processes, these elevated MLSS levels augment the capacity of color adsorption. In Fig 3.34, images depicting the permeates from MBR using CM and fabricated membranes.

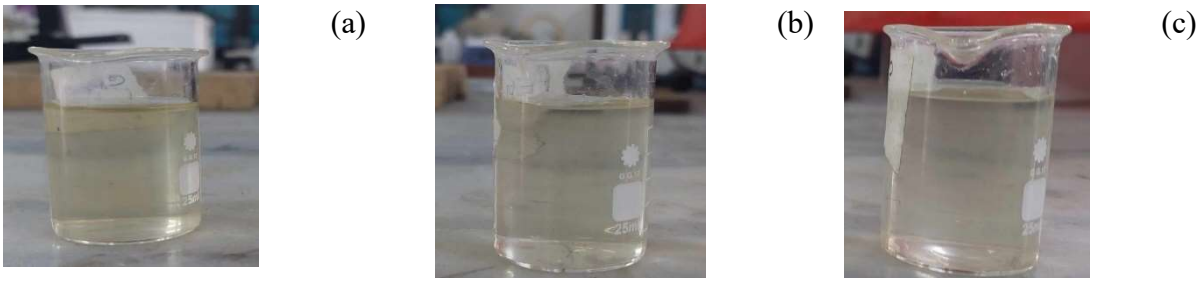

Fig 3.34: Visual representation of color removal by using (a) CM membrane (b) PES-PEG membrane, and (c) PES-PVP membrane

3.19.4 MBR fluxes of permeate of CM and PES blended membranes

Fig 3.35 illustrates the permeate flux (L/m^2h) from the CM, PES-PEG, and PES-PVP membranes and detail are presented in Table 3.28. Throughout the 70 days of operational period, the average fluxes from the CM, PEG, and PVP membranes were 39, 18, and 5 L/m^2h. Initially, all the membranes exhibited higher fluxes which gradually declined over the course of operation due to the fouling of the membranes. On the 42^{th} day, a physical cleaning procedure was executed on the membranes leading to substantial enhancement of the flux and regained. For instance, the initial fluxes of the CM, PES-PEG, and PES-PVP membranes were 86, 55, and 9 L/m^2h respectively which dropped down to 38, 17, and 4 L/m^2h after 39 days. However, following

physical cleaning, these fluxes significantly improved reaching approximately 70%, 42%, and 83% of their respective initial fluxes.

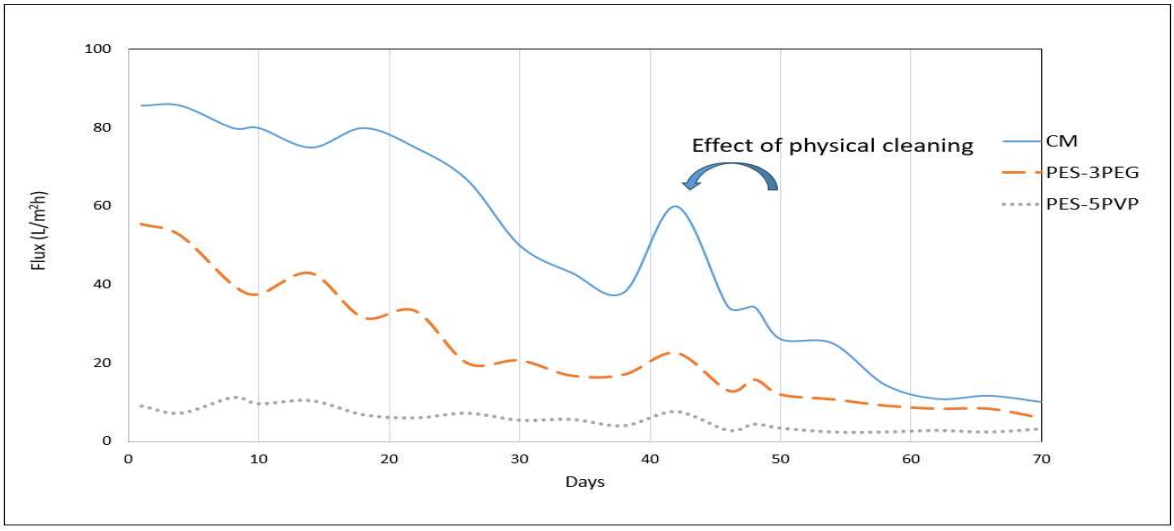

Fig 3.35: Fluxes of MBR permeate of CM and PES blended membranes

Table 3.28: MBR fluxes data of CM and PSF blended membranes

Day	CM (L/m^2h)	PES-3PEG (L/m^2h)	PES-5PVP (L/m^2h)
1	85.71	55.4	9
4	85.71	52.5	7.2
8	80	40	11.2
10	80	37.5	9.6
14	75	42.9	10.4
18	80	31.6	6.8
22	75	33.3	6
26	66.67	20	7.2
30	50	20.7	5.4
34	43	16.8	5.6
39	38	17.1	4
42	60	22.6	7.6
46	34.29	13	2.8
48	34.29	15.8	4.4
50	26.09	12	3.4
54	25	10.8	2.4
58	14.46	9.2	2.4
62	10.8	8.4	2.8
66	11.6	8.4	2.4
70	10	6	3.2

3.19.5 Bacteria removal of permeate of CM and PES blended membranes

Bacteria commonly display a variety of morphologies, taking on spherical shapes known for cocci, rod-shaped forms for bacilli, and spiral configurations for spirochetes. Their sizes range from approximately 1 to 2 μm and lengths spanning 5 to 10 μm (H.-D. Park et al., 2015). In the MBR sludge, a total of nine (09) bacteria were identified, each was presented in varying concentrations. The PES-PEG and PES-PVP membranes demonstrated high efficacy in bacteria removal which is detailed in Table 3.29. Significantly, in certain cases, these fabricated membranes displayed superior capabilities in filtering bacteria compared to CM.

Table 3.29: Bacteria removal of permeate of CM and PES blended membranes

Sample	Raw bacteria count (CFU/ml)	Microbiological Removal		
		CM (%)	PES-3PEG (%)	PES-5PVP (%)
Total aerobic bacterial count	170000	91.76	96.00	91.76
Total coliform count	150000	93.67	99.27	91.33
Total faecal coliform count	78000	93.97	99.74	99.36
Total yeast and mould	24000	99.98	95.00	99.17
E. coli	<10	89.00	78.00	89.00
Bacillus spp.	65000	81.23	84.62	81.54
Salmonella spp.	9300	99.91	99.96	99.96
Pseudomonas spp.	<10	89.00	78.00	89.00
Staphylococcus spp.	300	99	99	99

The membranes utilized in this MBR operation featured pore sizes ranging from 0.5 μm to 0.02 μm, falling below the average size of bacteria. This resulted in a significant level of bacterial removal, underscoring the effectiveness of membrane filtration in the MBR system. The efficiency of bacterial removal in the MBR system is enhanced by a combination of biodegradation, biosorption, and membrane retention processes (Faisal I. Hai et al., 2014). The biodegradation and biosorption emerge as the primary mechanism facilitating the reduction of pathogens in biological treatment processes, while the membrane primarily achieves pathogen reduction through size exclusion (Verbyla et al., 2019). Fig 3.36 visually depicts microorganism counts before (a) and after (b-d) treatment.

a b c d

Fig 3.36: Total aerobic bacteria in (a) raw feed and removal of total aerobic bacteria from (b) CM membrane (c) PES-3PEG membrane, and (d) PES-5PVP membrane

3.19.6 Comparison of MBR effluents (CM and PES blended) with standard values for irrigation

The effluents of CM, PES-3PEG, and PES-5PVP membranes using MBR were compared with the standard values of parameters for irrigation water are presented in Table 3.30. The COD values (mg/L) of permeates fell within the range of standard value, while BOD_5 values were slightly higher than the standard range. pH values also remained within the standard range. In terms of microbiological loads, the level of *E.Coli* and *pseudomonas spp.* in the permeates from all membranes were significantly lower than the standard ranges for irrigation, lake, and river water.

Table 3.30: Comparison of MBR permeates with standard values for irrigation water

Parameters	CM	PES-3PEG	PES-5PVP	Standard value for irrigation	Ref.
COD (mg/L)	325	364	351	400	BDS (DoE, 1997)
BOD (mg/L)	149	171	158	100	BDS (DoE, 1997)
pH	6.5	6.4	7.2	6-9	BDS (DoE, 1997)
E. Coli (CFU/100ml)	<10	<10	<10	≤ 1000	BDS (DoE, 1997) and WHO
Pseudomonas spp. (CFU/100ml)	<10	<10	<10	≤ 1000 (Lake and river water)	WHO

3.19.7 Real wastewater treatment by CM and PES-3PEG blended membranes using MBR

Real wastewater and sludge were collected from Flagship Dhaka CETP (BD), DEPZ, Savar. Tap water mixed with real wastewater in a 1:1 ratio (Malpei et al., 2003) and then filled into the MBR tank for treatment. Characteristics of tap water and mixed water (wastewater + tap water) were detailed in Table 3.31 and Table 3.32, respectively. A total of 46 days of MBR operation was carried out.

Table 3.31: **Characteristics of tap water**

Parameter	Value
Color	Colorless
Odor	Odorless
Tap water pH	7.0
TSS (mg/L)	Nil
TDS (mg/L)	234
Conductivity (ms/cm)	0.351
Ammonia (NH_3/NH_4^+) (mg/L)	Nil
Hardness (mg/L $CaCO_3$)	121

Table 3.32: **Characteristics of mixed water (real wastewater + tap water)**

Parameter	Value
Color	Brown
pH	6.8
COD (mg/L)	5960
BOD_5 (mg/L)	2250
TDS (mg/L)	256
Conductivity (ms/cm)	3.88
MLSS (g/L)	5.9

3.19.7.1 pH variation of permeate of CM and PES-3PEG membrane from real wastewater

Fig 3.37 depicts the pH variations over time, revealing similar trends for both the commercial and PES-3PEG membranes and details are presented in Table 3.33. As MBR system cannot take advantage of SRT longer than 30 days, it was notable that both membranes exhibited their lowest pH levels at 25-day.

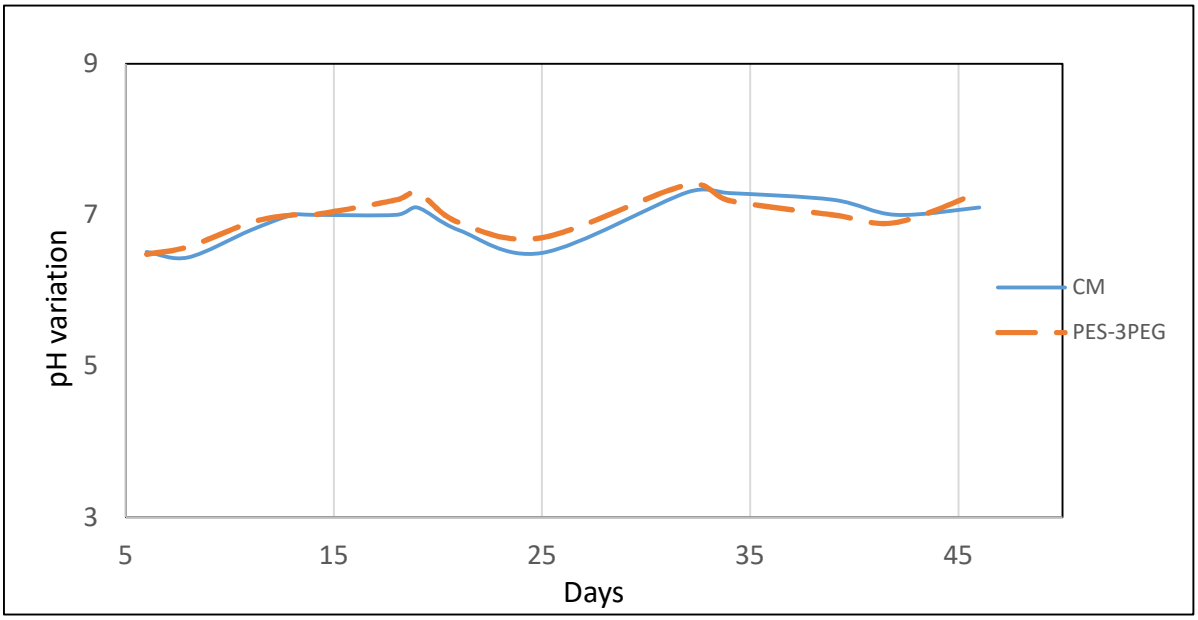

Fig 3.37: Variation of pH of permeates from CM and PES-3PEG membranes from real wastewater

Table 3.33: pH variation data of permeate of CM and PES-3PEG membranes from real wastewater

Day	CM	PES-3PEG
6	6.51	6.48
8	6.44	6.58
11	6.8	6.9
13	7	7
14	7	7
18	7	7.2
19	7.1	7.3
21	6.8	6.9
25	6.5	6.7
32	7.3	7.4
34	7.29	7.19
39	7.2	7
42	7	6.9
46	7.1	7.3

3.19.7.2 COD and BOD_5 removal of permeate from CM and PES-3PEG membranes from real wastewater

Fig 3.38 and Fig 3.39 illustrate the COD and BOD_5 removal results for real wastewater using MBR. It was found that the MBR exhibited remarkably high efficiency in organic matter removal across all utilized membranes, achieving approximately 93% removal for COD and 88-

89% for BOD_5 after 28 days of operation. However, there was a light decline thereafter attributed to the loss of activity of microorganisms.

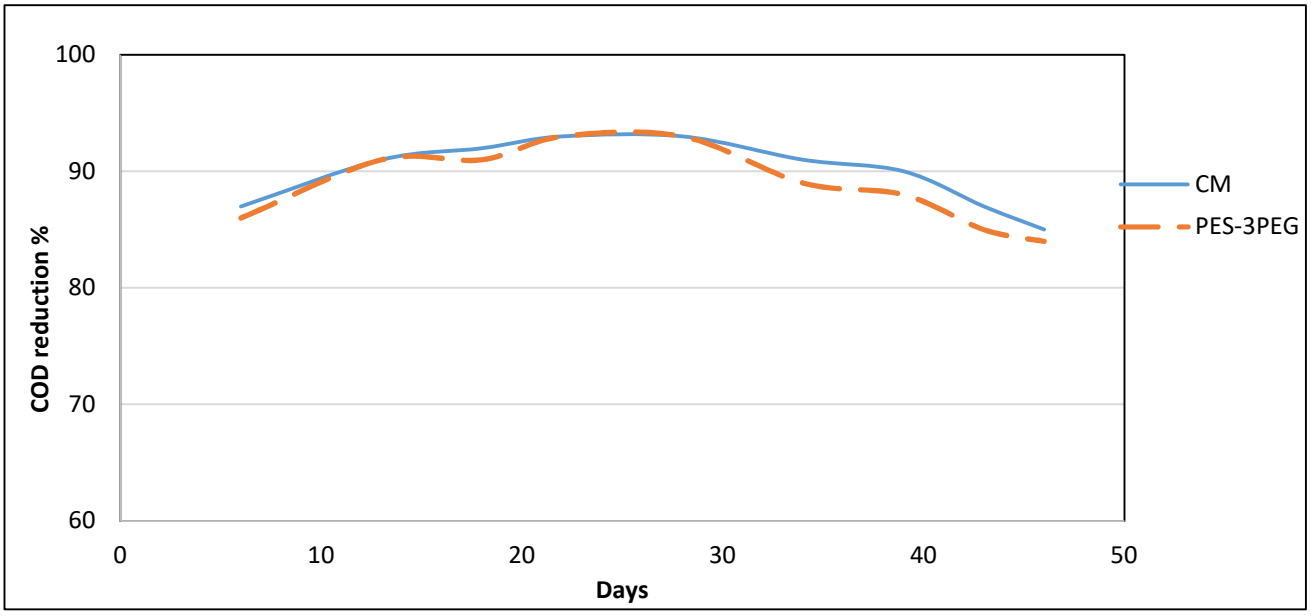

Fig 3.38: COD removal of permeate of CM and PES-3PEG membranes from real wastewater

Table 3.34: COD data of permeate of CM and PES-3PEG membranes from real wastewater

Day	CM removal %	PES-3 PEG removal %
6	87	86
13	91	91
18	92	91
22	93	92
28	93	93
34	91	89
39	90	88
43	87	85
46	85	84

It was noteworthy that similar to synthetic wastewater treatment using MBR, fabricated membranes exhibited equivalent efficiencies to commercial membrane in removing organic matter from real wastewater. Table 3.34 and Table 3.35 are showing the detail data of COD and BOD_5 removal, respectively.

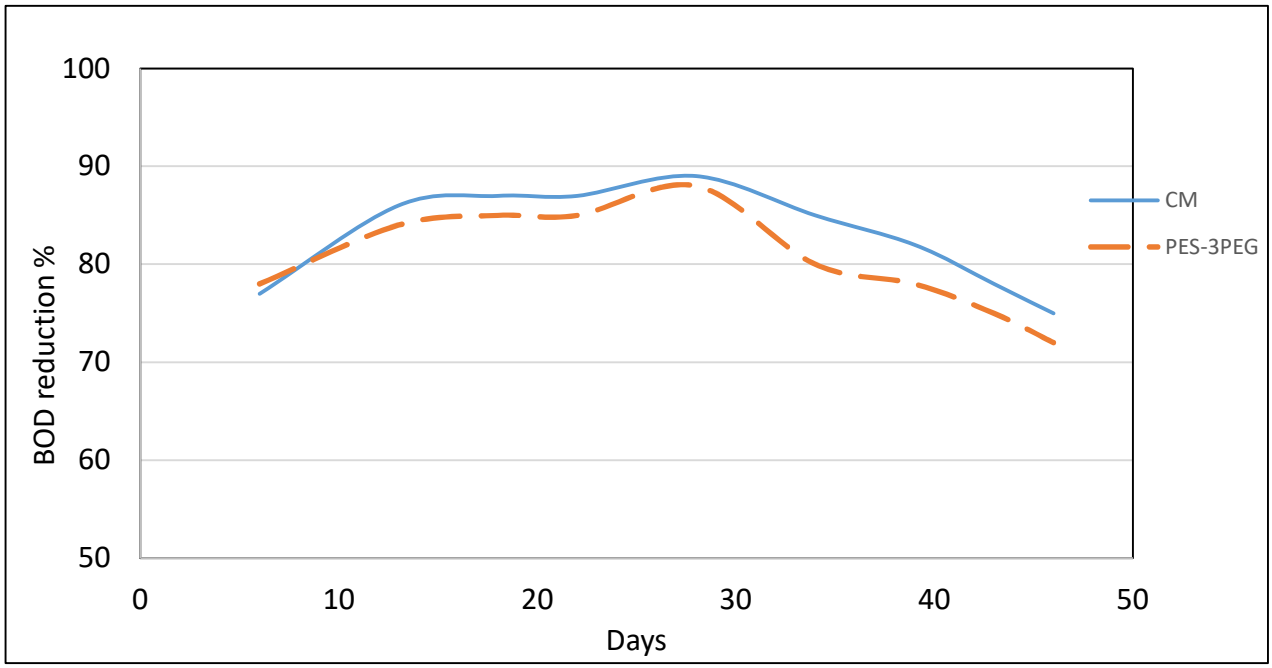

Fig 3.39: BOD_5 removal of permeate of CM and PES-3PEG membranes from real wastewater

Table 3.35: BOD_5 data of permeate of CM and PES-3PEG membranes from real wastewater

Day	CM removal %	PES-3PEG removal %
6	77	78
13	86	84
18	87	85
22	87	85
28	89	88
34	85	80
39	82	78
43	78	75
46	75	72

3.19.7.3 MBR fluxes of permeate of CM and PES-3PEG membranes from real wastewater

Fig 3.40 depicts the permeate flux from both the CM and PES-3PEG membranes with detail data presented in Table 3.36. Over the 46-day operational period, the average fluxes from the CM and PES-3PEG membranes were 32 and 13 L/m^2h, respectively. Initially, all membranes exhibited higher fluxes which gradually declined due to fouling over time.

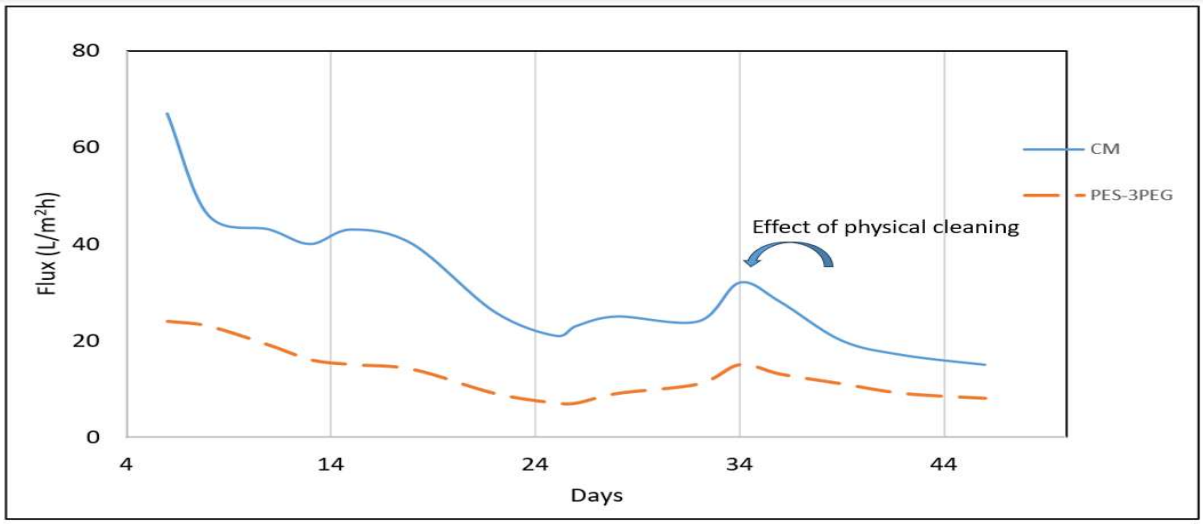

Fig 3.40: MBR fluxes of permeate of CM and PES-3PEG membranes from real wastewater

On the 34th day, a physical cleaning procedure was performed on the membranes resulting in a substantial enhancement of flux. For instance, the initial fluxes of the CM and PES-3PEG membranes were 67 and 24 L/m^{2}h respectively which decreased to 24 and 11 L/m^{2}h after 32 days. However, following physical cleaning, these fluxes significantly improved reaching approximately 49% and 63% of their respective initial fluxes.

Table 3.36: MBR permeate fluxes data of CM and PES-3PEG membranes from real wastewater

Day	CM (L/m^{2}h)	PES-3PEG (L/m^{2}h)
6	67	24
8	46	23
11	43	19
13	40	16
15	43	15
18	40	14
22	26	9
25	21	7
26	23	7
28	25	9
32	24	11
34	32	15
36	28	13
39	20	11
42	17	9
46	15	8

3.20 Cost analysis

Table 3.37 and Table 3.38 illustrate the material cost of PES-3PEG and PES-5PVP fabricated membranes. The total material cost was Tk 35460 m^{-2} (or \$296 m^{-2}) and Tk, 38920 m^{-2} (or \$324 m^{-2}), respectively.

Table 3.37: Cost analysis of PES-3PEG fabricated membrane

Components	Unit	Unit price (Tk)	Material required/m^2	Cost/m^2
PES polymer	gm	300	95	28500
DMF solvent	ml	4	390	1560
PEG additive	gm	100	15	1500
Hollytex-3256	m^2	3300	1	3300
Non-solvent	L	10	60	600
Total (taka)				Tk, 35460 \$296

Table 3.38: Cost analysis of PES-5PVP fabricated membrane

Components	Unit	Unit price (Tk)	Material required/m^2	Cost/m^2
PES polymer	gm	300	95	28500
DMF solvent	ml	4	380	1520
PVP additive	gm	200	25	5000
Hollytex-3256	m^2	3300	1	3300
Non-solvent	L	10	60	600
Total (taka)				Tk, 38920 \$324

These cost would increase slightly if additional expenses were included. In contrast, commercial PES-based membrane cost Tk 80000 m^{-2} (or \$666 m^{-2}). Therefore, it can be inferred that fabricated membranes are significantly less expensive than the commercial one.

CHAPTER 4: CONCLUSIONS, LIMITATIONS AND SCOPE OF FUTURE WORKS

4.1 Conclusions

In part 1, PSF-PEG and PSF-SA based blended membranes were prepared via the NIPS method utilizing a commercial grade PSF polymer. Among various support materials, the Hollytex-3256 nonwoven polyester fabric proved to be the optimal choice for creating a film with 23 wt.% PSF due to its compactness, smooth surface, and dimensional stability. PSF-PEG blended membrane with 5 wt.% PEG exhibited highest porosity (9.25%) and pure water flux (308 L/m^2h) compared to PSF-control membrane which has a 1.13 % porosity and a flux of 63 L/m^2h. On the other hand, PSF-SA blended membrane at 5 wt.% SA showed a porosity of only 3.21 % and a flux of 130 L/m^2h. This phenomenon is highlighting the efficacy of PEG as a pore-forming agent. Again, PSF-SA blended membranes displayed a lower contact angle, suggesting the potential SA to enhance membrane hydrophilicity. In MBR operation, PSF-PEG and PSF-SA blended membranes showed comparable results to the PES-based commercial membrane achieving approximately 90% removal of BOD_5 and COD. Regarding color removal efficiency, PSF-PEG and PSF-SA blended membranes exhibited about 70% color removal while the PES-based commercial membrane achieving a higher removal of 90%. Thus, the utilization of commercially available PSF polymer as a membrane material can be deemed effective particularly in enhancing the porosity of the fabricated membrane.

In part 2, PES-PEG and PES-PVP based hydrophilic blended membranes were fabricated employing the NIPS method. PES-PEG blended membrane with 3 wt.% PEG showed highest porosity (28.64%) and pure water flux (1328 L/m^2h) compared to PES-control membrane which had only 2.73% porosity and a flux of 226 L/m^2h. Conversely, PES-PVP blended membrane, at its optimum concentration of PVP (5 wt.%), exhibited a porosity of 15.04 % and a flux of 660 L/m^2h. On an average, under optimum conditions, PES-PEG blended membrane exhibited 101% higher fluxes compared to the PES-PVP-blended membrane, however it was approximately 82% of the PES-based commercial membrane (CM). Regarding hydrophilicity, both blended membranes demonstrated lower contact angles compared to the PES-control membrane. In MBR applications, PES-PEG and PES-PVP blended membranes exhibited 93-94 % BOD_5, 95-96% COD removal, and 93-94% color removal which were significantly comparable with that of PES-based commercial membrane. Despite the disparity in permeate flux, the fabricated membranes exhibited significant efficacy in removing microorganisms which was also comparable to that of the PES-based commercial membrane. In real wastewater treatment with

CM and PES-3PEG membranes using MBR, both the membranes achieving approximately 93% removal for COD and 88-89% for BOD_5.

Bangladesh faces significant challenges related to water pollution, especially in industrial sectors where untreated or inadequately treated wastewater is discharged directly into water bodies. The implementation of MBRs holds promise in enhancing water body quality, thereby fostering improved environmental and public health outcomes. As urban and industrial activities continue to grow, the demand for advanced wastewater treatment solutions such MBRs is likely to increase. By effectively leveraging MBR technology, Bangladesh can not only enhance wastewater management but also safeguard public health and advance its sustainable development objectives.

4.2 Limitations

As a result of the Covid-19 pandemic in Bangladesh since mid-2021, there have been disruption in both local and foreign material procurement. Additionally, various laboratories at the University of Dhaka have closed, hindering our ability to carry out the planned experimental procedures effectively.

4.3 Scope of future works

The following works could be explored to enhance our comprehension of the challenges related to membrane fabrication as well as treating these membranes in MBR:

- A more compact and dense support material (GSM> 82) needs to be used for reducing the base polymer concentration.
- Effects of humidity and temperature in the casting process can be studied.
- Coagulation bath compositions (solvent/non-solvent) need to be optimized.
- Optimizing operating parameters such as Sludge Retention Time (SRT), Hydraulic Retention Time (HRT), and Transmembrane Pressure (TMP) are essential to enhance the efficiency of the membrane filtration.
- The mode of operation of MBR should be changed from batch to continuous process to better simulate the industrial processes.
- Capital expenditures (CapEx) and operating expenses (OpEx) should be analyzed

References

Abdelrasoul, A., Doan, H. and Lohi, A. (2013), Fouling in Membrane Filtration and Remediation Methods, , in: *Mass Transfer - Advances in Sustainable Energy and Environment Oriented Numerical Modeling*. INTECH.

Aditya Kiran, S., Lukka Thuyavan, Y., Arthanareeswaran, G., Matsuura, T. and Ismail, A. F. (2016), Impact of Graphene Oxide Embedded Polyethersulfone Membranes for the Effective Treatment of Distillery Effluent. *Chemical Engineering Journal*, 286: 528–537. available at http://dx.doi.org/10.1016/j.cej.2015.10.091

Ahmad, M. S., Mohshim, D. F., Nasir, R., Mannan, H. A. and Mukhtar, H. (2018), Effect of Solvents on the Morphology and Performance of Polyethersulfone (PES) Polymeric Membranes Material for CO2/CH4 Separation, , in: *IOP Conference Series: Materials Science and Engineering 2018*.

Alenazi, Noof, Hussein, Mahmoud, Alamry, Khalid and Asiri, Abdullah (2018), Nanocomposite-Based Aminated Polyethersulfone and Carboxylate Activated Carbon for Environmental Application. A Real Sample Analysis. *C*, 4(2): 30.

Ali, Imran, Kim, Seu Run, Kim, Sung Pil and Kim, Jong Oh (2016), Recycling of Textile Wastewater with a Membrane Bioreactor and Reverse Osmosis Plant for Sustainable and Cleaner Production. *Desalination and Water Treatment*, 57(57): 27441–27449.

Aljanabi, Ali A.Abbas, Mousa, Noor Edin, Aljumaily, Mustafa M., Majdi, Hasan Sh, Yahya, Ali Amer, AL-Baiati, Mohammad N., Hashim, Noor, Rashid, Khaild T., Al-Saadi, Saad and Alsalhy, Qusay F. (2022), Modification of Polyethersulfone Ultrafiltration Membrane Using Poly(Terephthalic Acid-Co-Glycerol-g-Maleic Anhydride) as Novel Pore Former. *Polymers*, 14(16).

Alkawareek, Mahmoud Y., Akkelah, Boshra M., Mansour, Sara M., Amro, Hamza M., Abulateefeh, Samer R. and Alkilany, Alaaldin M. (2018), Simple Experiment to Determine Surfactant Critical Micelle Concentrations Using Contact-Angle Measurements. *Journal of Chemical Education*, 95(12): 2227–2232.

Alvi, Muhammad Azeem U.R., Khalid, Muhammad Waqas, Ahmad, Nasir M., Niazi, Muhammad Bilal K., Anwar, Muhammad Nabeel, Batool, Mehwish, Cheema, Waqas and Rafiq, Sikandar (2019), Polymer Concentration and Solvent Variation Correlation with the Morphology and Water Filtration Analysis of Polyether Sulfone Microfiltration Membrane. *Advances in Polymer Technology*, 2019.

American Membrane Technology Association (2016), Membrane Bioreactors for Wastewater Treatment. available at https://www.amtaorg.com/Membrane_Bioreactors_for_Wastewater_Treatment.html

Aminudin, Nurul Nabilah, Basri, Hatijah, Harun, Zawati, Yunos, Muhamad Zaini and Sean, Goh Pei (2013), Comparative Study on Effect of PEG and PVP as Additives on Polysulfone (PSF) Membrane Structure and Performance. *Jurnal Teknologi (Sciences and Engineering)*, 65(4): 47–51.

Amiri, Saba, Asghari, Alireza, Vatanpour, Vahid and Rajabi, Maryam (2020), Fabrication and Characterization of a Novel Polyvinyl Alcohol-Graphene Oxide-Sodium Alginate Nanocomposite Hydrogel Blended PES Nanofiltration Membrane for Improved Water Purification. *Separation and Purification Technology*, 250(June): 117216.

Anadão, Priscila, Sato, Laís Fumie, Wiebeck, Hélio and Díaz, Francisco Rolando Valenzuela (2010), Polysulfone Activated Carbon Composite Membranes. *Materials Science Forum*, 660–661: 1081–1086.

APHA (2017), *Standard Methods for Examination of Water and Wastewater*. American Public Health Association, Washington, DC, USA.

Armstrong, J. K., Wenby, R. B., Meiselman, H. J. and Fisher, T. C. (2004), The Hydrodynamic Radii of Macromolecules and Their Effect on Red Blood Cell Aggregation. *Biophysical Journal*, 87(6): 4259–4270.

Badani, Z., Ait-Amar, H., Si-Salah, A., Brik, M. and Fuchs, W. (2005), Treatment of Textile Waste Water by Membrane Bioreactor and Reuse. *Desalination*, 185(1–3): 411–417.

Baker, Richard. W (2012), *Membrane Technology and Application*. JOHN WILEY & SONS LTD.

Baker, Richard. W, E.L, Cussler., Eykamp, W, Koros, W.J, Riley, R.L and Strathmann, H (1990), *MEMBRANE SEPARATION SYSTEMS- A Research and Developmemnt Needs Assessment*.

Balster, Joerg (2013), Spiral Wound Membrane Module Joerg, , in: *Encyclopedia of Membranes*.

Ben, Fatma, Feki, Firas, Han, Junkuy, Isoda, Hiroko and Sayadi, Sami (2015), Treatment of Textile Wastewater by Submerged Membrane Bioreactor : In Vitro Bioassays for the Assessment of Stress Response Elicited by Raw and Reclaimed Wastewater In e. : 1–9.

Berkessa, Yifru Waktole, Yan, Binghua, Li, Tengfei, Jegatheesan, Veeriah and Zhang, Yang (2020), Treatment of Anthraquinone Dye Textile Wastewater Using Anaerobic Dynamic Membrane Bioreactor: Performance and Microbial Dynamics. *Chemosphere*, 238: 124539.

Bhattacharya, A. and Misra, B. N. (2004), Grafting: A Versatile Means to Modify Polymers: Techniques, Factors and Applications. *Progress in Polymer Science*, 29(8): 767–814.

Bikel, Matióas, Pünt, Ineke G.M., Lammertink, Rob G.H. and Wessling, Matthias (2009), Micropatterned Polymer Films by Vapor-Induced Phase Separation Using Permeable Molds. *ACS Applied Materials and Interfaces*, 1(12): 2856–2861.

Boonyungyuen, Wimonmas, Wonglertarak, Watcharapol and Wichitsathian, Boonchai (2014), Effect of Organic Loading Rate on the Performance of a Membrane Bioreactor (MBR) Treating Textile Wastewater, , in: *International Conference on Chemical, Environment & Biological Sciences (CEBS-2014) Sept. 17-18, 2014 Kuala Lumpur (Malaysia)*.

Brik, M., Schoeberl, P., Chamam, B., Braun, R. and Fuchs, W. (2006), Advanced Treatment of Textile Wastewater towards Reuse Using a Membrane Bioreactor. *Process Biochemistry*, 41(8): 1751–1757.

Carliell, C. M., Barclay, S. J., Naidoo, N., Buckley, C. A., Mulholland, D. A. and Senior, E. (1994), Anaerobic Decolorisation of Reactive Dyes in Conventional Sewage Treatment Processes. *Water SA*, 20(4): 341–344.

Chae Park, Hyun, Po Kim, Yoon, Yong Kim, Hwa and Soo Kang, Yong (1999), Membrane Formation by Water Vapor Induced Phase Inversion. *Journal of Membrane Science*, 156(2): 169–178.

Chakrabarty, B., Ghoshal, A. K. and Purkait, M. K. (2008), Preparation, Characterization and Performance Studies of Polysulfone Membranes Using PVP as an Additive. *Journal of Membrane Science*, 315(1–2): 36–47.

Chen, Xiaolin, Gao, Xueli, Wang, Weiwei, Wang, Duo, Gao, Congjie, Chen, Xiaolin, Gao, Xueli, Wang, Weiwei, Wang, Duo and Gao, Congjie (2010), Study of Sodium Alginate / Polysulfone Composite Nanofi Ltration Membrane. *Desalination and Water Treatment*, 18: 198–205.

Chen, Xing, Partheniadis, Ioannis, Nikolakakis, Ioannis and Al-Obaidi, Hisham (2020), Solubility Improvement of Progesterone from Solid Dispersions Prepared by Solvent Evaporation and Co-Milling. *Polymers*, 12(4).

Cheryan, Munir (1998), *Ultrafiltration and Microfiltration Handbook*. CRC press.

Chibowski, S and Paszkiewicz, M *Studies of Some Properties and the Structure of Polyethylene Glycol (PEG) Macromolecules Adsorbed on a TiO 2 Surface †*.

Cui, Z. F., Jiang, Y. and Field, R. W. (2010), *Fundamentals of Pressure-Driven Membrane Separation Processes*. Elsevier Ltd.

Cui, Zhaoliang, Tavajohi, Naser, Young, Suk, Myung, Jong, Taek, Kyung, Sanguineti, Aldo, Arcella, Vincenzo, Moo, Young and Drioli, Enrico (2013), Poly (Vinylidene Fl Uoride) Membrane Preparation with an Environmental Diluent via Thermally Induced Phase Separation. *Journal of Membrane Science*, 444: 223–236.

Dai, Zhongde, Ansaloni, Luca and Deng, Liyuan (2016), Recent Advances in Multi-Layer Composite Polymeric Membranes for CO2 Separation: A Review. *Green Energy and Environment*, 1(2): 102–128.

Daramola, Michael O., Aransiola, Elizabeth F. and Ojumu, Tunde V. (2012), Potential Applications of Zeolite Membranes in Reaction Coupling Separation Processes. *Materials*, 5(11): 2101–2136.

Das, Chandan and Gebru, Kibrom Alebel (2019), *Polymeric Membrane Synthesis, Modification, and Applications Electro-Spun and Phase Inverted Membranes*. CRC Press Taylor & Francis Group.

Deng, Baolin (2013), Effects of Polysulfone (PSf) Support Layer on the Performance of Thin-Film Composite (TFC) Membranes. *Journal of Chemical and Process Engineering*, 1.

Deowan, Shamim Ahmed, Galiano, Francesco, Hoinkis, Jan, Figoli, Alberto and Drioli, Enrico (2013), Submerged Membrane Bioreactor (SMBR) for Treatment of Textile Dye Wastewatertowards Developing Novel MBR Process, 259–264, in: *ICESD 2013: January 19-20, Dubai, UAE*.

Deowan, Shamim Ahmed, Galiano, Francesco, Hoinkis, Jan, Johnson, Daniel, Altinkaya, Sacide Alsoy, Gabriele, Bartolo, Hilal, Nidal, Drioli, Enrico and Figoli, Alberto (2016), Novel Low-Fouling Membrane Bioreactor (MBR) for Industrial Wastewater Treatment. *Journal of Membrane Science*, 510: 524–532.

Dey, Shuchismita and Islam, Ashraful (2015), A Review on Textile Wastewater Characterization in Bangladesh. *Resources and Environment*, 5(1): 15–44. available at http://journal.sapub.org/re

DoE (1997), *The Environment Conservation Rules, 1997*.

Dommati, Hitesh, Ray, Saikat Sinha, Wang, Jia Chang and Chen, Shiao Shing (2019), A Comprehensive Review of Recent Developments in 3D Printing Technique for Ceramic Membrane Fabrication for Water Purification. *RSC Advances*, 9(29): 16869–16883.

Espinal, Laura (2012), Porosity and Its Measurement, , in: Kaufmann, E. N. (Ed.), *Characterization of Materials*. John Wiley & Sons, Inc.

Ezugbe, Elorm Obotey and Rathilal, Sudesh (2020), Membrane Technologies in Wastewater Treatment: A Review. *Membranes*, 10(5).

Fane, A G Tony, Wang, Rong and Jia, Yue (2011), Membrane Technology: Past, Present and Future, , in: *Membrane and Desalination Technologies*. Humana Press Inc.

Fang, Xiaofeng, Li, Jiansheng, Li, Xin, Pan, Shunlong, Sun, Xiuyun, Shen, Jinyou, Han, Weiqing, Wang, Lianjun and Van der Bruggen, Bart (2017), Iron-Tannin-Framework Complex Modified PES Ultrafiltration Membranes with Enhanced Filtration Performance and Fouling Resistance. *Journal of Colloid and Interface Science*, 505: 642–652.

Federation, Water Environment (2012), *Membrane Bioreactors*. Water Environment Federation, Virginia.

Feng, Yingnan, Han, Gang, Chung, Tai Shung, Weber, Martin, Widjojo, Natalia and Maletzko, Christian (2017), Effects of Polyethylene Glycol on Membrane Formation and Properties of

Hydrophilic Sulfonated Polyphenylenesulfone (SPPSU) Membranes. *Journal of Membrane Science*, 531: 27–35. available at http://dx.doi.org/10.1016/j.memsci.2017.02.040

Ganesh, B. M., Isloor, Arun M. and Ismail, A. F. (2013), Enhanced Hydrophilicity and Salt Rejection Study of Graphene Oxide-Polysulfone Mixed Matrix Membrane. *Desalination*, 313: 199–207. available at http://dx.doi.org/10.1016/j.desal.2012.11.037

Grilli, Selene, Piscitelli, Daniela, Mattioli, Davide, Casu, Stefania and Spagni, Alessandro (2011), Textile Wastewater Treatment in a Bench-Scale Anaerobic-Biofilm Anoxic-Aerobic Membrane Bioreactor Combined with Nanofiltrat. *Journal of Environmental Science and Health*, 46: 1512–1518.

Gu, Minghao, Zhang, Jun, Wang, Xiaolin and Ma, Wenzhong (2006), Crystallization Behavior of PVDF in PVDF-DMP System via Thermally Induced Phase Separation. , 102: 3714–3719.

Guenoun, P., Garate, H., Deratani, A., Quemener, D., Pochat-Bohatier, C. and Bouyer, D. (2017), Fabrication of Novel Porous Membrane from Biobased Water-Soluble Polymer (Hydroxypropylcellulose). *Journal of Membrane Science*, 526: 212–220.

Gupta, Vandana and Anandkumar, J (2023), Membrane Processes, , in: Shah, Maulin. P. (Ed.), *Membrane and membrane based processes for wastewater treatment*. CRC press.

Hai, Faisal I., Riley, Thomas, Shawkat, Samia, Magram, Saleh F. and Yamamoto, Kazuo (2014), Removal of Pathogens by Membrane Bioreactors: A Review of the Mechanisms, Influencing Factors and Reduction in Chemical Disinfectant Dosing. *Water* , 6(12): 3603–3630.

Hai, Faisal Ibney, Yamamoto, Kazuo and Fukushi, Kensuke (2005), Different Fouling Modes of Submerged Hollow-Fiber and Flat-Sheet Membranes Induced by High Strength Wastewater with Concurrent Biofouling. *Desalination*, 180(1–3): 89–97.

Hai, Faisal Ibney, Yamamoto, Kazuo and Lee, Chung Hak (2014), *Membrane Biological Reactors*. IWA.

Haia, Faisal I, Yamamoto, Kazuo and Lee, Chung-Hak (2014), Introduction to Membrane Biological Reactors, 1–1, in: Haia, F. I., Yamamoto, K., and Lee, C.-H. (Eds.), *Membrane Biological Reactors Theory, Modeling, Design, Management and Applications to Wastewater Reuse*. IWA Publishing.

Hamedi, Hamideh, Ehteshami, Majid, Mirbagheri, Seyed Ahmad, Rasouli, Seyed Abbas and Zendehboudi, Sohrab (2019), Current Status and Future Prospects of Membrane Bioreactors (MBRs) and Fouling Phenomena: A Systematic Review. *Canadian Journal of Chemical Engineering*, 97(1): 32–58.

Hassan, Nazmul, Kabir, A N M Hamidul, Rahman, Moshikur and Islam, Rafiqul (2014), Treatment of Textile Wastewater by Electro-Coagulation and Activated Sludge Process. , 1(6): 58–63.

Hołda, Agnieszka K. and Vankelecom, Ivo F.J. (2015), Understanding and Guiding the Phase Inversion Process for Synthesis of Solvent Resistant Nanofiltration Membranes. *Journal of Applied Polymer Science*, 132(27): 1–17.

Huang, Rong-rong, Hoinkis, Jan, Hu, Qi and Koch, Florian (2009), Treatment Treatment of Dyeing Wastewater by Hollow Fiber Membrane Biological Reactor. *Desalination and Water*, 11: 288–293.

Hussein, Tamara Kawther, Jasim, Nidaa Adil and Al-Madhhachi, Abdul Sahib T. (2023), The Performance of Microfiltration Using Hydrophilic and Hydrophobic Membranes for Phenol Extraction from a Water Solution. *ChemEngineering*, 7(2): 26.

Hwang, Taeseon, Oh, Joon Suk, Yim, Woosoon, Nam, Jae Do, Bae, Chulsung, Kim, Hyung Ick and Kim, Kwang Jin (2016), Ultrafiltration Using Graphene Oxide Surface-Embedded Polysulfone Membranes. *Separation and Purification Technology*, 166: 41–47.

Ibney, Faisal, Yamamoto, Kazuo and Fukushi, Kensuke (2006), Development of a Submerged Membrane Fungi Reactor for Textile Wastewater Treatment. *Desalination*, 192: 315–322.

Idris, Alamin, Man, Zakaria, Maulud, Abdulhalim S. and Khan, Muhammad Saad (2017), Effects of Phase Separation Behavior on Morphology and Performance of Polycarbonate Membranes. *Membranes*, 7(2).

Ionita, Mariana, Pandele, Andreea Madalina, Crica, Livia and Pilan, Luisa (2014), Improving the Thermal and Mechanical Properties of Polysulfone by Incorporation of Graphene Oxide. *Composites Part B: Engineering*, 59: 133–139.

Iorhemen, Oliver Terna, Hamza, Rania Ahmed and Tay, Joo Hwa (2016), Membrane Bioreactor (Mbr) Technology for Wastewater Treatment and Reclamation: Membrane Fouling. *Membranes*, 6(2).

Işik, Mustafa and Sponza, Delia Teresa (2008), Anaerobic/Aerobic Treatment of a Simulated Textile Wastewater. *Separation and Purification Technology*, 60(1): 64–72.

De Jager, D., Sheldon, M. S. and Edwards, W. (2012), Membrane Bioreactor Application within the Treatment of High-Strength Textile Effluent. *Water Science and Technology*, 65(5): 907–914.

Jeon, Sungil, Karkhanechi, Hamed, Fang, Li-feng, Cheng, Liang, Ono, Takahiro, Nakamura, Ryota and Matsuyama, Hideto (2017), Novel Preparation and Fundamental Characterization of Polyamide 6 Self- Supporting Hollow Fiber Membranes via Thermally Induced Phase Separation (TIPS). *Journal of Membrane Science*.

Jiang, Lan Ying (2016), Asymmetric Membrane, , in: *Encyclopedia of Membranes*. Springer-Verlag Berlin Heidelberg.

Juhn, Il, Ramaswamy, Senthilkumar, Krantz, William B and Greenberg, Alan R (2010), Poly (Ethylene Chlorotrifluoroethylene) Membrane Formation via Thermally Induced Phase Separation (TIPS). *Journal of Membrane Science*, 362(1–2): 211–220.

Jung, Bumsuk, Joon, Ki Yoon, Kim, Bokyung and Rhee, Hee Woo (2004), Effect of Molecular Weight of Polymeric Additives on Formation, Permeation Properties and Hypochlorite Treatment of Asymmetric Polyacrylonitrile Membranes. *Journal of Membrane Science*, 243(1–2): 45–57.

Kahrs, Catharina and Schwellenbach, Jan (2020), Membrane Formation via Non-Solvent Induced Phase Separation Using Sustainable Solvents: A Comparative Study. *Polymer*, 186: 122071.

Kalayni (2020), Artificial Inorganic Membranes Market Report 2019. *Prnewsprim*. available at https://www.prnewsprime.com/2020/03/artificial-inorganic-membranes-market-report-2019/

Kalyani, Swayampakula, Smitha, Biduru, Sridhar, Sundergopal and Krishnaiah, Abburi (2008), Pervaporation Separation of Ethanol-Water Mixtures through Sodium Alginate Membranes. *Desalination*, 229(1–3): 68–81.

Kant, Rita (2012), Textile Dyeing Industry an Environmental Hazard. *Natural Science*, 04(01): 22–26.

Kassim Shaari, Norin Zamiah, Abd Rahman, Norazah, Sulaiman, Nurul Aida and Mohd Tajuddin, Ramlah (2017), Thin Film Composite Membranes: Mechanical and Antifouling Properties. *MATEC Web of Conferences*, 103.

Khorsand-Ghayeni, Mohammad, Barzin, Jalal, Zandi, Mojgan and Kowsari, Mojegan (2017), Fabrication of Asymmetric and Symmetric Membranes Based on PES/PEG/DMAc. *Polymer Bulletin*, 74(6): 2081–2097.

Khulbe, K.C, Feng, C and Matsuura.T (2010), The Art of Surface Modification of Synthetic Polymeric Membranes. *Journal of Applied Polymer Science*, 115(5): 855–895.

Kim, In Chul, Yun, Hyung Gu and Lee, Kew Ho (2002), Preparation of Asymmetric Polyacrylonitrile Membrane with Small Pore Size by Phase Inversion and Post-Treatment Process. *Journal of Membrane Science*, 199(1): 75–84.

Kim, Jeong F, Jung, Jun T, Wang, Ho H, Suk, Y, Moore, Theodore, Sanguineti, Aldo, Lee, Young M, Moore, Theodore, Sanguineti, Aldo, Drioli, Enrico and Lee, Young M (2016), Microporous PVDF Membranes via Thermally Induced Phase Separation (TIPS) and Stretching Methods. *Journal of Membrane Science*.

Konsowa, A. H., Eloffy, M. G. and El-Taweel, Y. A. (2013), Treatment of Dyeing Wastewater Using Submerged Membrane Bioreactor. *Desalination and Water Treatment*, 51(4–6): 1079–1090.

Konsowa, A H, Eloffy, M G and El-Taweel, Y.A (2013), Treatment Treatment of Dyeing Wastewater Using Submerged Membrane Bioreactor. *Desalination and Water*, 51: 1079–1090.

Kumar, S., Nandi, B. K., Guria, C. and Mandal, A. (2017), Oil Removal from Produced Water by Ultrafiltration Using Polysulfone Membrane. *Brazilian Journal of Chemical Engineering*, 34(2): 583–596.

Ladewig, Bradley and Al-Shaeli, Muayad Nadhim Zemam (2017), *Fundamentals of Membrane Bioreactors*. Springer Nature Singapore Pte Ltd.

Ladewing, Bradley and Al-Shaeli, Muayad Nadhim Zemam (2017), *Fundamentals of Membrane Reactors*. Springer Nature Singapore Pte Ltd.

Lee, Hyuck Jai, Jung, Bumsuk, Kang, Yong Soo and Lee, Hoosung (2004), Phase Separation of Polymer Casting Solution by Nonsolvent Vapor. *Journal of Membrane Science*, 245(1–2): 103–112.

Lee, Jaewoo, Chae, Hee Ro, Won, Young June, Lee, Kibaek, Lee, Chung Hak, Lee, Hong H., Kim, In Chul and Lee, Jong min (2013), Graphene Oxide Nanoplatelets Composite Membrane with Hydrophilic and Antifouling Properties for Wastewater Treatment. *Journal of Membrane Science*, 448: 223–230.

Li, Chia Ling, Wang, Da Ming, Deratani, André, Quémener, Damien, Bouyer, Denis and Lai, Juin Yih (2010), Insight into the Preparation of Poly(Vinylidene Fluoride) Membranes by Vapor-Induced Phase Separation. *Journal of Membrane Science*, 361(1–2): 154–166.

Li, Zhong-kun, Lang, Wan-zhong, Miao, Wei and Guo, Ya-jun (2016), Preparation and Properties of PVDF/SiO2@GO Nanohybrid Membranes via Thermally Induced Phase Separation Method. *Journal of Membrane Science*.

Liang, Hong-qing, Wu, Qing-yun, Wan, Ling-shu, Huang, Xiao-jun and Xu, Zhi-kang (2013), Polar Polymer Membranes via Thermally Induced Phase Separation Using a Universal Crystallizable Diluent. *Journal of Membrane Science*, 446: 482–491.

Lorena, Salazar, Martì, Crespi and Roberto, Salazar (2011), Comparative Study between Activated Sludge versus Membrane Bioreactor for Textile Wastewater. *Desalination and Water Treatment*, 35(1–3): 101–109.

Lubello, CCaffaz, Simone and Caretti, Cecilia (2007), MBR Pilot Plant for Textile Wastewater Treatment and Reuse. *Water Science & Technology*, 55(10): 115–124.

Lubello, Claudio and Gori, Riccardo (2004), Membrane Bio-Reactor for Advanced Textile Wastewater Treatment and Reuse. *Water Science and Technology*, 50(2): 113–119.

Luong, Tan Vu, Schmidt, S., Deowan, S. A., Hoinkis, J., Figoli, A. and Galiano, F. (2016), Membrane Bioreactor and Promising Application for Textile Industry in Vietnam. *Procedia CIRP*, 40(September 2015): 419–424.

Madaeni, S. S. and Taheri, A. H. (2009), Preparation of Pes Ultrafiltration Membrane for Treatment of Emulsified Oily Wastewater: Effect of Solvent and Non-Solvent on Morphology and Performance. *Journal of Polymer Engineering*, 29(4): 183–198.

Mahmoudian, Mehdi, Kochameshki, Mahmoud Ghasemi, Mahdavi, Hossein, Vahabi, Henri and Enayati, Mojtaba (2018), Investigation of Structure-Performance Properties of a Special Type of Polysulfone Blended Membranes. *Polymers for Advanced Technologies*, 29(10): 2690–2700.

Malik, Tabassum, Razzaq, Humaira, Razzaque, Shumaila, Nawaz, Hifza, Siddiqa, Asima, Siddiq, Mohammad and Qaisar, Sara (2019), Design and Synthesis of Polymeric Membranes Using Water-Soluble Pore Formers: An Overview. *Polymer Bulletin*, 76(9): 4879–4901. available at https://doi.org/10.1007/s00289-018-2616-3

Malpei, F, Bonomo, L and Rozzi, A (2003), Feasibility Study to Upgrade a Textile Wastewater Treatment Plant by a Hollow Fibre Membrane Bioreactor for Effluent Reuse. *Water Science and Technology*. available at https://iwaponline.com/wst/article-pdf/47/10/33/421995/33.pdf

Mansourizadeh, A., Ismail, A. F., Abdullah, M. S. and Ng, B. C. (2010), Preparation of Polyvinylidene Fluoride Hollow Fiber Membranes for CO2 Absorption Using Phase-Inversion Promoter Additives. *Journal of Membrane Science*, 355(1–2): 200–207.

Matošić, Marin, Crnek, Vlado, Jakopović, Helena Korajlija and Mijatović, Ivan (2009), MUNICIPAL WASTEWATER TREATMENT IN A MEMBRANE BIOREACTOR. *Fresenius Environmental Bulletin*, 18(12): 2275–2281.

Matsuyama, Hideto, Okafuji, Hajime, Maki, Taisuke, Teramoto, Masaaki and Kubota, Noboru (2003), Preparation of Polyethylene Hollow Fiber Membrane via Thermally Induced Phase Separation. *Journal of Membrane Science*, 223: 119–126.

Maximous, Nermen, Nakhla, G, Wan, W and Wong, K (2009), Preparation , Characterization and Performance of Al 2 O 3 / PES Membrane for Wastewater Filtration. , 341: 67–75.

McKeen, Laurence W. (2012), Markets and Applications for Films, Containers, and Membranes. *Permeability Properties of Plastics and Elastomers*: 59–75.

McWilliam, Andrew (2019), Membrane Bioreactors: Global Markets. *BCC publication*. available at https://www.bccresearch.com/market-research/membrane-and-separation-technology/membrane-bioreactors.html

Mei, Shuo, Xiao, Changfa and Hu, Xiaoyu (2011), Preparation of Porous PVC Membrane via a Phase Inversion Method from PVC/DMAc/Water/Additive. *Journal of Applied Polymer Science*, 120: 557–562.

Menut, P., Su, Y. S., Chinpa, W., Pochat-Bohatier, C., Deratani, A., Wang, D. M., Huguet, P., Kuo, C. Y., Lai, J. Y. and Dupuy, C. (2008), A Top Surface Liquid Layer during Membrane Formation Using Vapor-Induced Phase Separation (VIPS)-Evidence and Mechanism of Formation. *Journal of Membrane Science*, 310(1–2): 278–288.

Miller, Daniel J., Dreyer, Daniel R., Bielawski, Christopher W., Paul, Donald R. and Freeman, Benny D. (2017), Surface Modification of Water Purification Membranes. *Angewandte Chemie*, 56(17): 4662–4711.

Moghimifar, Vahid, Raisi, Ahmadreza and Aroujalian, Abdolreza (2014), Surface Modification of Polyethersulfone Ultrafiltration Membranes by Corona Plasma-Assisted Coating TiO2 Nanoparticles. *Journal of Membrane Science*, 461: 69–80.

Mokkapati, V. R.S.S., Koseoglu-Imer, Derya Yuksel, Yilmaz-Deveci, Nurmiray, Mijakovic, Ivan and Koyuncu, Ismail (2017), Membrane Properties and Anti-Bacterial/Anti-Biofouling Activity of Polysulfone-Graphene Oxide Composite Membranes Phase Inversed in Graphene Oxide Non-Solvent. *RSC Advances*, 7(8): 4378–4386.

Mondal, Sourav, Purkait, Mihir Kumar and De, Sirshendu (2018), Emulsion Liquid Membrane, , in: *Advances in Dye Removal Technologies*. Springer Nature Singapore Pte Ltd.

Mulder, Marcel (1996), *Basic Principles of Membrane Technology*. KLUWER ACADEMIC PUBLISHERS.

Mulder, Marcel (2000), Phase Inversion Membranes, 3331–3346, in: *Encyclopedia of Separation Science*. Academic Press.

Mulyati, S., Aprilia, S., Safiah, Syawaliah, Armando, M. A. and Mawardi, H. (2017), The Effect of Poly Ethylene Glycol Additive on the Characteristics and Performance of Cellulose Acetate Ultrafiltration Membrane for Removal of Cr(III) from Aqueous Solution, , in: *IOP Conference Series: Materials Science and Engineering, Volume 352, The 7th AIC-ICMR on Sciences and Engineering 2017 18–20 October 2017, Banda Aceh, Indonesia*. Institute of Physics Publishing.

Mulyati, S., Aprilia, S., Safiah, Syawaliah, Armando, M. A. and Mawardi, H. (2018), The Effect of Poly Ethylene Glycol Additive on the Characteristics and Performance of Cellulose Acetate Ultrafiltration Membrane for Removal of Cr(III) from Aqueous Solution. *IOP Conference Series: Materials Science and Engineering*, 352(1).

Nabilah Aminudin, Nurul, Basri, Hatijah, Harun, Zawati, Zaini Yunos, Muhamad and Pei Sean, Goh (2013), Comparative Study on Effect of PEG and PVP as Additives on Polysulfone (PSF) Membrane Structure and Performance. *Jurnal Teknologi*, 65: 2180–3722. available at www.jurnalteknologi.utm.my

Nadour, Meriem, Boukraa, Fatima, Ouradi, Adel and Benaboura, Ahmed (2017), Effects of Methylcellulose on the Properties and Morphology of Polysulfone Membranes Prepared by Phase Inversion. *Material Research*, 20(2): 339–348.

Najjar, Ahmad, Sabri, Souhir, Al-Gaashani, Rashad, Kochkodan, Viktor and Atieh, Muataz Ali (2019), Enhanced Fouling Resistance and Antibacterial Properties of Novel Graphene Oxide-Arabic Gum Polyethersulfone Membranes. *Applied Sciences (Switzerland)*, 9(3).

Nasseri, Simin, Ebrahimi, Shima, Abtahi, Mehrnoosh and Saeedi, Reza (2018), Synthesis and Characterization of Polysulfone/Graphene Oxide Nano-Composite Membranes for Removal of Bisphenol A from Water. *Journal of Environmental Management*, 205: 174–182.

Nath, Kaushik (2008), *Membrane Separation Processes*. Prentice-Hall of India, New Delhi, 110001.

Nawi, Normi Izati Mat, Chean, Ho Min, Shamsuddin, Norazanita, Bilad, Muhammad Roil, Narkkun, Thanitporn, Faungnawakij, Kajornsak and Khan, Asim Laeeq (2020), Development of Hydrophilic PVDF Membrane Using Vapour Induced Phase Separation Method for Produced Water Treatment. *Membranes*, 10(6): 1–17.

Nawi, Normi Izati Mat, Sait, Nur Rifqah, Bilad, Muhammad Roil, Shamsuddin, Norazanita, Jaafar, Juhana, Nordin, Nik Abdul Hadi, Narkkun, Thanitporn, Faungnawakij, Kajornsak and Mohshim, Dzeti Farhah (2021), Polyvinylidene Fluoride Membrane via Vapour Induced Phase Separation for Oil/Water Emulsion Filtration. *Polymers*, 13(3): 1–17.

Nguyen, Thang, Roddick, Felicity A. and Fan, Linhua (2012), Biofouling of Water Treatment Membranes: A Review of the Underlying Causes, Monitoring Techniques and Control Measures. *Membranes*, 2(4): 804–840.

Niren, P. and Jigisha, P. (2011), Textile Wastewater Treatment Using a UF Hollow-Fibre Submerged Membrane Bioreactor (SMBR). *Environmental Technology*, 32(11): 1247–1257.

Omnexus (2021), Glass Transition Temperature. available at https://omnexus.specialchem.com/polymer-properties/properties/glass-transition-temperature

Pandy, P Senthur (2015), Treatment of Textile Effluent Using Submerged Membrane Bioreactor. *International Journal of Science, Environment*, 4(2): 305–317.

Parhi, P. K. (2013), Supported Liquid Membrane Principle and Its Practices: A Short Review. *Journal of Chemistry*, 2013.

Park, Hee-Deung, Chang, In-Soung and Lee, Kwang-Jin (2015), *Principles of Membrane Bioreactors for Wastewater Treatment*. CRC Press.

Park, Myoung Jun, Phuntsho, Sherub, He, Tao, Nisola, Grace M., Tijing, Leonard D., Li, Xue Mei, Chen, Gang, Chung, Wook Jin and Shon, Ho Kyong (2015), Graphene Oxide Incorporated Polysulfone Substrate for the Fabrication of Flat-Sheet Thin-Film Composite Forward Osmosis Membranes. *Journal of Membrane Science*, 493: 496–507.

PCI membranes Classic Series Tubular Membranes. available at https://www.pcimembranes.com/classic-series-tubular-membranes/

Pervin, Rumiaya, Ghosh, Pijush and Basavaraj, Madivala G. (2019a), Tailoring Pore Distribution in Polymer Films via Evaporation Induced Phase Separation. *RSC Advances*, 9(27): 15593–15605.

Pervin, Rumiaya, Ghosh, Pijush and Basavaraj, Madivala G. (2019b), Tailoring Pore Distribution in Polymer Films via Evaporation Induced Phase Separation. *RSC Advances*, 9(27): 15593–15605.

Peydayesh, Mohammad, Bagheri, Maryam, Mohammadi, Toraj and Bakhtiari, Omid (2017), Fabrication Optimization of Polyethersulfone (PES)/Polyvinylpyrrolidone (PVP) Nanofiltration Membranes Using Box-Behnken Response Surface Method. *RSC Advances*, 7(40): 24995–25008.

Pinnau, I and Freeman, B.D (2000), *Membrane Formation and Modification*. American Chemical Society.

Plisko, T. V., Penkova, A. V., Burts, K. S., Bildyukevich, A. V., Dmitrenko, M. E., Melnikova, G. B., Atta, R. R., Mazur, A. S., Zolotarev, A. A. and Missyul, A. B. (2019), Effect of Pluronic F127 on Porous and Dense Membrane Structure Formation via Non-Solvent Induced and Evaporation Induced Phase Separation. *Journal of Membrane Science*, 580: 336–349.

Porter, M.C (1990), *Handbook of Industrial Membrane Technology*. Noyes Publication, USA.

Purkait, Mihir Kumar and Singh, Randeep (2018), *Membrane Technology in Separation Science*. CRC press, Taylor & Francis Group.

Purkait, Mihir Kumar, Sinha, Manish Kumar, Mondal, Piyal and Singh, Randeep (2018), Introduction to Membranes, , in: *Interface Science and Technology*.

Qu, Ping, Tang, Huanwei, Gao, Yuan, Zhang, Li-Ping and Wang, Siqun (2010), Polyethersulfone/Cellulose Membrane. *BioResources*, 5(4): 2323–2336.

Radjenovi, Jelena, Matosic, Martin, Mijatovic, Ivan, Petrovic, Mira and Barceló, Damia (2008), Membrane Bioreactor (MBR) as an Advanced Wastewater Treatment Technology, 37–101, in: *Emerging Contaminants from Industrial and MunicipalWaste,*. Springer Berlin Heidelberg.

Rajabzadeh, Saeid, Liang, Cui, Ohmukai, Yoshikage, Maruyama, Tatsuo and Matsuyama, Hideto (2012), Effect of Additives on the Morphology and Properties of Poly (Vinylidene Fluoride) Blend Hollow Fiber Membrane Prepared by the Thermally Induced Phase Separation Method. *Journal of Membrane Science*, 423–424: 189–194.

Rashid, Khalid T., Alayan, Haiyam M., Mahdi, Alyaa E., Al-Baiati, Mohammad N., Majdi, Hasan Sh, Salih, Issam K., Ali, Jamal M. and Alsalhy, Qusay F. (2022), Novel Water-Soluble Poly(Terephthalic-Co-Glycerol-g-Fumaric Acid) Copolymer Nanoparticles Harnessed as Pore Formers for Polyethersulfone Membrane Modification: Permeability–Selectivity Tradeoff Manipulation. *Water (Switzerland)*, 14(9).

Ravishankar, Harish, Christy, Jens and Jegatheesan, Veeriah (2018), Graphene Oxide (GO)-Blended Polysulfone (PSf) Ultrafiltration Membranes for Lead Ion Rejection. *Membranes*, 8(3).

Ren, Jizhong and Wang, Rong (2011), Preparation of Polymeric Membranes, , in: *Handbook of Environmental Engineering: Membrane and Desalination Technologies*. Springer Science + Business Media.

Report, Market Analysis (2017), Membrane Bioreactor Market Size, Share & Trends Analysis Report. available at https://www.grandviewresearch.com/industry-analysis/membrane-bioreactor-mbr-market

Ripoche, Anne, Menut, Paul, Dupuy, Claude, Caquineau, Hubert and Deratant, Andre (2002), Poly(Ether Imide) Membrane Formation by Water Vapour Induced Phase Inversion. *Macromol. Symp.*, 48: 37–48.

Rondon, Hector, El-cheikh, William, Alicia, Ida, Boluarte, Rodriguez, Chang, Chia-yuan, Bagshaw, Steve, Farago, Leanne, Jegatheesan, Veeriah and Shu, Li (2015), Bioresource Technology Application of Enhanced Membrane Bioreactor (EMBR) to Treat Dye Wastewater. *BIORESOURCE TECHNOLOGY*, 183: 78–85.

Roy, Chapol Kumar, Jahan, Miskat Ara Akhter and Rahman, Shafkat Shamim (2018), Characterization and Treatment of Textile Wastewater by Aquatic Plants (Macrophytes) and Algae. *European Journal of Sustainable Development Research*, 2(3). available at http://www.lectitopublishing.nl/Article/Detail/characterization-and-treatment-of-textile-wastewater-by-aquatic-plants-macrophytes-and-algae

Saha, Pradip, Mozumder, Salatul Islam and Hoinkis, Jan (2014), MBR Technology for Textile Wastewater Treatment : First Experience in Bangladesh. *Membrane Water Treatment*, 5: 197–204.

SAMCO (2018), What Are the Different Types of Membrane Fouling and What Causes Them. available at https://www.samcotech.com/types-of-membrane-fouling-and-causes/

Sarbatly, Rosalam (2020), *Membrane Technology for Water and Wastewater Treatment in Rural Regions* . IGI Global, USA.

Schoeberl, Paul, Brik, Mounir, Bertoni, Marina, Braun, Rudolf and Fuchs, Werner (2005), Optimization of Operational Parameters for a Submerged Membrane Bioreactor Treating Dyehouse Wastewater. *Separation and Purification Technology*, 44: 61–68.

Scott, K. (1995), Membrane Materials, Preparation and Characterisation. *Handbook of Industrial Membranes*: 187–269.

Sharaai, Amir Hamzah, Mahmood, Noor Zalina and Sulaiman, Abdul Halim (2009), Life Cycle Impact Assessment (LCIA) of Potable Water Treatment Process in Malaysia: Comparison between Dissolved Air Flotation (DAF) and Ultrafiltration (UF) Technology. *Australian Journal of Basic and Applied Sciences*, 3(4): 3625–3632.

Şimşek, Esra Nur, Akdağ, Akın and Çulfaz-Emecen, P. Zeynep (2016), Modification of Poly(Ether Sulfone) for Antimicrobial Ultrafiltration Membranes. *Polymer*, 106: 91–99.

Sinha, M K and Purkait, M K (2013), Increase in Hydrophilicity of Polysulfone Membrane Using Polyethylene Glycol Methyl Ether. *Journal of Membrane Science*.

Solak, Ebru Kondolot and Şanli, Oya (2010), Use of Sodium Alginate-Poly(Vinyl Pyrrolidone) Membranes for Pervaporation Separation of Acetone/Water Mixtures. *Separation Science and Technology*, 45(10): 1354–1362.

Solak, Ebru Kondolot and Şanlı, Oya (2011), Separation Performance of Sodium Alginate/Poly Vinyl Pyrrolidone Membranes for Aqueous/Dimethylformamide Mixtures by Vapor Permeation and Vapor Permeation with Temperature Difference Methods. *Advances in Chemical Engineering and Science*, 01(04): 305–312.

Song, Kyung-guen, Kim, Yuri and Ahn, Kyu-hong (2008), Effect of Coagulant Addition on Membrane Fouling and Nutrient Removal in a Submerged Membrane Bioreactor. *Desalination*, 221: 467–474.

Spagni, Alessandro, Casu, Stefania and Grilli, Selene (2012), Decolourisation of Textile Wastewater in a Submerged Anaerobic Membrane Bioreactor. *Bioresource Technology*, 117: 180–185.

Srivastava, Harsha P, Arthanareeswaran, G, Anantharaman, N and Starov, Victor M (2011), Performance of Modi Fi Ed Poly (Vinylidene Fl Uoride) Membrane for Textile Wastewater Ultra Fi Ltration. , 282: 87–94.

Su, Y. S., Kuo, C. Y., Wang, D. M., Lai, J. Y., Deratani, A., Pochat, C. and Bouyer, D. (2009), Interplay of Mass Transfer, Phase Separation, and Membrane Morphology in Vapor-Induced Phase Separation. *Journal of Membrane Science*, 338(1–2): 17–28.

Su, Yi, Chen, Cuixian, Li, Yongguo and Li, Jiding (2007), PVDF Membrane Formation via Thermally Induced Phase Separation. *Journal of Macromolecular Science, Part A: Pure and Applied Chemistry*, 44(1): 99–104.

Sun, Huawei, Zhang, Yufeng, Zhang, Zhaohui, Zhao, Heng and Liu, Enhua (2010), Application of Coagulation +Hydrolytic Acidification+Tubular Membrane Bioreactor(MBR) System in Printing and Dyeing Wastewater Treatment. *Modern Applied Science*, 4(2): 41–48.

Sundar, V. J., Ramesh, R., Rao, P. S., Saravanan, P., Sridharnath, B. and Muralidharan, C. (2001), Water Management in Leather Industry. *Journal of Scientific and Industrial Research*, 60(6): 443–450.

Tamime, A.Y (2013), *Membrane Processing* (A. Y. Tamime, Ed.). Blackwell Publishing Ltd.

Tan, Xue Mei and Rodrigue, Denis (2019), A Review on Porous Polymeric Membrane Preparation. Part I: Production Techniques with Polysulfone and Poly (Vinylidene Fluoride). *Polymers*, 11(8).

Tomietto, Pacôme, Loulergue, Patrick, Paugam, Lydie and Audic, Jean Luc (2020), Biobased Polyhydroxyalkanoate (PHA) Membranes: Structure/Performances Relationship. *Separation and Purification Technology*, 252: 117419.

Treatment, Membrane and Bio, Membrane (2008), Membrane Bio-Reactors. *American Membrane Technology Association*: 1–7.

Tsai, H. A., Kuo, C. Y., Lin, J. H., Wang, D. M., Deratani, A., Pochat-Bohatier, C., Lee, K. R. and Lai, J. Y. (2006), Morphology Control of Polysulfone Hollow Fiber Membranes via Water Vapor Induced Phase Separation. *Journal of Membrane Science*, 278(1–2): 390–400.

Tsai, J. T., Su, Y. S., Wang, D. M., Kuo, J. L., Lai, J. Y. and Deratani, A. (2010), Retainment of Pore Connectivity in Membranes Prepared with Vapor-Induced Phase Separation. *Journal of Membrane Science*, 362(1–2): 360–373.

Tsakiridou, Georgia, Reppas, Christos, Kuentz, Martin and Kalantzi, Lida (2019), A Novel Rheological Method to Assess Drug-Polymer Interactions Regarding Miscibility and Crystallization of Drug in Amorphous Solid Dispersions for Oral Drug Delivery. *Pharmaceutics*, 11(12).

Uddin, Mohsin and Maruf Billah, S M (2022), Textile Wastewater Treatment Using Membrane Bioreactor: Opportunities and Challenges in Bangladesh, , in: *5th International Conference on Industrial & Mechanical Engineering and Operations Management*.

Ulbricht, Mathias (2006), Advanced Functional Polymer Membranes. *Polymer*, 47(7): 2217–2262.

Upadhyaya, Lakshmeesha, Qian, Xianghong and Ranil Wickramasinghe, S. (2018), Chemical Modification of Membrane Surface — Overview. *Current Opinion in Chemical Engineering*, 20: 13–18.

Urducea, Cristina Bărdacă, Nechifor, Aurelia Cristina, Dimulescu, Ioana Alina, Oprea, Ovidiu, Nechifor, Gheorghe, Totu, Eugenia Eftimie, Isildak, Ibrahim, Albu, Paul Constantin and Bungău, Simona Gabriela (2020), Control of Nanostructured Polysulfone Membrane Preparation by Phase Inversion Method. *Nanomaterials*, 10(12): 1–20.

Velu, S., Muruganandam, L. and Arthanareeswaran, G. (2015), Preparation and Performance Studies on Polyethersulfone Ultrafiltration Membranes Modified with Gelatin for Treatment of Tannery and Distillery Wastewater. *Brazilian Journal of Chemical Engineering*, 32(1): 179–189.

Venault, Antoine and Chang, Yung (2013), Surface Hydrophilicity and Morphology Control of Anti-Biofouling Polysulfone Membranes via Vapor-Induced Phase Separation Processing. *Journal of Nanoscience and Nanotechnology*, 13(4): 2656–2666.

Verbyla, Matthew E. and Rousselot, Olivier (2019), Membrane Bioreactors, , in: Mihelcic, J. R. and Verbyla, M. E. (Eds.), *Water and Sanitation for the 21st Century: Health and Microbiological Aspects of Excreta and Wastewater Management (Global Water Pathogen Project)*. Michigan State University. available at https://www.waterpathogens.org/book/membrane-bioreactors

Wang, K., Abdala, A. A., Hilal, N. and Khraisheh, M. K. (2017), Mechanical Characterization of Membranes, 259–306, in: *Membrane Characterization*. Elsevier Inc.

Wang, Lawrence K, Chen, Jiaping Paul, Hung, Yung-Tse and Shammas, N. k (2011), *Membrane and Desalination Technologies*. Humana Press Inc.

Wang, Miao, Huang, Yuan Wei, Chen, Yan, Yan, Xi, Xu, Wen Yan and Lang, Wan Zhong (2019), Poly(Vinylidene Fluoride) Membranes Fabricated by Vapor-Induced Phase Separation (VIPS) for the Adsorption Removal of VB12 from Aqueous Solution. *Journal of Applied Polymer Science*, 136(45): 1–11.

Wu, Qing-yun, Wan, Ling-shu and Xu, Zhi-kang (2012), Structure and Performance of Polyacrylonitrile Membranes Prepared via Thermally Induced Phase Separation. *Journal of Membrane Science*, 409–410: 355–364.

Xu, Hang, Li, Dongni, Liu, Yao, Jiang, Yinshan, Li, Fangfei and Xue, Bing (2019), Preparation of Halloysite/Polyvinylidene Fluoride Composite Membrane by Phase Inversion Method for Lithium Ion Battery. *Journal of Alloys and Compounds*, 790: 305–315.

Xue, Yuyan and Lian, Jingyan (2014), The Effects of Solvent on Polysulfone Membrane Structure. *Advanced Materials Research*, 930: 278–281.

Ye, Qian, Cheng, Lihua, Zhang, Lin, Xing, Li and Chen, Huanlin (2011), Preparation of Symmetric Network PVDF Membranes for Protein Adsorption via Vapor-Induced Phase Separation. *Journal of Macromolecular Science, Part B: Physics*, 50(10): 2004–2022.

Yeow, M. L., Liu, Y. T. and Li, K. (2004), Morphological Study of Poly(Vinylidene Fluoride) Asymmetric Membranes: Effects of the Solvent, Additive, and Dope Temperature. *Journal of Applied Polymer Science*, 92(3): 1782–1789.

Yigit, N O, Uzal, N, Koseoglu, H, Harman, I, Yukseler, H and Yetis, U (2009), Treatment of a Denim Producing Textile Industry Wastewater Using Pilot-Scale Membrane Bioreactor. *Desalination*, 240(1–3): 143–150.

You, S. J., Tseng, D. H., Ou, S. H. and Chang, W. K. (2007), Performance and Microbial Diversity of a Membrane Bioreactor Treating Real Textile Dyeing Wastewater. *Environmental Technology*, 28(8): 935–941.

Yuan, Hao, Jin, Lahua, Luo, Dan and Ge, Chen (2018), Modification Effect of Nano-Graphene Oxide on Properties and Structure of Polysulfone Ultrafiltration Membrane. *Journal of Environmental Protection*, 09(11): 1185–1195.

Yunos, Muhamad Zaini, Harun, Zawati, Basri, H and Ismail, Ahmad Fauzi (2012), Effects of Water as Non-Solvent Additive on Performance of Polysulfone Ultrafiltration Membrane. *Advanced Materials Research*, 488–489: 46–50.

Yurtsever, Adem, Sahinkaya, Erkan, Aktaş, Özgür, Uçar, Deniz, Özer, Ç and Wang, Zhiwei (2015), Performances of Anaerobic and Aerobic Membrane Bioreactors for the Treatment of Synthetic Textile Wastewater. *BIORESOURCE TECHNOLOGY*.

Zaerpour, Masoud (2014), Design, Cost & Benefit Analysis of a Membrane Bioreactor.

Zhao, Jian, Luo, Gaoxing, Wu, Jun and Xia, Hesheng (2013), Preparation of Microporous Silicone Rubber Membrane with Tunable Pore Size via Solvent Evaporation-Induced Phase Separation. *ACS Applied Materials and Interfaces*, 5(6): 2040–2046.

Zhao, Qian, Xie, Rui, Luo, Feng, Faraj, Yousef, Liu, Zhuang, Ju, Xiao Jie, Wang, Wei and Chu, Liang Yin (2018), Preparation of High Strength Poly(Vinylidene Fluoride) Porous Membranes with Cellular Structure via Vapor-Induced Phase Separation. *Journal of Membrane Science*, 549: 151–164.

Zhao, Song, Wang, Zhi, Wang, Jixiao, Yang, Shangbao and Wang, Shichang (2011), PSf/PANI Nanocomposite Membrane Prepared by in Situ Blending of PSf and PANI/NMP. *Journal of Membrane Science*, 376(1–2): 83–95.

Zheng, Libing, Wang, Jun, Yu, Dawei, Zhang, Yong and Wei, Yuansong (2018), Preparation of PVDF-CTFE Hydrophobic Membrane by Non-Solvent Induced Phase Inversion: Relation between Polymorphism and Phase Inversion. *Journal of Membrane Science*.

Zheng, Xiang and Liu, Junxin (2006), Dyeing and Printing Wastewater Treatment Using a Membrane Bioreactor with a Gravity Drain. *Desalination*, 190: 277–286.

Zinadini, Sirus, Zinatizadeh, Ali Akbar, Rahimi, Masoud, Vatanpour, Vahid and Zangeneh, Hadis (2014), Preparation of a Novel Antifouling Mixed Matrix PES Membrane by Embedding Graphene Oxide Nanoplates. *Journal of Membrane Science*, 453: 292–301.

Zuo, Ji-hao, Li, Zhong-kun, Wei, Chao, Yan, Xi, Chen, Yan and Lang, Wan-zhong (2019), Fine Tuning the Pore Size and Permeation Performances of Thermally Induced Phase Separation (TIPS) -Prepared PVDF Membranes with Saline Water as Quenching Bath. *Journal of Membrane Science*, 577(December 2018): 79–90.

Introduction to Membrane. available at http://www.separationprocesses.com/Membrane/MT_Chp07d.htm#:~:text=A liquid membrane (LM) is,aqueous solutions or gas mixtures.

(2024), Membrane Bioreactor Market Size, Share & Trends Analysis Report By Product (Hollow Fiber), By Configuration (Submerged), By Application (Municipal), By Region, And Segment Forecasts, 2023 - 2030. available at https://www.grandviewresearch.com/industry-analysis/membrane-bioreactor-mbr-market [31 May 2024].